INTERNATIONAL SCHOOL FOR ADVANCED STUDIES

CONDENSED MATTER SECTOR

EXCHANGE AND CORRELATION ENERGY IN THE ADIABATIC CONNECTION FLUCTUATION-DISSIPATION THEORY BEYOND RPA

Author:
Nicola Colonna

Supervisor:
Prof. **Stefano de Gironcoli**

A thesis submitted for the degree of Doctor of Philosophy
Academic year 2013/2014

October 2014

Contents

Chapter 1

Introduction

Shortly after Erwin Schrödinger formulated his famous equation describing the behavior of matter at the atomic scale, P.M. Dirac immediately realized what would have been the next demanding task pointing out that: "the underlying physical laws necessary for the mathematical theory of a large part of physics and the whole of chemistry are thus completely known, and the difficulty is only that the exact application of these laws leads to equations much too complicated to be soluble" [1]. Indeed in the last decades enormous efforts have been devoted to the development of approximate methods for the solution of the Schrödinger equation, most of them relying on the use of computational techniques. However, staying within wave function-based methods one has to face what Walter Kohn in his Nobel lecture [2] defined the "exponential wall". As the number of particles increases the dimension of the Hilbert space and the complexity of the many-body wave-function grow exponentially preventing the practical application of these methods but also posing doubts on the effective possibility to understand such complicated mathematical objects.

Shifting the emphasis from the wave function to the density as the basic quantity for the description of many-particle systems, Density Functional Theory (DFT) [3] provides a complementary insight for a better understanding of complex systems. Unlike the many-body wave function, the particle density is a *physical* quantity, independent on the representation and always depends on three spatial coordinates only, regardless of the dimension of the system; it thus turns out to be a much easier object to deal with when the dimension of the system increases. Beside this appealing conceptual advantage, the real strength of DFT is its favorable price/performance ratio compared with correlated wave function-based methods. In its formulation due to W. Kohn and L. Sham [4], DFT allows to compute the ground

state density and total energy of a many-particle system simply solving a set of single particle Schrödinger-like equations. This can be done with a computational cost that grows as a power of the number of particles whereas, as mentioned before, an exact solution of the Schrödinger equation requires a time that grows exponentially with the size of the system. Thanks to the constant improvements which have been making the method acceptably accurate for quantum-chemical applications, DFT is now by far the most widely used electronic structure method and its undeniable importance in physics and chemistry is evidenced by the 1998 award of the Nobel Prize to Walter Kohn "for his development of the density-functional theory" [2].

Although exact in principle, DFT relies, in all its practical applications, on approximate treatments of the unknown exchange and correlation energy functional, the most widely used being the local spin density approximation (LSDA) [4, 5] and its generalized gradient corrections (GGAs) [6, 7]. Both these approximations have been proved to successfully predict the properties of a wide class of electronic systems but still there exist many situations in which they perform poorly or even fail qualitatively. One such fundamental problem that has become increasingly apparent as the systems that could be treated have become larger, is the description of dispersion interactions. Although a weak interaction *per se*, dispersion interaction is ubiquitous and can add up to give a substantial contribution to the interaction in large assemblies of atoms and molecule thus becoming very important in systems like, for instance, biomolecules, adsorbates or nanomaterials. Dispersion forces originate from the correlation between electron density fluctuations in widely separated region of space and therefore can not be captured by standard approximations for the exchange-correlation functional which have an intrinsic local or semi-local nature.

Another class of materials for which standard Density Functional Approximations (DFAs) badly fail is represented by the *strongly correlated* systems. Strong correlations is usually meant to refer to situations where multiple determinants associated with degeneracy or near degeneracy are needed and a single-particle picture becomes inadequate. However it is understood that this is not a failure of DFT itself, which is actually based on a determinant of single-particle Kohn-Sham (KS) orbitals, but just a break-down of current DFAs. In this respect many different corrective approaches have been developed for *ab initio* calculations on strongly correlated systems ranging from Self Interaction Correction [8] to Exact-Exchange and hybrid functionals [9] to DFT+U [10].

However, rather than introducing *ad hoc* corrections to describe selected problems, it would be highly desirable to find a new class of functionals that perform uniformly better than the

present one as already happened passing from LDA to GGAs and more recently with the development of hybrid functionals. In this respect it is illuminating to start with a formal exact way of constructing the exchange and correlation functional using the Adiabatic Connection Fluctuation-Dissipation (ACFD) theory [11, 5, 12]. In this framework an *exact expression* for the exchange-correlation energy can be derived in terms of the density-density response functions of a continuous set of fictitious systems defining a path that couples the non-interacting KS system with the real many-body interacting one. The formalism thus provide a powerfull theoretical framework for a *systematic* development of advanced functionals but also a practical way to compute accurate correlation energies. Moreover all ACFD methods treat the exchange energy exactly thus cancelling out the spurious self-interaction error present in Hartree energy and the correlation energy is fully non-local and automatically includes van der Waals interactions. Indeed the most successful DFAs specifically designed to treat dispersion interactions descend from the exact expression of the correlation energy derived from the ACFD theory [13, 14, 15].

Although much more expensive than simple approximation to it, a direct evaluation of the exact formula is also possible when the interacting density-density response function is given. A Dyson equation-like linking the latter to its non-interacting (KS) counterpart can be derived from the time dependent density functional theory (TDDFT) but still requires suitable approximation for the exchange-correlation kernel to be solved. Nevertheless it has been shown that using the Random Phase Approximation (RPA), i.e. completely neglecting the unknown exchange and correlation kernel, plus a local-density correction for short range correlation, leads to a qualitatively correct description of van der Waals interactions [16, 17, 18, 19] and static correlation as seen for instance when studying dissociation of molecules in open-shell fragments [20, 21].

These encouraging results obtained already at the lowest level of approximations, indicate the potential offered by an exact treatment of the ACFD formula for the evaluation of accurate exchange and correlation energy and encourage to insist in this direction and develop futher improvements. In this Thesis we will illustrate how combining the general ACFD framework with a many-body approach along the adiabatic-connection path leads to a systematic scheme for computing increasingly accurate correlation energies. Resorting to a many-body perturbation approach allows to practically define an expansion for the exchange-correlation kernel in a power series of the electron-electron interaction and thus to proceed order-by-order toward increasingly accurate approximations for the linear density response function and hence for the correlation energy via the Adiabatic Connection formula. Applying this scheme to first

order we recover the RPAx (or EXXRPA) approximation [22, 23, 24] for which we propose a novel and efficient implementation based on an eigenvalue decomposition of the interacting time-dependent density response function in the limit of vanishing electron-electron interaction.

The Thesis is organized as follows. In the next Chapter we will describe the theoretical framework underlying the present work with a special emphasis on Kohn-Sham density functional theory. A brief review of the most widely used exchange-correlation functionals is given before introducing the Adiabatic Connection Fluctuation-Dissipation formalism and the exact formula for the exchange-correlation energy in terms of density-density linear response functions. The Dyson equation for the latter is introduced within the time dependent generalization of DFT and the simple RPA approximation is reviewed from both computational and physical point of views highlighting its successes and limitations. A general and systematic scheme aiming at computing increasingly accurate correlation energies within the ACFD framework is described at the beginning of Chapter 3 and applied to first order, recovering the so called RPAx approximation. Our efficient implementation for the calculation of correlation energies at the RPAx level is also described here with some details on its plane-wave and pseudo-potential implementation. We then test the performance of the RPAx approximation on selected systems in Chapter 4, highlighting its successes and finding simple corrections for its limitations.

The results presented in Chapter 3 and Chapter 4 are contained in two publications:

1. N. L. Nguyen, N. Colonna, and S. de Gironcoli, Phys. Rev. B 90, 045138 (2014).
2. N. Colonna, M. Hellgren, and S. de Gironcoli, Phys. Rev. B 90,125150 (2014).

Chapter 2

Theoretical background

In this Chapter we will introduce the theoretical background underlying the present work. The standard wave-function formulation of the many-electron problem and its density-functional restatement are briefly described in Sections 2.1 and 2.2, together with an overview of the most common approximations for the exchange-correlation energy functional. In Section 2.3 we will introduce the Adiabatic Connection Fluctuation-Dissipation theory which provides the general theoretical framework the present work is based on for the development of a new and advanced class of exchange-correlation functionals. As an example of such ACFD-derived functionals, we will review the Random Phase Approximation highlighting its successes and limitations.

2.1 The many-body electronic problem

Ordinary matter such as atoms, molecules and condensed matter, is built up by mutually interacting electrons and nuclei. From a standard quantum-mechanical point of view they are described by the many-body wavefunction, $|\Psi\rangle$, solution of the well-known Schrödinger equation:

$$\hat{H}|\Psi\rangle = \mathcal{W}|\Psi\rangle \tag{2.1}$$

where $\mathcal{W}$ is the total energy of the system. For a generic system of electrons and nuclei in reciprocal interaction via Coulomb forces, the non-relativistic Hamiltonian $\hat{H}$ can be written

as:

$$\hat{H} = -\frac{\hbar^2}{2m_e}\sum_i \nabla_i^2 - \sum_{i,I}\frac{Z_I e^2}{|\mathbf{r}_i - \mathbf{R}_I|} + \frac{1}{2}\sum_{i\neq j}\frac{e^2}{|\mathbf{r}_i - \mathbf{r}_j|} - \sum_I \frac{\hbar^2}{2M_I}\nabla_I^2 + \frac{1}{2}\sum_{I\neq J}\frac{Z_I Z_J e^2}{|\mathbf{R}_I - \mathbf{R}_J|} \tag{2.2}$$

where electrons are denoted by lower case subscripts and nuclei, with charge $Z_I e$ and mass M_I, by upper case subscripts. The terms appearing in Eq. (2.2) represent the kinetic energy of the electrons, the electron-nucleus attractive potential energy, the electron-electron repulsive potential energy, the kinetic energy of the nuclei and the nucleus-nucleus repulsive potential energy. This extremely complicated problem is, in practice, impossible to treat both analytically and numerically, and appropriate approximations can not be avoided. The very fundamental one is the *Born-Oppenheimer approximation* [25]. It is based on the large difference between the masses of nuclei and electrons which allows to decouple the dynamics of the fast degrees of freedom (the electrons) from the dynamics of the slow variables (the nuclei). In a first stage the nuclei can be regarded as fixed in selected spatial configurations, and attention is focused on the so called potential energy surfaces $E_i(\{\mathbf{R}_I\})$ which specify the electronic energies E_i as a function of the chosen nuclear positions $\{\mathbf{R}_I\}$. Then the dynamics of the nuclear degrees of freedom is determined by the nuclear kinetic energy and by the effective potential energies $E_i(\{\mathbf{R}_I\})$. Formally this amount to write the total wavefunction as a product of an electronic and a nuclear wavefunction

$$\Psi(\{\mathbf{r}_i, \mathbf{R}_I\}) = \Phi(\{\mathbf{R}_I\})\psi(\{\mathbf{r}_i\};\{\mathbf{R}_I\}) \tag{2.3}$$

where $\Phi(\{\mathbf{R}_I\})$ is the solution of the nuclear equation

$$\left[-\sum_I \frac{\hbar^2}{2M_I}\nabla_I^2 + E_i(\{\mathbf{R}_I\})\right]\Phi(\{\mathbf{R}_I\}) = \mathcal{W}\Phi(\{\mathbf{R}_I\}), \tag{2.4}$$

and $\psi(\{\mathbf{r}_i\};\{\mathbf{R}_I\})$ satisfies the Schrödinger equation for the electrons moving in the external potential of the nuclei kept fixed in the configuration $\{\mathbf{R}_I\}$

$$\left[-\frac{\hbar^2}{2m_e}\sum_i \nabla_i^2 - \sum_{i,I}\frac{Z_I e^2}{|\mathbf{r}_i - \mathbf{R}_I|} + \frac{1}{2}\sum_{i\neq j}\frac{e^2}{|\mathbf{r}_i - \mathbf{r}_j|} + \frac{1}{2}\sum_{I\neq J}\frac{Z_I Z_J e^2}{|\mathbf{R}_I - \mathbf{R}_J|}\right]\psi(\{\mathbf{r}_i\};\{\mathbf{R}_I\}) = E_i(\{\mathbf{R}_I\})\psi(\{\mathbf{r}_i\};\{\mathbf{R}_I\}). \tag{2.5}$$

Although the Born-Oppenheimer approximation greatly simplifies the original problem, Eq. (2.5) is still a formidable complicated task due to the presence of the electron-electron interaction. Solving the many-electron problem requires further approximations and it is the main object of electronic structure methods.

2.1.1 Electronic structure in practice

Soon after the formulation of the Schrödinger equation, the first attempts to solve the many-electron problem appeared; in 1927 D. R. Hartree introduced a procedure to calculate approximate wave functions and energies for atoms and ions [26], pioneering the self-consistent field (scf) approach and setting the stage for many of the numerical methods still in use today. Hartree method was later refined by Fock [27] who recognized the importance of correlation effects due to the Pauli exclusion principle and performed the first calculations using properly antisymmetrized Slater-determinant wave-functions, the first example of what is now know as Hartree-Fock method. Electronic correlations, beyond the exchange effects, originating from the electron-electron interaction, are in some cases very important and difficult to describe and represent the great challenge of electronic structure theory. Correlated methods for total energy calculation routinely used by the quantum chemistry community, such as Many-Body Perturbation Theory (MBPT), e.g. Møller-Plesset perturbation theory [28], Configuration Interaction (CI) [29] or Coupled Cluster theory [30], are able, in most of the case, to describe the electronic correlation but are computationally very demanding thus limiting their application to systems with a small number of electrons typically no more than a few tens. On the other hand mean-field approaches based on a single-particle description of the system, have much cheaper computational costs but, in their early developments, did not give accurate results since the correlation effects beyond the Pauli exclusion principle were completely neglected. This scenario which can be summarized as a compromise between accuracy (correlated methods in quantum chemistry) and efficiency (mean-field approaches) has been gradually changing in the last decades thanks to the advent of DFT. Unlike other mean-field single-particle methods, the one based on DFT gives in principle an exact description of the electronic ground state. The continuous progress in the development of accurate exchange-correlation functionals, improving their ability to describe an increasingly wider class of materials, has made DFT the most widely used approach for quantitative calculations on realistic systems in physics, chemistry and material science.

2.2 Density Functional Theory

In traditional many-body methods the wave-function is the central quantity. It is a mathematical object which contains a great deal of information about the system and usually much

more than we want. Moreover since it is a function of $3N$ variables[1], it is not easy to calculate, store and in general to deal with when the number of electrons in the system increases. In density functional theory the emphasis shifts from the wave-function to the electron density, $n(\mathbf{r})$, which is a much more easy object to treat and always depends on three spatial coordinates only, regardless of the dimension of the system.

Actually the idea of using the density as a key quantity to describe the properties of an electronic system, dates back to 1927; in the early days of quantum mechanics there was no practical way of using the Schrödinger equation to determine the electronic structure of many-electron systems; forced by these difficulties Thomas [31] and Fermi [32] separately proposed a simple approximate method for computing the energy of atoms starting from statistical arguments and using the electronic density as the central quantity. In the original Thomas-Fermi method the kinetic energy of the interacting system is "locally" approximated by the kinetic energy of a non-interacting homogeneous electron gas with density equal to the local density at any given point. Then two classical terms, one for the electron-nucleus interaction and one for the electron-electron electrostatic interaction, are added while the exchange and correlation contributions are completely neglected. Although the model was later extended by Dirac who formulated the local approximation for the exchange energy still in use today, the local-density approximation adopted for the kinetic energy is a too large source of error, preventing the application of this approach to real systems.

Even though at that time it was not know whether the total energy could be formally expressed in terms of density alone, the Thomas-Fermi method was a first attempt of density functional approach to the many-electron problem and as such can be viewed as a precursor to modern DFT. It was only in 1964 that DFT was put on a firm theoretical footing by Hohenberg and Kohn who published their famous paper demonstrating that any properties of a many-electron system can be viewed as a functional of the ground state electronic density alone. One year later Kohn and Sham formulation of DFT was established paving the way for DFT as the most widely used computational method for electronic structure calculations.

2.2.1 The Hohenberg-Kohn theorems

DFT is based on two theorems first proved by Hohenberg and Kohn (HK) [3]. The first one states that for any system of interacting particles in an external potential $V_{ext}(\mathbf{r})$, the potential $V_{ext}(\mathbf{r})$ is determined uniquely, up to an additive constant, by the ground state particle density

[1] A factor two has to be added if spin is also considered

$n_0(\mathbf{r})$. Since the Hamiltonian is fully determined, except for a constant shift of the total energy, it follows that the many-body wavefunctions for all the electronic states are determined. Therefore *all properties of the system are completely determined by the ground state density* $n_0(\mathbf{r})$.

The second theorem states that a *universal function* for the total energy $E[n]$ in terms of the density $n(\mathbf{r})$ can be defined, valid for any external potential $V_{ext}(\mathbf{r})$. Given a particular $V_{ext}(\mathbf{r})$, the exact ground state energy of the system is the global minimum of the functional

$$E[n] = F[n] + \int d\mathbf{r}\, V_{ext}(\mathbf{r}) n(\mathbf{r}) \tag{2.6}$$

and the density that minimizes this functional is the exact ground state density $n_0(r)$. Here $F[n] = T[n] + E_{int}[n]$ includes all the internal energies, kinetic and potential, of the interacting electron system and must be universal[2] in the sense that it depends on the density alone and not on the external potential $V_{ext}(\mathbf{r})$.

The HK theorems clearly state that any property of the electronic system can be expressed as a functional of the ground state density; however they do not give any prescription on how to construct these functionals. Looking at the ground state density itself is not enough in order to understand the properties of a generic electronic system; what one really needs are the explicit expressions for the functionals relating the density to the desired observable quantities. This is true for any property of the system and becomes a crucial point, because of the variational principle, as long as the total energy functional is concerned. All direct approximation of the total energy functional in terms of density alone, e.g. the Thomas-Fermi theory, give poor results. It is the approach proposed by Kohn and Sham that proved a major step forward toward accurate DFT calculations.

2.2.2 The Kohn-Sham equations

The central idea in the Kohn-Sham (KS) approach [4] is to replace the difficult interacting many-body system described by the Hamiltonian in Eq. (2.5) with an auxiliary system that can be solved more easily. In the KS method one *assumes* that the ground state density of the original interacting system of electrons is equal to that of a non-interacting system of electrons moving in an effective local potential $v_{KS}(\mathbf{r})$. This leads to single-particle equations whose solution gives the ground state density and energy of the original interacting system.

In order to define what is the effective local potential $v_{KS}(\mathbf{r})$, the HK energy functional

[2] Here "universal" means the same for all electron systems. Different functionals have to be defined for different kinds of particle depending on their masses and interactions.

$E[n]$ is decomposed as

$$E[n] = T_s[n] + E_H[n] + \int d\mathbf{r}\, v_{ext}(\mathbf{r})n(\mathbf{r}) + E_{xc}[n] \tag{2.7}$$

where $T_s[n]$ is the kinetic energy of the non-interacting system and can be explicitly written in terms of single particle wavefunctions $|\phi_i\rangle$

$$T_s[n] = \sum_{i=1}^{N}\langle\phi_i| - \frac{\hbar^2}{2m_e}\nabla^2|\phi_i\rangle = \frac{\hbar^2}{2m_e}\sum_{i=1}^{N}\int d\mathbf{r}\, |\nabla\phi_i(\mathbf{r})|^2, \tag{2.8}$$

$E_H[n]$ is the classical Hartree term representing the electrostatic interaction energy of the electronic density distribution

$$E_H[n] = \frac{e^2}{2}\int d\mathbf{r}d\mathbf{r}'\, \frac{n(\mathbf{r})n(\mathbf{r}')}{|\mathbf{r}-\mathbf{r}'|}, \tag{2.9}$$

and $E_{xc}[n]$, *defined* by Eq (2.7), is the still unknown exchange and correlation (xc) energy functional. From the stationary property of Eq. (2.7) one obtains the equation:

$$\int \delta n(\mathbf{r}) \left\{ \frac{\delta T_s[n]}{\delta n(\mathbf{r})} + v_{ext}(\mathbf{r}) + v_H(\mathbf{r}) + v_{xc}(\mathbf{r}) - \mu \right\} d\mathbf{r} = 0 \tag{2.10}$$

where μ is a Lagrange multiplier imposed to keep fixed the total number of electrons,

$$v_H(\mathbf{r}) = e^2 \int d\mathbf{r}' \frac{n(\mathbf{r}')}{|\mathbf{r}-\mathbf{r}'|} \tag{2.11}$$

is the Hartree potential and $v_{xc}(\mathbf{r})$ is the exchange-correlation (xc) potential defined as the functional derivative of the xc energy with respect to the density:

$$v_{xc}(\mathbf{r}) := \frac{\delta E_{xc}[n]}{\delta n(\mathbf{r})}. \tag{2.12}$$

Within the HK theory, Eq. (2.10) describes a system of non-interacting electrons moving in an effective local potential, $v_{KS}(\mathbf{r})$, sum of the external, the Hartree and the exchange-correlation contributions. Therefore one obtain the density which satisfies this equation simply by solving self-consistently the KS equations:

$$\begin{aligned} &\left[-\frac{\hbar^2}{2m_e}\nabla^2 + v_{KS}[n](\mathbf{r}) \right] \phi_i(\mathbf{r}) = \epsilon_i \phi_i(\mathbf{r}), \\ &n(\mathbf{r}) = \sum_{i=1}^{N} |\phi_i(\mathbf{r})|^2, \\ &v_{KS}[n](\mathbf{r}) = v_{ext}(\mathbf{r}) + v_H[n](\mathbf{r}) + v_{xc}[n](\mathbf{r}). \end{aligned} \tag{2.13}$$

Here the functional dependence of the KS potential and its individual contributions on the density has been highlighted. Finally the total energy of the interacting system is simply

related to the eigenvalues, ϵ_i, of the KS equations (2.13) by

$$E[n] = \sum_i^N \epsilon_i - E_H[n] + E_{xc}[n] - \int d\mathbf{r}\, v_{xc}(\mathbf{r}) n(\mathbf{r}). \tag{2.14}$$

It's worth mentioning that if the xc functional were known exactly, the self-consistent solution of the KS equations would give the correct ground state density and energy of the interacting system. Therefore the KS method, unlike other mean-field independent-particle approaches, incorporates the effects of the interactions and correlations among the particles and gives, in principle, an exact description of the electronic ground state. However, in practice, one has to resort to some reasonable approximations for the unknown xc functional.

In a nutshell, the breakthrough of the KS theory is that by treating exactly the independent electron kinetic energy and the long-range Hartree terms, the remaining exchange and correlation functional can be reasonably approximated, in most of the situations, by very simple local functionals of the density. Within these local approximations the KS method becomes very similar to the Hartree approach but in addition it also includes exchange and correlation effects making KS-DFT very attractive from a computational point of view.

2.2.3 Solving the Kohn-Sham equations: plane-wave and pseudopotential method

The numerical solution of the KS equations (2.13) is a matter of computational strategy and convenience. One can either use a discretized form of the differential operators and wavefunctions on a real-space grid or expand the orbitals in a complete basis set. In the latter case the integro-differential KS equations can be recast into a linear algebra problem which can be solved by a variety of available numerical methods. Plane waves, together with the pseudopotential method and the fast Fourier transform (FFT) algorithm, provide a powerful tool for the efficient solution of the KS equations.

In a periodic system the orbitals are usually required to be normalized and obey periodic boundary conditions in a volume Ω that is allowed to go to infinity. Following the derivation in Ref. [33], the eigenfunctions of the KS problem can by written as

$$\phi_i(\mathbf{r}) = \sum_{\mathbf{q}} c_{i,\mathbf{q}} \times \frac{1}{\sqrt{\Omega}} \exp\left(i\mathbf{q}\cdot\mathbf{r}\right) \equiv \sum_{\mathbf{q}} c_{i,\mathbf{q}} \times |\mathbf{q}\rangle \tag{2.15}$$

where $c_{i,\mathbf{q}}$ are the coefficients representing the orbital ϕ_i in the basis of orthonormal plane waves $|\mathbf{q}\rangle$ satisfying

$$\langle \mathbf{q}|\mathbf{q}'\rangle = \frac{1}{\Omega}\int_\Omega d\mathbf{r}\, \exp(-i\mathbf{q}'\cdot\mathbf{r}) \exp(i\mathbf{q}\cdot\mathbf{r}) = \delta_{\mathbf{q},\mathbf{q}'}. \tag{2.16}$$

The KS equations (2.13) in Fourier space reads

$$\sum_{\mathbf{q}}\langle\mathbf{q}'|\hat{H}_{KS}|\mathbf{q}\rangle c_{i,\mathbf{q}} = \epsilon_i \sum_{\mathbf{q}}\langle\mathbf{q}'|\mathbf{q}\rangle c_{i,\mathbf{q}} = \epsilon_i c_{i,\mathbf{q}'}. \tag{2.17}$$

The kinetic operator $\hat{T}$ is diagonal in Fourier space and its matrix elements are simply given by

$$\langle\mathbf{q}'|\hat{T}|\mathbf{q}\rangle = \langle\mathbf{q}'|-\frac{\hbar^2}{2m_e}\nabla^2|\mathbf{q}\rangle = \frac{\hbar^2}{2m_e}|q|^2\delta_{\mathbf{q}',\mathbf{q}}. \tag{2.18}$$

For a crystal the potential V_{KS} has the periodicity imposed by the lattice and can be expressed as a sum of Fourier components

$$V_{KS}(\mathbf{r}) = \sum_m V_{KS}(\mathbf{G}_m)\exp(i\mathbf{G}_m\cdot\mathbf{r}) \tag{2.19}$$

where $\mathbf{G}_m$ are the reciprocal lattice vectors[3] and

$$V_{KS}(\mathbf{G}_m) = \frac{1}{\Omega_{cell}}\int_{\Omega_{cell}} d\mathbf{r}\; V_{KS}(\mathbf{r})\exp(-i\mathbf{G}\cdot\mathbf{r}), \tag{2.20}$$

with Ω_{cell} the volume of the primitive cell. Therefore the matrix elements of the potential

$$\langle\mathbf{q}'|\hat{V}_{KS}|\mathbf{q}\rangle = \sum_m V_{KS}(\mathbf{G}_m)\delta_{\mathbf{q}'-\mathbf{q},\mathbf{G}_m} \tag{2.21}$$

are different from zero only if $\mathbf{q}$ and $\mathbf{q}'$ differ by a reciprocal lattice vector $\mathbf{G}_m$. Denoting with $\mathbf{k}$ a proper wave-vector in the first Brilloiun zone, one can always define $\mathbf{q} = \mathbf{k}+\mathbf{G}_m$ and $\mathbf{q}' = \mathbf{k}+\mathbf{G}_{m'}$ meaning that the Hamiltonian becomes block-diagonal and each block corresponds to a vector $\mathbf{k}$ in the first Brillouin zone. The KS equations for any given $\mathbf{k}$ become

$$\sum_{m'} H_{m,m'}(\mathbf{k})c_{i,m'}(\mathbf{k}) = \epsilon_i(\mathbf{k})c_{i,m}(\mathbf{k}), \tag{2.22}$$

where

$$H_{m,m'}(\mathbf{k}) = \frac{\hbar^2}{2m_e}|\mathbf{k}+\mathbf{G}_m|^2\delta_{m,m'} + V_{KS}(\mathbf{G}_m-\mathbf{G}_{m'}). \tag{2.23}$$

The eigenfunction $\phi_i(\mathbf{r})$ can be labeled by the vector $\mathbf{k}$ as well and can be written

$$\phi_{i,\mathbf{k}}(\mathbf{r}) = \sum_m c_{i,m}\times\frac{1}{\sqrt{\Omega}}\exp[i(\mathbf{k}+\mathbf{G}_m)\cdot\mathbf{r}] = \exp(i\mathbf{k}\cdot\mathbf{r})\frac{1}{\sqrt{N_{cell}}}u_{i,\mathbf{k}}(\mathbf{r}) \tag{2.24}$$

where N_{cell} is the number of primitive cells in the total volume, $\Omega = \Omega_{cell}N_{cell}$ and

$$u_{i,\mathbf{k}}(\mathbf{r}) = \frac{1}{\sqrt{\Omega_{cell}}}\sum_m c_{i,m}(\mathbf{k})\exp(i\mathbf{G}_m\cdot\mathbf{r}) \tag{2.25}$$

[3] See for instance Ref. [33] or Ref. [34] for the definition of the reciprocal lattice.

are functions which have the periodicity of the lattice and are orthonormal in one primitive cell. Eq. (2.24) is nothing but the well known Bloch theorem. The eigenpairs solution of the KS Hamiltonian can therefore be labeled by a wave vector $\mathbf{k}$ belonging to the first Brillouin zone and by an index i representing the discrete set of eigenvalues of the Hamiltonian at any given vector $\mathbf{k}$. As the volume Ω goes to infinity and the system approaches the macroscopic limit, the allowed values of $\mathbf{k}$ becomes very dense and the eigenvalues $\epsilon_i(\mathbf{k})$ become continuous bands.

Although the periodicity of the lattice allows to select only a discrete set of plane waves (PW), the representation of the Hamiltonian and its eigenfunctions for any value of $\mathbf{k}$ requires in principle an infinite number of such plane waves with wave vectors $\mathbf{k} + \mathbf{G}_m$. In practice since the valence wavefunctions are in general smooth and slowly varying functions, the high wave-vector components in the PW expansion are small enough, allowing for the truncation of the expansion. The plane waves used in a calculation are usually chosen to have a kinetic energy smaller than a given cut-off E_{cut}

$$\frac{\hbar^2}{2m_e}|\mathbf{k} + \mathbf{G}_m|^2 \leq E_{cut} \tag{2.26}$$

meaning that the convergence with respect to the number of plane waves can be easily checked by increasing the parameter E_{cut}.

While in the region between the nuclei the valence wavefuncions are slowly varying and thus can be easily described using a PW expansion, close to the nuclei positions, because of the orthogonality condition with respect to the core-electrons wavefunctions, they still vary strongly. In order to use an acceptable number of PW also in the core region, the strong variations of the valence wavefunctions can be " smoothened" resorting to the *pseudopotential method*.

The pseudopotential idea arises from the fact that many relevant properties of a system, such as bonding, chemical reactivity and many response functions, are mostly related to valence electrons only. Core electrons often play minor roles and can be regarded as a rigid object forming, together with the corresponding nucleus, a background of ion cores. In this picture the combined effects of the nucleus plus the core electrons on the valence electrons via Coulomb interaction is replaced by an effective potential which is called *pseudopotential*. These potentials are required to give smooth and nodeless pseudowave-functions which are identical to the all-electron wave-functions outside a given radius and smooth enough in the core region in order to be well represented by a small number of plane waves.

The operation required to build an *ab-initio* pseudopotential are basically three:

1 an all-electron calculation within some DFT approximation (LDA, GGA etc...) is performed for a single atom in order to obtain the electronic states;

2 the core states are kept in the ground state of the atomic configuration while the valence states are pseudized in such a way to be identical to the all-electron ones outside a given cut-off radius and smooth and nodeless in the core region;

3 the KS problem is inverted in order to find the corresponding pseudopotentials.

The additional requirement that the norm of the wave-functions is conserved leads to the so called *norm-conserving pseudopotentials* [35]. This condition is crucial to ensure the correct scattering properties around the atomic reference energy and leads to much more accurate results if compared to empirical pseudopotentials that do not fulfill this requirement.

A new class of pseudopotentials has been later proposed by Vanderbilt called *ultrasoft pseudopotential* [36]. The constraint on the total charge is relaxed allowing for the construction of very smooth pseudowavefunctions with a sensible reduction of the number of PW needed for the expansion. At the same time the atomic scattering properties are not compromised. Although the approach is technically rather complicated it allows to speed up the calculation especially for elements, like for instance N, O and F, whose norm-conserving pseudopotentials are still quite "hard" thus requiring a significant amount of Fourier components to be well represented.

2.2.4 Approximations for the xc functional

Already in their original paper Kohn and Sham pointed out that for systems characterized by a slowly varying density the xc energy can be locally approximated by the xc energy of a homogeneous electron gas with a density equal to the local density of the inhomogeneous system. This leads to the Local Density Approximation (LDA):

$$E_{xc}^{\mathrm{LDA}}[n] = \int d\mathbf{r}\, \varepsilon_{xc}(n(\mathbf{r}))n(\mathbf{r}) \tag{2.27}$$

where $\varepsilon_{xc}(n)$ is the exchange and correlation energy per particle in an electron gas with uniform density n, for which parametrizations [37, 8, 38] based on accurate Quantum Monte Carlo results [39] exist. By construction LDA is exact in the limit of uniform density and, as expected, works very well for systems with densities that vary slowly over space. However the success of LDA is far more than originally expected; highly non-homogeneous systems

such as atoms, molecules and metal surfaces are indeed reasonably described by LDA. A partial explanation for this success of the LDA is a systematic error cancellation: typically, LDA underestimates E_c but overestimates E_x, resulting in unexpectedly good values of E_{xc}. This error cancellation is not accidental, but systematic, and caused by the fact that for any density the LDA xc hole (see Eq. (2.38) and Eq. (2.39) for a definition of the xc hole) satisfies the correct sum rule

$$\int d\mathbf{r}' \; n_{xc}^{LDA}(\mathbf{r}, \mathbf{r}') = -1 \tag{2.28}$$

which is only possible if integrated errors in n_x^{LDA} cancel with those of n_c^{LDA}.

These encouraging results motivated the community to develop many extensions on the LDA by including also the gradient of the density into the functional. The first attemps in this direction leads to the so colled "gradient-expansion approximations" (GEAs) in which one tries to systematically calculate gradient-corrections of the form $|\nabla n(\mathbf{r})|$, $|\nabla n(\mathbf{r})|^2$, $\nabla^2 n(\mathbf{r})$, etc., to the LDA. However it immediately turned out that inclusion of low-order gradient corrections almost never improves on the LDA, and often even worsens it. In the early eighties it was realized that instead of power-series-like systematic gradient expansions one could experiment with more general functions of $n(\mathbf{r})$ and $\nabla n(\mathbf{r})$, without requiring an order by order expansion. This leads to the so called Generalized Gradient approximations (GGAs) which are usually defined as:

$$E_{xc}^{\mathrm{GGA}}[n] = \int d\mathbf{r} \; \varepsilon_x(n(\mathbf{r}))F_{xc}(n(\mathbf{r}), \nabla n(\mathbf{r}))n(\mathbf{r}) \tag{2.29}$$

where ε_x is the exchange energy per particle of a homogeneous electron gas with a density equal to the local density of the inhomogeneous system and F_{xc} is an enhancement factor over the local exchange which depends on the local density $n(\mathbf{r})$ and on its variation $\nabla n(\mathbf{r})$. Depending on the different expressions for F_{xc} several GGAs have been developed; in particular, GGAs used in quantum chemistry typically proceed by fitting parameters to test sets of selected molecules. On the other hand, GGAs used in physics tend to emphasize exact constraints. Nowadays the most popular (and most reliable) GGAs are PBE (denoting the functional proposed in 1996 by Perdew, Burke and Ernzerhof [7]) in physics, and BLYP (denoting the combination of Becke's 1988 exchange functional [6] with the 1988 correlation functional of Lee, Yang and Parr [40]) in chemistry. In the last few years a consensus has developed about a few GGAs that are qualitatively similar for systems of physical interest and which are able to give reliable results for all main types of chemical bonds (covalent, ionic, metallic and hydrogen bridge) and to significantly improve over the LDA providing in many cases the accuracy required by the chemistry community.

A step up in what Perdew called the "Jacob's ladder" toward the heaven of chemical accuracy[4] is represented by the *hybrid functionals* characterized by a combination of orbital-dependent Hartree-Fock and an explicit density functional. The physical insight behind this class of functionals is that the xc energy can be exactly expressed as an integral over a coupling constant tuning the electron-electron interaction (see Sections below) and the contribution when the interaction is turned off is exactly the Hartree-Fock exchange energy. The construction of hybrid functionals involves a certain amount of empiricism in the choice of functionals that are mixed and in the optimization of the weight factors given to the HF and DFT terms. Formally, this might be considered a drawback, but in practice hybrid functionals have proven to be the most successful exchange-correlation functionals for chemical applications.

All the functionals mentioned so far are built using informations from occupied states only. Exact exchange used for the construction of hybrid functionals can be combined with exact partial correlation, making use of the virtual KS states in addition to the occupied ones. Examples are the Random Phase Approximation (RPA) and its modifications. One particularly convenient approach to derive such functionals is the so called *adiabatic connection fluctuation-dissipation theory*, which is a powerful tool to obtain, in principle, the exact ground state total energy of an interacting many-body system.

2.3 The Adiabatic Connection Fluctuation-Dissipation Theory

The most disappointing drawback of the different approximations briefly described in Sec. 2.2.4, is probably the fact that it is extremely difficult to find a systematic way to improve them. In this respect it is illuminating to start with a formally exact way of constructing the xc energy functional using the Adiabatic Connection Fluctuation-Dissipation Theory. This elegant approach has been derived independently by Langreth and Perdew[11, 12], and by Gunnarsson and Lundqvist [5] and provide a route to overcome the shortcomings of standard LDA/GGA density functional theory. In particular i) an exact expression for the exchange-correlation energy in term of density-density response function can be derived from the ACFD theorem providing a promising way to develop systematic improvements for the xc functional; ii) all ACFD methods treat the exchange energy exactly thus canceling out the spurious self-interaction error present in Hartree energy; moreover iii) the correlation energy is fully non-

[4] The so-called "chemical accuracy" requires calculations with an error of not more than about 1 kcal/mol = 0.04336 eV/particle.

local and automatically includes long-range van der Waals interactions.

The starting point for the derivation is the *adiabatic-connection* technique which allows to exactly define the ground-state energy of an interacting many-body system. Then in the DFT context one can use the *fluctuation-dissipation theorem* to obtain an exact expression for the exchange-correlation energy in term of density-density response functions meaning that any approximation for the latter directly translates into an approximate DFT exchange-correlation functional.

2.3.1 Adiabatic Connection Formula

The basic idea of the adiabatic connection is to introduce a continuous set of coupling-strength (λ) dependent Hamiltonians $\hat{H}(\lambda)$ which connect a reference non-interacting Hamiltonian $\hat{H}_0 = \hat{H}(\lambda = 0)$ with the target many-body Hamiltonian $\hat{H} = \hat{H}(\lambda = 1)$ describing the Coulomb-interacting electronic system. This is usually done with a smooth turning-on of the electron-electron interaction controlled by the coupling-strength parameter λ. The choice of the reference Hamiltonian and of the adiabatic-connection path is not unique. In DFT context the natural choice is to set the path in such a way to keep the electron density constant along the way and fixed to its physical value (the ground state density of the interacting system) meaning that the reference non-interacting Hamiltonian is just the KS Hamiltonian. Then when the electron-electron interaction is turned-on a non-trivial λ-dependent local potential $v_\lambda(\mathbf{r})$ is introduced in such a way to keep the density constant along the path. For a generic value of λ the Hamiltonian can be written as:

$$\hat{H}_\lambda = \hat{T} + \lambda \hat{W} + \hat{V}_\lambda \tag{2.30}$$

where $\hat{W} = e^2 \sum_{i<j}^{N} |\mathbf{r}_i - \mathbf{r}_j|^{-1}$ and $\hat{V}_\lambda = \sum_{i=1}^{N} v_\lambda(\mathbf{r}_i)$. The local multiplicative potential $v_\lambda(\mathbf{r})$ is such that at $\lambda = 1$, it is equal to the external potential $v_{ext}(\mathbf{r})$ (usually the nuclear potential) of the fully interacting system while at $\lambda = 0$ it coincides with the KS potential $v_{KS}(\mathbf{r})$. A schematic representation of the adiabatic connection in the DFT context is shown in Fig. 2.1 Using the Hellmann-Feynman theorem we can easily define the derivative of the energy with respect to the external parameter λ

$$\frac{dE(\lambda)}{d\lambda} = \frac{d}{d\lambda}\langle \Psi_\lambda | \hat{H}_\lambda | \Psi_\lambda \rangle = \langle \Psi_\lambda | \hat{W} | \Psi_\lambda \rangle + \langle \Psi_\lambda | \frac{\hat{V}_\lambda}{d\lambda} | \Psi_\lambda \rangle, \tag{2.31}$$

where Ψ_λ denotes the ground-state of $\hat{H}_\lambda$. Integrating this equation over λ between zero and one, the total ground-state energy $E = E(\lambda = 1)$ of the interacting system is obtained:

$$E = E_0 + \int_0^1 d\lambda \, \langle \Psi_\lambda | \hat{W} | \Psi_\lambda \rangle + \int d\mathbf{r} \, n(\mathbf{r})[v_{ext}(\mathbf{r}) - v_{KS}(\mathbf{r})], \tag{2.32}$$

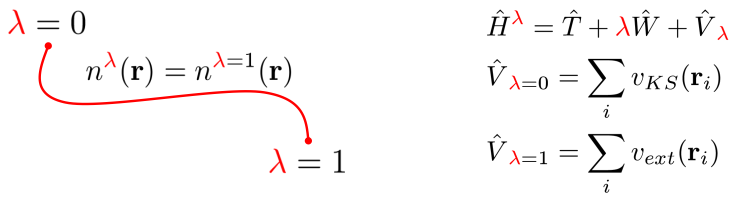

Figure 2.1: Schematic representation of the adiabatic coupling connection in a DFT context. Starting from the non-interacting KS system ($\lambda = 0$), the electron-electron interaction is turned on and a local potential $\hat{V}_{\lambda}$ is introduced in such a way to keep the density fixed along the path.

with $E_0 = E(\lambda = 0)$ being the energy of the non-interacting KS system and where the fact that the density is independent on λ has been exploited in the second integral. Using the standard decomposition for the energies E_0 and E

$$\begin{aligned} E_0 &= T_s + \int d\mathbf{r}\; n(\mathbf{r}) v_{KS}(\mathbf{r}) \\ E &= T_s + \int d\mathbf{r}\; n(\mathbf{r}) v_{ext}(\mathbf{r}) + E_H + E_{xc}, \end{aligned} \tag{2.33}$$

we are left with the well know identity

$$E_H + E_{xc} = \int_0^1 d\lambda\; \langle \Psi_\lambda | \hat{W} | \Psi_\lambda \rangle = \int_0^1 d\lambda\; W(\lambda). \tag{2.34}$$

We can rewrite the electron-electron interaction operator $\hat{W}$ as

$$\hat{W} = \frac{e^2}{2} \sum_{j \neq k}^{N} \frac{1}{|\mathbf{r}_j - \mathbf{r}_k|} = \frac{e^2}{2} \sum_{j \neq k}^{N} \int d\mathbf{r} \int d\mathbf{r}' \; \frac{\delta(\mathbf{r} - \mathbf{r}_j)\delta(\mathbf{r}' - \mathbf{r}_k)}{|\mathbf{r} - \mathbf{r}'|}, \tag{2.35}$$

which in terms of the density operator $\hat{n}(\mathbf{r}) = \sum_j \delta(\mathbf{r} - \mathbf{r}_j)$ becomes

$$\hat{W} = \frac{e^2}{2} \int d\mathbf{r} \int d\mathbf{r}' \; \frac{1}{|\mathbf{r} - \mathbf{r}'|} \left[\hat{n}(\mathbf{r})\hat{n}(\mathbf{r}') - \hat{n}(\mathbf{r})\delta(\mathbf{r} - \mathbf{r}') \right]. \tag{2.36}$$

Inserting Eq. (2.36) into Eq. (2.34) we find

$$W(\lambda) = \frac{e^2}{2} \int d\mathbf{r} \int d\mathbf{r}' \; \frac{1}{|\mathbf{r} - \mathbf{r}'|} \left[\langle \hat{n}(\mathbf{r})\hat{n}(\mathbf{r}') \rangle_\lambda - n(\mathbf{r})\delta(\mathbf{r} - \mathbf{r}') \right] \tag{2.37}$$

where $\langle \cdots \rangle_\lambda$ means an average on the ground-state $|\Psi_\lambda\rangle$. Introducing the density fluctuation operator $\delta\hat{n}(\mathbf{r}) = \hat{n}(\mathbf{r}) - n(\mathbf{r})$ we can isolate the Hartree term and obtain an *exact expression* for the exchange-correlation energy

$$\begin{aligned} E_{xc} =& \frac{e^2}{2} \int_0^1 d\lambda \int d\mathbf{r} \int d\mathbf{r}' \; \frac{1}{|\mathbf{r} - \mathbf{r}'|} \left[\langle \delta\hat{n}(\mathbf{r})\delta\hat{n}(\mathbf{r}') \rangle_\lambda - \hat{n}(\mathbf{r})\delta(\mathbf{r} - \mathbf{r}') \right] \\ =& \frac{e^2}{2} \int_0^1 d\lambda \int d\mathbf{r} \int d\mathbf{r}' \; \frac{n_{xc}^{\lambda}(\mathbf{r}, \mathbf{r}')n(\mathbf{r})}{|\mathbf{r} - \mathbf{r}'|}. \end{aligned} \tag{2.38}$$

Here

$$n_{xc}^{\lambda}(\mathbf{r},\mathbf{r}') = \frac{\langle \delta\hat{n}(\mathbf{r})\delta\hat{n}(\mathbf{r}')\rangle_{\lambda}}{n(\mathbf{r})} - \delta(\mathbf{r}-\mathbf{r}') \tag{2.39}$$

is the formal expression for the so-called xc hole which show that $n_{xc}^{\lambda}(\mathbf{r},\mathbf{r}')$ is intimately related to the density-density correlation function.

The *fluctuation-dissipation* theorem (FDT) [41, 42] can be used to establish a link between the density-density correlation (*fluctuation*) to the response properties of the system (*dissipation*). The theorem state that a system at thermodynamic equilibrium responses to a small external perturbation in the same way it responses to spontaneous internal fluctuations in absence of the perturbation. In this context the zero-temperature FDT leads to

$$\langle \delta\hat{n}(\mathbf{r})\delta\hat{n}(\mathbf{r}')\rangle_{\lambda} = -\frac{\hbar}{\pi}\int_0^{\infty} d\omega \Im\left[\chi_{\lambda}(\mathbf{r},\mathbf{r}';\omega)\right] = -\frac{\hbar}{\pi}\int_0^{\infty} du \chi_{\lambda}(\mathbf{r},\mathbf{r}';iu) \tag{2.40}$$

where $\chi_{\lambda}(\mathbf{r},\mathbf{r}';\omega)$ and $\chi_{\lambda}(\mathbf{r},\mathbf{r}';iu)$ are the density-density response function of the λ-scaled interacting system evaluated for real and imaginary frequencies. In the second identity we moved the integration path onto the imaginary axis in the complex-frequency plane exploiting the fact that $\chi(\mathbf{r}',\mathbf{r}';\omega)$ is analytic in the upper-half plane. Then we used the fact that $\chi(\mathbf{r},\mathbf{r}';iu)$ is a real function. For numerical evaluation the integration over imaginary frequencies is more suitable because it avoids the poles (related to the excitations energies of the system) that the response function presents on the real axis. Combining Eq. (2.40) with Eq. (2.38) the ACFD formula for the xc energy is obtained

$$E_{xc} = -\frac{1}{2}\int_0^1 d\lambda \int d\mathbf{r}d\mathbf{r}' \frac{e^2}{|\mathbf{r}-\mathbf{r}'|}\left\{\frac{\hbar}{\pi}\int_0^{\infty}\chi_{\lambda}(\mathbf{r},\mathbf{r}';iu)\,du + \delta(\mathbf{r}-\mathbf{r}')n(\mathbf{r})\right\}. \tag{2.41}$$

Notice that if $\chi_{\lambda}(\mathbf{r},\mathbf{r}';iu)$ is replaced by the non-interacting KS density-density response function $\chi_0(\mathbf{r},\mathbf{r}';iu)$, which has the familiar expression in terms of KS orbitals $\phi_i(\mathbf{r})$, KS eigenvalues ϵ_i and occupation number f_i

$$\chi_0(\mathbf{r},\mathbf{r}';iu) = \sum_{i,j}(f_i - f_j)\frac{\phi_i^*(\mathbf{r})\phi_j(\mathbf{r})\phi_j^*\mathbf{r}'\phi_i(\mathbf{r}')}{\epsilon_i - \epsilon_j + i\hbar u}, \tag{2.42}$$

the so-called KS exact-exchange energy E_x is recovered

$$E_x = -\frac{e^2}{2}\int d\mathbf{r}d\mathbf{r}' \frac{|\sum_i^{occ}\phi_i^*(\mathbf{r})\phi_i(\mathbf{r}')|^2}{|\mathbf{r}-\mathbf{r}'|}. \tag{2.43}$$

E_x has the same expression as the Hartree-Fock exchange energy but it is evaluated with the KS orbitals. The xc energy in Eq. (2.41) can be thus separated into the KS exact exchange energy, E_x, and the correlation energy, E_c, which can be expressed in terms of interacting and

non-interacting density-density response functions as

$$E_c = -\frac{\hbar}{2\pi}\int_0^1 d\lambda \int du \, \mathrm{Tr}\left\{v\left[\chi_\lambda(iu) - \chi_0(iu)\right]\right\}, \tag{2.44}$$

where $v = e^2/|\mathbf{r} - \mathbf{r}'|$ is the Coulomb kernel and the compact notation "Tr" means a trace over the spatial coordinates $\mathbf{r}$ and $\mathbf{r}'$. The interacting response function χ_λ can be related to its non-interacting counterpart resorting to the generalization of DFT for time-dependent phenomena.

2.3.2 Time-dependent linear density response

The time-independent Hohenberg-Kohn-Sham theory described in previous section has been extended to time-dependent phenomena by Runge and Gross [43] who proved that for any given initial state and interparticle interaction there exist a one-to-one mapping between time-dependent densities and time-dependent external potentials. As a consequence of this connection, if the time-dependent density of an interacting system can be reproduced in a fictitious system of non-interacting electrons moving under the influence of an effective time-dependent potential $v_{KS}[n](\mathbf{r}, t)$, this potential is a universal functional of $n(\mathbf{r}, t)$. Accordingly, the time-dependent density of the interacting system can be obtained from

$$n(\mathbf{r}, t) = \sum_j^N |\phi_j(\mathbf{r}, t)| \tag{2.45}$$

where the orbitals $\phi_j(\mathbf{r}, t)$ satisfies the the so-called time-dependent KS (TDKS) equations

$$i\hbar\frac{\partial}{\partial t}\phi_j(\mathbf{r}, t) = \left(-\frac{\hbar^2}{2m_e}\nabla^2 + v_{KS}[n](\mathbf{r}, t)\right)\phi_j(\mathbf{r}, t), \tag{2.46}$$

and the TDKS potential can be defined to be the sum of the external potential, the Hartree potential and the xc potential

$$v_{KS}[n](\mathbf{r}, t) = v_{ext}(\mathbf{r}, t) + \int d\mathbf{r}' \frac{n(\mathbf{r}', t)}{|\mathbf{r} - \mathbf{r}'|} + v_{xc}[n](\mathbf{r}, t). \tag{2.47}$$

Eq. (2.47) *defines* the time-dependent xc potential which is an unknown functional of the time-dependent density and needs to be adequately approximated for any practical applications.

As far as weakly perturbations are concerned one can use linear response theory and the basic theorem of TDDFT to formally derive an exact representation of the linear density response $n_1(\mathbf{r}, t)$ of an interacting many-body system in terms of the response function of the corresponding KS system and a frequency-dependent xc kernel.

Consider an electronic system moving in a static external potential $v_0(\mathbf{r})$ (typically the nuclear potential) until time $t = t_0$ when a time-dependent perturbation $v_1(\mathbf{r}, t)$ is switched on. Assuming that for $t < t_0$ the system was in its ground-state, the initial density $n_0(\mathbf{r})$ is simply given by the solution of the ordinary KS problem in Eq. (2.13). In a perturbative regime, i.e., for sufficient small $v_1(\mathbf{r}, t)$ the density can be expanded into a Taylor series with respect to the perturbation $v_1(\mathbf{r}, t)$

$$n(\mathbf{r}, t) = n_0(\mathbf{r}) + n_1(\mathbf{r}, t) + n_2(\mathbf{r}, t) + \dots \tag{2.48}$$

where the subscript indicates the order of the perturbation. The first-order density response is given by

$$n_1(\mathbf{r}, t) = \int dt' \int d\mathbf{r}' \, \chi(\mathbf{r}, t, \mathbf{r}', t') v_1(\mathbf{r}', t') \tag{2.49}$$

where we have introduced the density-density response function

$$\chi(\mathbf{r}, t, \mathbf{r}', t') = \left. \frac{\delta n(\mathbf{r}, t)}{\delta v_{ext}(\mathbf{r}', t')} \right|_{v_0}. \tag{2.50}$$

Notice that owing to the static HK theorem, the unperturbed potential $v_0 = v_{ext}[n_0]$ is a functional of the unperturbed ground-state density n_0, meaning that the density-density response function $\chi(\mathbf{r}, t, \mathbf{r}', t')$ is a functional of n_0 as well.

For the corresponding non-interacting KS system the density-density response function (which has a non interacting form) is formally given by

$$\chi_0(\mathbf{r}, t, \mathbf{r}', t') = \frac{\delta n(\mathbf{r}, t)}{\delta v_{KS}(\mathbf{r}', t')}. \tag{2.51}$$

Since the external potential $v_{ext}(\mathbf{r}, t)$ uniquely determines the density $n(\mathbf{r}, t)$[5] and, thanks to the Runge-Gross theorem, the density uniquely determine the effective potential $v_{KS}(\mathbf{r}, t)$, a unique functional $v_{KS}[v_{ext}]$ can be formally defined such that the density of non-interacting particles moving in $v_{KS}(\mathbf{r}, t)$ is identical with the density of Coulomb-interacting particles moving in the external potential $v_{ext}(\mathbf{r}, t)$ [44]. By virtue of the functional chain rule, the functional derivative of v_{KS} with respect to v_{ext} provides a link between the interacting density-density response function χ and the non-interacting one χ_0:

$$\begin{aligned} \chi(\mathbf{r}, t, \mathbf{r}', t') &= \int d\mathbf{r}_1 \, dt_1 \, \frac{\delta n(\mathbf{r}, t)}{\delta v_{KS}(\mathbf{r}_1, t_1)} \left. \frac{\delta v_{KS}(\mathbf{r}_1, t_1)}{\delta v_{ext}(\mathbf{r}', t')} \right|_{n_0} \\ &= \int d\mathbf{r}_1 \, dt_1 \, \chi_0(\mathbf{r}, t, \mathbf{r}_1, t_1) \left. \frac{\delta v_{KS}(\mathbf{r}_1, t_1)}{\delta v_{ext}(\mathbf{r}', t')} \right|_{n_0} \end{aligned} \tag{2.52}$$

[5] In this case there is no additional dependence on the initial many-body ground-state. By virtue of the static HK theorem the initial many-body ground-state is uniquely determined by the initial ground state density n_0 meaning that, in this case, the time-dependent density is a functional of the external potential alone.

Using the definition of v_{KS} in Eq. (2.47) and once more the functional chain rule, the functional derivative of v_{KS} with respect to v_{ext} becomes:

$$\left.\frac{\delta v_{KS}(\mathbf{r}_1,t_1)}{\delta v_{ext}(\mathbf{r}',t')}\right|_{n_0} = \delta(t_1-t')\delta(\mathbf{r}_1-\mathbf{r}') + \int d\mathbf{r}_2\, dt_2 \left[\frac{\delta(t_1-t_2)}{|\mathbf{r}_1-\mathbf{r}_2|} + \frac{\delta v_{xc}(\mathbf{r}_1,t_1)}{\delta n(\mathbf{r}_2,t_2)}\right] \frac{\delta n(\mathbf{r}_2,t_2)}{\delta v_{ext}(\mathbf{r}',t')}. \tag{2.53}$$

Replacing into Eq. (2.52) and using the definitions Eq. (2.50) and Eq. (2.51), a Dyson-like equation is obtained relating the interacting and the non-interacting density-density response functions

$$\begin{aligned}\chi(\mathbf{r},t,\mathbf{r}',t') = \chi_0(\mathbf{r},t,\mathbf{r}',t') + \int d\mathbf{r}_1\, dt_1 \int d\mathbf{r}_2\, dt_2\, \chi_0(\mathbf{r},t,\mathbf{r}_1,t_1) \times \\ \times \left[\frac{\delta(t_1-t_2)}{|\mathbf{r}_1-\mathbf{r}_2|} + f_{xc}(\mathbf{r}_1,t_1,\mathbf{r}_2,t_2)\right] \chi(\mathbf{r}_2,t_1,\mathbf{r}',t')\end{aligned} \tag{2.54}$$

where the time-dependent xc kernel [45, 44, 46]

$$f_{xc}(\mathbf{r},t,\mathbf{r}',t') := \left.\frac{\delta v_{xc}[n](\mathbf{r},t)}{\delta n(\mathbf{r}',t')}\right|_{n_0} \tag{2.55}$$

is a functional of the initial ground-state density n_0. If we take the Fourier transformation of Eq. (2.54) passing from time domain to (imaginary) frequency domain and insert the scaling parameter λ, we get the desired relation between the (scaled) interacting response function and the non-interacting one

$$\chi_\lambda(iu) = \chi_0(iu) + \chi_0(iu)[\lambda v + f_{xc}^\lambda(iu)]\chi_\lambda(iu) \tag{2.56}$$

where spatial coordinates dependence is implicit in the matrix notation. The system of Eqs. (2.56), (2.44) and (2.42) can be closed, thus allowing to compute the correlation energy, once the xc kernel f_{xc}^λ is specified. In this context the simplest approximation is the *random-phase approximation* (RPA) where the xc kernel is simply neglected and only the frequency-independent Coulomb or Hartree kernel is taken into account.

2.3.3 The Random Phase Approximation

The random phase approximation was introduced in the context of quantum many-body theory for the first time by Bohm and Pines[47, 48, 49, 50] during the 1950s extending concepts and techniques of quantum electrodynamics to the study of solids and nuclei. But it was only in the late 1970s that the RPA was formulated in the context of DFT and it took until recent years to be applied as a first principle electronic structure method. Within the ACFD framework described in previous sections it amounts to replace the interacting response function

with its RPA approximation given by the solution of the Dyson-like equation

$$\chi_\lambda^{\mathrm{RPA}}(iu) = \chi_0(iu) + \lambda\chi_0(iu)v\chi_\lambda^{\mathrm{RPA}}(iu). \tag{2.57}$$

It has been shown, see for instance Ref [51], that RPA yields the correct $1/R^6$ long range behavior for the interaction energy of well-separated closed shell subsystems such as van der Waals compounds; moreover RPA correctly describes static correlation [21, 52], as seen for instance when studying H_2 dissociation. Beside this encouraging results RPA is known to overestimate the correlation energies and thus to poorly describe total energies [53, 54] and in this respect various approaches have been developed that introduce "ad hoc" corrections or modifications to RPA [55, 56, 57].

From a practical point of view the greatest limitation of RPA, and its modifications or extensions, is its computational cost which is much more considerable compared to conventional LDA or GGAs functionals, preventing its widespread use in chemistry and material science. However also in this field great improvements have been achieved with respect to initial implementations which had very unfavorable scaling with the size of the system. In particular for what concern plane wave based implementations the scaling is $O[N^4]$ automatically, but some expedients can be used to speed up the calculations. A straightforward plane-wave and pseudo-potential implementation [18] requires the diagonalization of the KS Hamiltonian for all occupied and unoccupied orbitals so that the KS response function $\chi_0(iu)$ can be explicitly calculated from its definition in Eq. (2.42). Then the Dyson equation for the RPA response function $\chi_\lambda^{RPA}(iu)$ has to be solved for a discrete set of values of the coupling-constant λ and imaginary frequency iu. Finally the RPA correlation energy is obtained integrating over these variables. An obvious disadvantage of this kind of implementation is that a great number of unoccupied state has to be calculated in order to get well-converged correlation energies. Therefore the KS problem has to be solved using full matrix diagonalization techniques which have unfavorable scaling if compared to iterative diagonalization methods commonly used to calculate KS orbitals and energies. Moreover the representation of the response functions in reciprocal space requires to store very large matrices and solving the Dyson equation, which becomes a linear equation relating full matrices, is memory-demanding and cpu-time-comsuming, thus limiting the size of the systems that can be treated.

Recently Nguyen and de Gironcoli [58, 59] and Galli and coworkers [60] independently proposed an alternative implementation based on the eigenvalues decomposition of the RPA dielectric function $\varepsilon^{RPA}(iu) = 1 - v\chi^0(iu)$, efficiently computed resorting to iterative density response calculations in the framework of Density Functional Perturbation Theory (DFPT) [61].

In this context the RPA correlation energy can be written as

$$E_c^{RPA} = \frac{\hbar}{2\pi}\int_0^\infty du \sum_\alpha [e_\alpha(iu) + \ln(1 - e_\alpha(iu))] \tag{2.58}$$

where $e_\alpha(iu)$ are the eigenvalues of the operator $v\chi_0(iu)$

$$v\chi_0|z_\alpha\rangle = e_\alpha|z_\alpha\rangle. \tag{2.59}$$

Eq. (2.58) can be easily derived combining the RPA Dyson equation (2.57) with the equation above:

$$v\chi_\lambda^{RPA}|z_\alpha\rangle = v\chi_0|z_\alpha\rangle + \lambda v\chi_\lambda^{RPA}v\chi_0|z_\alpha\rangle = e_\alpha|z_\alpha\rangle + \lambda e_\alpha v\chi_\lambda^{RPA}|z_\alpha\rangle. \tag{2.60}$$

This relation shows that $v\chi_\lambda^{RPA}$ has the same eigenpotentials $|z_\alpha\rangle$ of $v\chi_0$ while its eigenvalues are simply related to e_α by the relation:

$$v\chi_\lambda^{RPA}|z_\alpha\rangle = \frac{e_\alpha}{1 - \lambda e_\alpha}|z_\alpha\rangle \tag{2.61}$$

The trace appearing in the general expression for the correlation energy in Eq. (2.44) is simply given by the sum over eigenvalues of $v\chi_\lambda^{RPA}$ and $v\chi_0$. Analytical integration over the coupling constant λ leads to the final expression for the RPA correlation energy in Eq. (2.58). Since only a small fraction of the eigenvalues e_α differs significantly from zero [62], the full spectrum is not needed and only the "most relevant" eigenvalues a_α and eigenvectors $|z_\alpha\rangle$ can be efficiently calculated using an iterative diagonalization procedure. Moreover the matrix elements of $v\chi_0(iu)$ needed during the diagonalization procedure can be efficiently computed resorting to the linear response technique of DFPT since the action of $v\chi_0(iu)$ on a generic potential $|\omega_\alpha\rangle$ is essentially the linear density variation induced by the potential itself.

The computational cost of this alternative RPA implementation is reduced from $N_{pw\chi_0}^2 N_{occ} N_{vir}$ to $N_{pw\psi} N_{occ}^2 N_{eig}$ where $N_{pw\chi_0}$ and $N_{pw\psi}$ are the number of plane waves for the expansions of the KS response function and the KS single particle orbitals, N_{occ} and N_{vir} are the number of occupied and virtual KS state and N_{eig} is the number of the relevant eigenvalues of the dielectric function. Althought the general scaling is still $O[N^4]$ the iterative diagonalization implementation allows a reduction of the prefactor estimated to be $100 - 1000$ [58, 59].

Despite the efforts in trying to reduce the computational woarkload of RPA calculations, they still remain computationally very demanding. For this reason, most of the RPA calculation are limited to a post self-consistent correction where the xc energy is computed from the charge density obtained from a self-consistent calculation performed with a more traditional xc functional. This implies that the results may depend strongly on the imput orbitals so that

when using different exchange-correlation functional or different basis set, the final RPA total energy also differs [20, 19]. In principle self consistent field (scf) RPA calculations can be done by relying on the optimized effective potential (OEP) method which provides a way to compute the local multiplicative potential that minimizes a given orbital dependent energy functional. The first *ante-litteram* example of scf-RPA within the OEP framework dates back to more than 20 years ago when Godby, Schlüter and Sham solved the Sham-Schlüter equation to obtain the effective KS potential of a few semiconductor systems [63, 64]. However they did not compute the RPA ground state total energy. More recently fully scf-RPA calculations have been performed for closed shell atoms [54, 65] showing that the RPA potentials in these systems bear a close resemblance to the exact correlation potentials. Soon after applications to simple molecules appeared [66, 67, 68]. For what concerns plane wave implementations, an efficient way to compute the scf-RPA energy and potential has been recently proposed by Nguyen *et al.* [69, 70], stemming from the non-scf implementation of Nguyen and de Gironcoli [58] paving the way for extensive calculations also for extended systems. The functional derivative of the RPA correlation energy E_c^{RPA} with respect to the density $n(\mathbf{r})$ defines the RPA correlation potentials $v_c^{RPA}(\mathbf{r})$ and can be written as

$$v_c^{RPA}(\mathbf{r}) = \frac{\delta E_c^{RPA}}{\delta n(\mathbf{r})} = \int d\mathbf{r}' \frac{\delta E_c^{RPA}}{\delta v_{KS}(\mathbf{r}')} \cdot \frac{\delta v_{KS}(\mathbf{r}')}{\delta n(\mathbf{r})} \tag{2.62}$$

where the functional chain rule has been used. This integral equation defines the OEP problem and can be solved when the functional derivative of the RPA energy with respect to the KS potential in given. In the implementation based on the dielectric-function diagonalization, this amounts to calculate the derivative of the eigenvalues $a_\alpha(iu)$ appearing in Eq. (2.58) with respect to $v_{KS}(\mathbf{r})$; infact

$$\frac{\delta E_c^{RPA}}{\delta v_{KS}(\mathbf{r}')} = -\frac{\hbar}{2\pi} \int du \sum_\alpha \frac{a_\alpha}{1-a_\alpha} \cdot \frac{\delta a_\alpha}{\delta v_{KS}(\mathbf{r})}. \tag{2.63}$$

Nguyen *et al.* [69, 70] derived an exact expression for $\delta a_\alpha / \delta v_{KS}(\mathbf{r})$ just in terms of KS orbitals and its first order variations and showed how to efficently compute it resorting, again, to linear response technique of DFPT. Moreover they have shown that the additional computational cost for this operation is a fraction of the one needed to compute E_c, meaning that beside E_c^{RPA} one can also abtain its functional derivative $\delta E_c^{RPA} / \delta v_{KS}(\mathbf{r}')$ basically at the same computational cost. Once $\delta E_c^{RPA} / \delta v_{KS}(\mathbf{r}')$ is given, the OEP equation (2.62) is solved using an efficient iterative scheme.

However, employing the RPA in a self consistent manner seems not enough to overcome all the already mentioned shortcomings of the RPA. In particular the total energies from scf

RPA calculations are bound to be even worse that those from non-scf RPA ones. The reason is that the RPA correlation energy is too large in magnitude leading to a too low total energy. Going from non-scf to scf calculations of the RPA correlation energy, the total energy becomes even lower because of the variational nature of the RPA energy functional leading to worse results.

2.3.4 Beyond the Random Phase Approximation

In the previous section we have briefly described virtues and vices of RPA. In order to correct for the latter various approaches have been developed that introduce corrections or modifications to the RPA. It is generally accepted that RPA is able to correctly describe long-range interaction but it is not adequate when short-range correlation are concerned. Perdew and coworkers [55] proposed a first modification, named RPA+, in which a local or semi-local correction is added to the standard RPA. This formally amount to approximate what is left outside the RPA correlation energy with a local or semi-local functional:

$$\Delta E_c^{RPA} = E_c - E_c^{RPA} \sim \int d\mathbf{r}\, n(\mathbf{r}) \left(\epsilon_c[n(\mathbf{r})] - \epsilon_c^{RPA}[n(\mathbf{r})] \right) \tag{2.64}$$

where E_c is the exact correlation energy of the non-homogeneous system and ϵ_c and ϵ_c^{RPA} the correlation energy per particle and its RPA counterpart of the homogeneous electron gas. The RPA+ correction, although good for total energy, does not improve the description of energy differences and in particular the atomization energies of small molecules [20].

The basic idea of RPA+ scheme, i.e. of retaining only the long-range behavior of RPA, is also exploited in the *range-separated* approaches [56]. In this case the short-range RPA contribution is completely removed (and not just corrected as in the RPA+ scheme) and replaced by a local, semi-local or hybrid functional. The computational efficiency and the accuracy in describing atomization energies take advantage from this approach, however at the price of introducing an empirical parameter that controls the range-separation.

In Ref [57] the inclusion of *single-excitation* contribution has been suggested as a possible solution of the RPA deficiencies. It is a second-order contribution to the energy which is neglected at the RPA level. Adding this term to the RPA energy improves the accuracy of van der Waals bonded molecules [57] which are generally underbinded at RPA level. Also atomization energies of covalent molecules [71] benefit from the inclusion of this term.

Staying within the ACFD framework, a rigorous possibility to address the shortcomings of RPA is to add an exchange-correlation contribution to the kernel appearing in the Dyson equation (2.56) looking for better approximations for the interacting response function. To

the best of our knowledge very little is known about the exchange-correlation kernel. The most common approximations for f_{xc}, are based on properties of the HEG (see, for instance, Refs. [72], [73] and [74] for a review), the simplest being the Adiabatic Local Density Approximation (ALDA) where the non-locality and the frequency dependence of the kernel are completely neglected. A truly non-local (but still adiabatic) approximation for f_{xc} has been derived by Petersilka *et al.* starting from the time-dependent generalization of the approximate OEP scheme proposed by Krieger, Li, and Iafrate [75].

Recently the expression for the full frequency-dependent exact-exchange contribution to f_{xc} has been derived by Göerling [76, 77, 78] within the time-dependent optimized effective potential (TDOEP) framework and by Hellgren and von Barth [79, 80] from a variational formulation of the MBPT. It defines, together to the Coulomb kernel, the full first order contribution to f_{xc}[6], and, if plugged into the Dyson equation (2.56), leads to an approximation for the response function, known in litterature as RPAx or EXXRPA, which is on the same level of the RPA but correctly takes into account all the first order contributions to the kernel in the interaction strength λ.

In the next Chapter we set the RPAx approximation within a general scheme which in principle allows to compute contributions to the kernel beyond the exact-exchange one, by establishing a link between the TDDFT expression for the response function in Eq. (2.56) and the power expansion of χ_λ in the interaction strength, which can be obtained resorting to the well-established Görling -Levy Perturbation Theory (GLPT) [81] along the adiabatic-connection path. Combining this MBPT approach with the ACFD theory provides a promising and powerful tool for the *systematic* development of new and advanced functionals.

[6] Both the Hartree and the exchange energy are linear in the coupling strength λ, meaning that both the Coulomb and the exchange kernel contribute to linear order.

Chapter 3

Advanced exchange-correlation functionals from ACFD Theory

In this Chapter we will derive a strategy for a systematic *improvement of the xc energy integrating the general framework of the ACFD theory with a many-body perturbation approach along the adiabatic connection path. Applying our strategy to first order leads to the random-phase plus exact-exchange kernel approximation, known in literature as RPAx. In Sec. 3.2 we will describe an efficient approach to solve the RPAx equation based on an eigenvalue decomposition of the full-interacting density response function in the limit of vanishing electron-electron interaction. Details of a plane-wave implementation are also supplied.*

3.1 Systematic improvement of the correlation energy

Within the ACFD formalism the central quantity defining the correlation energy is the (scaled) linear density response function $\chi_\lambda(iu)$ which is linked to the KS response function $\chi_0(iu)$ via the Dyson-like equation (2.56), and thus ultimately to the (scaled) exchange and correlation kernel f_{xc}^λ:

$$\begin{aligned} E_c &= -\frac{\hbar}{2\pi}\int_0^1 d\lambda \int du \ \mathrm{Tr}\left\{v\left[\chi_\lambda(iu)-\chi_0(iu)\right]\right\} \\ \chi_\lambda(iu) &= \chi_0(iu)+\chi_0(iu)[\lambda v + f_{xc}^\lambda(iu)]\chi_\lambda(iu). \end{aligned} \tag{3.1}$$

Any approximation for f_{xc}^λ will turns into a corresponding approximation for the response function and for the correlation energy. As already pointed out in Section 2.3.4, to the best of our knowledge, very little is known about how to obtain explicitly the exchange-correlation

kernel. In the following we will describe a general scheme which allows us to formally define a power expansion for f_{xc}^{λ}, by establishing a link between the TDDFT expression for the response function in Eq. (3.1) and the power expansion of χ_λ in the interaction strength, which can be obtained from a many-body approach along the adiabatic-connection path.

The starting point of our derivation is the λ-dependent Hamiltonian in Eq. (2.30) which describes the continuous set of fictitious systems defining the adiabatic-connection path. We already pointed out that for $\lambda = 1$ the local potential $v_\lambda(\mathbf{r})$ is equal to the external potential (usually the nuclear potential) of the fully interacting system and $\hat{H}_{\lambda=1}$ coincides with the fully interacting Hamiltonian, while for $\lambda = 0$ the local potential coincides with the KS potential and $\hat{H}_{\lambda=0}$ is the KS Hamiltonian. For intermediate values of λ an explicit expression for the local λ-dependent potential has been derived by Görling and Levy [81]:

$$v_\lambda(\mathbf{r}) = v_{KS}(\mathbf{r}) - \lambda[v_H(\mathbf{r}) + v_x(\mathbf{r})] - \frac{\delta E_c^\lambda[n]}{\delta n(\mathbf{r})} \tag{3.2}$$

where $v_{KS}(\mathbf{r})$ is the KS potential, $v_H(\mathbf{r})$ is the Hartree potential, $v_x(\mathbf{r})$ is the local exchange potential defined as the functional derivative of the exact KS exchange energy E_x in Eq. (2.43) with respect to the density, and $\delta E_c^\lambda / \delta n(\mathbf{r})$ is the correlation contribution to the local potential. The λ-dependent Hamiltonian in Eq. (2.30) becomes

$$\hat{H}_\lambda = \hat{H}_{KS} + \lambda[\hat{W} - \hat{V}_{Hx}] - \hat{V}_c^\lambda \tag{3.3}$$

where $\hat{H}_{KS}$ is the KS Hamiltonian while the operators $\hat{V}_{Hx}$ and $\hat{V}_c^\lambda$ are simply given by:

$$\hat{V}_{Hx} = \sum_{i=1}^{N} v_H(\mathbf{r}_i) + v_x(\mathbf{r}_i), \qquad \hat{V}_c^\lambda = \sum_{i=1}^{N} \frac{E_c^\lambda[n]}{\delta n(\mathbf{r}_i)}. \tag{3.4}$$

Once the many-body λ-dependent Hamiltonian is given, one can use a systematic perturbative approach, specifically the well-established Görling-Levy Perturbation Theory [81], in order to find increasingly more accurate xc kernels and energies. The basic idea is to establish a link between the TDDFT expression for the response function in Eq. (3.1) and the power expansion of χ_λ in the interaction strength, which can be obtained from the GLPT along the adiabatic-connection path.

We start by considering the power expansion for the xc kernel $f_{xc}^\lambda = \lambda f_x + \lambda^2 f_c^{(2)} + \ldots$; to first order in the interaction strength λ, not only the Hartree term v, defining the RPA, but also an exchange contribution f_x enters in the definition of the kernel, reflecting the fact that the Hartree and the exchange energy are both linear in the interaction. Explicitely writing the

Dyson equation (2.56) order by order in λ

$$\begin{aligned}\chi_\lambda =&\chi_0+\\ &+\lambda\left[\chi_0\left(v_c+f_x\right)\chi_0\right]+\\ &+\lambda^2\left[\chi_0\left(v_c+f_x\right)\chi_0\left(v_c+f_x\right)\chi_0+\chi_0 f_c^{(2)}\chi_0\right]+\\ &+\ldots,\end{aligned} \tag{3.5}$$

it can be seen that the first order kernel, $v_c + f_x$, is intimately related to the first-order variation of χ_λ with respect to λ and similarly higher order correlation contributions to the kernel are related to the corresponding power in the χ_λ expansion. Therefore i) we can define an arbitrarily accurate approximation to the density-density response function considering the expansion of the kernel up to a desired order in λ:

$$\chi_\lambda^{(n)} = \chi_0 + \chi_0[\lambda v_c + \lambda f_x + \ldots + \lambda^n f_c^{(n)}]\chi_\lambda^{(n)}; \tag{3.6}$$

where ii) the kernel up to order λ^n can be exactly determined by comparing with the λ^n expansion of χ_λ from GLPT and iii) the solution of the Dyson equation for $\chi_\lambda^{(n)}$ leads to a density-density response function which is exact to order λ^n but also contains, although in an approximate way, all higher-order terms.

In order to solve the Many Body Hamiltonian in Eq. (3.3) so as to obtain the xc kernel to a given order in λ, the xc potential, and hence the xc energy, must be known up to the same level. This apparent circular dependence does not actually hinder the application of the procedure since, thanks to the coupling constant integration involved in Eq. (3.1), the knowledge of the xc energy, and therefore its functional derivatives, up to order λ^n only depends on the xc kernel up to order λ^{n-1}. Our strategy can thus be applied in a sequential way where higher and higher orders in λ can be *systematically* included as follows:

$$\begin{aligned}&E_0 \xrightarrow{\delta/\delta n} v_{KS} \xrightarrow{GLPT} \chi_0 \xrightarrow{ACFD}\\ \rightarrow&E_x \xrightarrow{\delta/\delta n} v_x \xrightarrow{GLPT} \left(f_x, \chi_\lambda^{(1)}\right) \xrightarrow{ACFD}\\ \rightarrow&E_c^{(r2)} \xrightarrow{\delta/\delta n} v_c^{(2)} \xrightarrow{GLPT} \left(f_c^{(2)}, \chi_\lambda^{(2)}\right) \xrightarrow{ACFD}\\ \rightarrow&E_c^{(r3)} \rightarrow \ldots\end{aligned} \tag{3.7}$$

To 0^{th} order, i.e. replacing χ_λ with its non-interacting counterpart χ_0, the exact-exchange KS energy is obtained; moving to the next step, the exact-exchange kernel can be derived from first order many-body perturbation theory and the RPAx approximation [22, 24, 79] for the

correlation energy, i.e. $E_c^{(r2)}$, is recovered. We stress here that $E_c^{(rn)}$ refers to an approximation of the correlation energy which is exact to order λ^n but also contains, via the Dyson equation, contributions to all order and should not be confused with the n^{th} perturbative correction to the correlation energy in GLPT [81].

The mathematical complexity of this sequential procedure increases very rapidly and make extremely hard its application already at the second order; nevertheless the prescription is in principle given. The functional derivative of $E_c^{(r2)}$ with respect to the density defines the exact λ^2 correction to the Hamiltonian in Eq. (3.3) and allows to apply GLPT to second order and hence to have access to the corresponding second-order contribution to the xc kernel. Solving the Dyson equation with the improved kernel defines a new approximation for the response function $\chi_\lambda^{(2)}$ which is exact up to second order. Plugging $\chi_\lambda^{(2)}$ into the ACFD formula (3.1), leads to a new approximation for the correlation energy, $E_c^{(3r)}$, which is exact to order λ^3 but also contains, although in an approximate way, all higher-order terms.

Essentially this scheme can be regarded as a revised version of the standard GLPT [81, 82, 77] with the additional step provided by the solution of the Dyson equation for the response function and the calculation of a non-perturbative correlation energy (all order in the coupling-constant appears in $E_c^{(r2)}$ and following approximation to E_c) from the ACFD formula in Eq. (3.1). In this way we expect this approach to be applicable also to small gap or metallic systems where finite-order many-body perturbation theories break down [83, 73].

Having introduced the general framework, we apply our strategy to first order in the coupling strength, hence we focus on the frequency-dependent exact-exchange kernel f_x and on the calculation of the contribution $E_c^{(r2)}$ to the correlation energy (previously denoted as RPAx [79, 23] or EXXRPA [22, 24, 52]) for which we propose a novel and efficient implementation.

3.2 RPA plus exact-exchange kernel

The RPAx problem is completely specified by the following two equations:

$$\begin{aligned} E_c^{(r2)} &= -\frac{\hbar}{2\pi}\int_0^1 d\lambda \int du\ \mathrm{Tr}\left\{v\left[\chi_\lambda^{(1)}(iu) - \chi_0(iu)\right]\right\} \\ \chi_\lambda^{(1)}(iu) &= \chi_0(iu) + \lambda\chi_0(iu)[v + f_x(iu)]\chi_\lambda^{(1)}(iu), \end{aligned} \tag{3.8}$$

whose solution is a matter of computational strategy. Our implementation for computing the RPAx correlation energy is based on an eigenvalue decomposition of the time-dependent response function χ_λ in the limit of vanishing coupling constant. The scheme, described below,

is a generalization of the implementation proposed by Nguyen and de Gironcoli [58, 59] for computing RPA correlation energies briefly introduced in Sec. 2.3.3.

3.2.1 An efficient scheme for RPAx energy calculation

Let us start by defining the following generalized eigenvalue problem:

$$-\chi_0[v_c + f_x]\chi_0|\omega_\alpha\rangle = a_\alpha[-\chi_0]|\omega_\alpha\rangle \tag{3.9}$$

where the eigenpairs $\{|\omega_\alpha\rangle, a_\alpha\}$ and all the operators implicitly depend on the imaginary frequency iu and the spatial coordinates dependencies are implicit in the matrix notation. Once the solution of the generalized eigenvalue problem (3.9) is available, the trace in Eq. (3.8) is simply given by

$$\begin{aligned}\mathrm{Tr}\left[v\left(\chi_\lambda^{(1)} - \chi_0\right)\right] &= -\sum_\alpha \langle\omega_\alpha|\chi_0 v(\chi_\lambda^{(1)} - \chi_0)|\omega_\alpha\rangle \\ &= \sum_\alpha \left(1 - \frac{1}{1-\lambda a_\alpha}\right)\langle\omega_\alpha|\chi_0 v\chi_0|\omega_\alpha\rangle\end{aligned} \tag{3.10}$$

where the second identity can be derived as follows: removing $[-\chi_0]$ from both sides of Eq. (3.9) it becomes $(v + f_x)\chi_0|\omega_\alpha\rangle = a_\alpha|\omega_\alpha\rangle$ and substituting into the Dyson equation (3.8) for $\chi_\lambda^{(1)}$ we get:

$$\begin{aligned}\chi_\lambda^{(1)}|\omega_\alpha\rangle &= \chi_0|\omega_\alpha\rangle + \lambda\chi_\lambda^{(1)}(v + f_x)\chi_0|\omega_\alpha\rangle \\ &= \chi_0|\omega_\alpha\rangle + \lambda a_\alpha\chi_\lambda^{(1)}|\omega_\alpha\rangle.\end{aligned} \tag{3.11}$$

Thus the action of $\chi_\lambda^{(1)}$ on the eigenvectors $|\omega_\alpha\rangle$ simply becomes:

$$\chi_\lambda^{(1)}|\omega_\alpha\rangle = \chi_0|\omega_\alpha\rangle + \lambda a_\alpha\chi_\lambda^{(1)}|\omega_\alpha\rangle \quad \Rightarrow \quad \chi_\lambda^{(1)}|\omega_\alpha\rangle = \frac{\chi_0|\omega_\alpha\rangle}{1-\lambda a_\alpha} \tag{3.12}$$

from which Eq. (3.10) immediately follows. The integration over the coupling constant in Eq. (3.8) can be done analytically and leads to the final expression for the RPAx correlation energy

$$E_c^{(r2)} = -\frac{\hbar}{2\pi}\int_0^\infty du \sum_\alpha \frac{\langle\omega_\alpha|\chi_0 v\chi_0|\omega_\alpha\rangle}{a_\alpha(iu)}\left\{a_\alpha(iu) + \ln[1 - a_\alpha(iu)]\right\}, \tag{3.13}$$

which is indeed completely specified once the solution of the generalized eigenvalue problem in Eq. (3.9) is given. Notice that if the exchange kernel f_x is neglected the RPA correlation energy given in Eq. (2.58) is recovered. Moreover Eq. (3.9) and Eq. (3.13) show that knowledge of $h_x = \chi_0 f_x \chi_0$ is sufficient for computing the RPAx correlation energy and the exact-exchange

kernel f_x is not explicitly needed. In the next sections we will derive an expression for $h_x = \chi_0 f_x \chi_0$ in terms of the KS eigenvalues and eigenfunctions and their first-order corrections only, and show how it can be efficiently computed resorting to the linear-response techniques of density functional perturbation theory [61].

3.2.2 The exact-exchange kernel

The exact expression for $h_x = \chi_0 f_x \chi_0$ in terms of the KS eigenvalues and eigenfunctions has been derived by Görling starting from the time-dependent optimized potential method equation[76, 77] and by Hellgren and von Barth starting from the variational formulation of many-body perturbation theory [54, 79]. In this work we propose an alternative derivation staying within the general scheme described in the previous Section and show how the desired matrix elements of h_x can be efficiently computed resorting to the linear-response techniques of density functional perturbation theory [61]. In our implementation for computing the RPAx correlation energy only the eigenvalues and eigenvectors of $h_{Hx} = \chi_0(v + f_x)\chi_0$ are needed. We thus now derive an exact expression for the matrix elements of h_{Hx} exploiting the fact that it is simply the first-order variation of χ_λ with respect to the coupling strength λ.

Let us start by considering the matrix element of χ_0 on two arbitrary, α and β, time-dependent perturbing potentials $\Delta V = \Delta V(\mathbf{r})e^{ut}$ at imaginary frequency $\omega = iu$

$$\chi_0^{\alpha\beta}(iu) = \langle \Delta^\alpha V | \chi_0 | \Delta^\beta V \rangle = \int d\mathbf{r}\, \Delta^\alpha V^*(\mathbf{r}) \Delta^\beta n(\mathbf{r}; iu). \tag{3.14}$$

Assuming that the non-interacting KS Hamiltonian has a non degenerate ground state, the linear response density Δn at imaginary frequency $\omega = iu$ can be written as

$$\Delta n(\mathbf{r}; iu) = \langle \Phi_0 | \hat{n}(\mathbf{r}) | \Delta\Phi_0^{(+)} + \Delta\Phi_0^{(-)} \rangle, \tag{3.15}$$

where $|\Delta\Phi_0^{\pm}\rangle$ are the first-order corrections to the KS Slater determinant $|\Phi_0\rangle$ due to the perturbation ΔV, and satisfy the linearized time-dependent KS equations

$$[H_{KS} - (E_0 \pm iu)]|\Delta\Phi_0^{(\pm)}\rangle + \Delta V|\Phi_0\rangle = 0 \tag{3.16}$$

being $E_0 = \langle \Phi_0 | \hat{H}_{KS} | \Phi_0 \rangle$ the ground state energy. Using Eq. (3.15), Eq. (3.14) can thus be written as

$$\chi_0^{\alpha\beta}(iu) = \langle \Phi_0 | \Delta^\alpha V^* | \Delta^\beta \Phi_0^{(+)} + \Delta^\beta \Phi_0^{(-)} \rangle. \tag{3.17}$$

In order to compute the first-order variation of the response function in the coupling strength λ, i.e. h_{Hx}, we switch on the (static) first-order perturbation $\delta\hat{V} = \hat{W} - \hat{V}_{Hx}$ (see

Eq. (3.3)) and we compute its effect on the matrix elements in Eq. (3.17). As already pointed out in Sec. 3.1, the correlation contribution to the local potential $\hat{V}_c^\lambda$ appearing in Eq. (3.3) is at least of order λ^2, since E_c^λ is, hence it does not contribute to the first-order correction to χ_0 which is completely determined by $\delta\hat{V}$:

$$\begin{aligned} h_{Hx}^{\alpha\beta} = \delta\chi_0^{\alpha\beta} = &\langle \delta\Phi_0 | \Delta^\alpha V^* | \Delta^\beta \Phi_0^{(+)} + \Delta^\beta \Phi_0^{(-)} \rangle \\ &+ \langle \Phi_0 | \Delta^\alpha V^* | \delta\Delta^\beta \Phi_0^{(+)} + \delta\Delta^\beta \Phi_0^{(-)} \rangle \end{aligned} \tag{3.18}$$

where $|\delta\Delta\Phi_0\rangle$ is obtained by taking the linear variation of Eq (3.16)

$$\left[H_{KS} - (E_0 \pm iu)\right] |\delta\Delta\Phi_0^{(\pm)}\rangle + \left[\delta V - \delta E_0\right] |\Delta\Phi_0^{(\pm)}\rangle + \Delta V |\delta\Phi_0\rangle = 0 \tag{3.19}$$

while the variation $|\delta\Phi_0\rangle$ satisfies the linearized time-independent Schrödinger equation

$$[H_{KS} - E_0]|\delta\Phi_0\rangle + [\delta V - \delta E_0]|\Phi_0\rangle = 0 \tag{3.20}$$

with $\delta E_0 = \langle \Phi_0 | \delta V | \Phi_0 \rangle$.

With a simple manipulation it's easy to show that $\delta\chi_0$ depends only on the ground state wavefunction and its first-order corrections (and not on the second order correction $|\delta\Delta\Phi_0\rangle$). Multiplying the h.c. of Eq. (3.16) on the right by $|\delta\Delta\Phi_0\rangle$ and Eq. (3.19) on the left by $\langle\Delta\Phi_0|$ the following identities are obtained:

$$\begin{aligned} &\langle \Delta^\alpha \Phi_0^{(+)} | [H_{KS} - (E_0 - iu)] | \delta\Delta^\beta \Phi_0^{(-)} \rangle + \langle \Phi_0 | \Delta^\alpha V^* | \delta\Delta^\beta \Phi_0^{(-)} \rangle = 0 \\ &\langle \Delta^\alpha \Phi_0^{(+)} | [H_{KS} - (E_0 - iu)] | \delta\Delta^\beta \Phi_0^{(-)} \rangle + \langle \Delta^\alpha \Phi_0^{(+)} | [\delta V - \delta E_0] | \Delta^\beta \Phi_0^{(-)} \rangle + \langle \Delta^\alpha \Phi_0^{(+)} | \Delta^\beta V | \delta\Phi_0 \rangle = 0 \end{aligned} \tag{3.21}$$

$$\begin{aligned} &\langle \Delta^\alpha \Phi_0^{(-)} | [H_{KS} - (E_0 + iu)] | \delta\Delta^\beta \Phi_0^{(+)} \rangle + \langle \Phi_0 | \Delta^\alpha V^* | \delta\Delta^\beta \Phi_0^{(+)} \rangle = 0 \\ &\langle \Delta^\alpha \Phi_0^{(-)} | [H_{KS} - (E_0 + iu)] | \delta\Delta^\beta \Phi_0^{(+)} \rangle + \langle \Delta^\alpha \Phi_0^{(-)} | [\delta V - \delta E_0] | \Delta^\beta \Phi_0^{(+)} \rangle + \langle \Delta^\alpha \Phi_0^{(-)} | \Delta^\beta V | \delta\Phi_0 \rangle = 0 \end{aligned} \tag{3.22}$$

Comparing the two couple of identities, one for each signs $(\pm)$, an expression for $\langle \Phi_0 | \Delta^\alpha V^* | \delta\Delta^\beta \Phi_0^{(-)} + \delta\Delta^\beta \Phi_0^{(+)} \rangle$ is obtained where the second order corrections cancel out:

$$\begin{aligned} \langle \Phi_0 | \Delta^\alpha V^* | \delta\Delta^\beta \Phi_0^{(+)} + \delta\Delta^\beta \Phi_0^{(-)} \rangle = &+ \langle \Delta^\alpha \Phi_0^{(+)} + \Delta^\alpha \Phi_0^{(-)} | \Delta V^\beta | \delta\Phi_0 \rangle \\ &+ \langle \Delta^\alpha \Phi_0^{(+)} | \delta V - \delta E_0 | \Delta^\beta \Phi_0^{(-)} \rangle \\ &+ \langle \Delta^\alpha \Phi_0^{(-)} | \delta V - \delta E_0 | \Delta^\beta \Phi_0^{(+)} \rangle. \end{aligned} \tag{3.23}$$

Substituting into Eq. (3.18), leads to the final expression for $h_{vx}^{\alpha\beta}$:

$$\boxed{\begin{aligned} h_{Hx}^{\alpha\beta} = &+ \langle \delta\Phi_0 | \Delta^\alpha V^* | \Delta^\beta \Phi_0^{(+)} + \Delta^\beta \Phi_0^{(-)} \rangle + \langle \Delta^\alpha \Phi_0^{(-)} + \Delta^\alpha \Phi_0^{(+)} | \Delta^\beta V | \delta\Phi_0 \rangle \\ &- \left[\langle \Delta^\alpha \Phi_0^{(+)} | \Delta^\beta \Phi_0^{(-)} \rangle + \langle \Delta^\alpha \Phi_0^{(-)} | \Delta^\beta \Phi_0^{(+)} \rangle \right] \delta E_0 \\ &+ \langle \Delta^\alpha \Phi_0^{(+)} | \delta V | \Delta^\beta \Phi_0^{(-)} \rangle + \langle \Delta^\alpha \Phi_0^{(-)} | \delta V | \Delta^\beta \Phi_0^{(+)} \rangle . \end{aligned}} \tag{3.24}$$

Eq. (3.24) together with Eq. (3.16) and Eq. (3.20) defines the matrix elements $h_{Hx}^{\alpha\beta}$ as a function of the KS Slater determinant $|\Phi_0\rangle$ and its first-order corrections $|\Delta\Phi_0^{\pm}\rangle$ and $|\delta\Phi_0\rangle$. Introducing their definitions in terms of the single particle KS orbitals, $|\phi_a\rangle$'s, and their first-order variations, $|\Delta\phi_a^{(\pm)}\rangle$'s and $|\delta\phi_a\rangle$'s, Eq. (3.24) becomes:

$$\begin{aligned} h_{Hx}^{\alpha\beta} = &+ \sum_{ab}^{occ} \langle \Delta^\alpha \phi_a^{(-)} \phi_b | W | \Delta^\beta \phi_b^{(+)} \phi_a \rangle + \sum_{ab}^{occ} \langle \Delta^\alpha \phi_a^{(+)} \phi_b | W | \Delta^\beta \phi_b^{(-)} \phi_a \rangle \\ &+ \sum_{ab}^{occ} \langle \Delta^\alpha \phi_a^{(-)} \phi_b | W | \Delta^\beta \phi_b^{(-)} \phi_a \rangle + \sum_{ab}^{occ} \langle \Delta^\alpha \phi_a^{(+)} \phi_b | W | \Delta^\beta \phi_b^{(+)} \phi_a \rangle \\ &- \sum_{ab}^{occ} \langle \Delta^\alpha \phi_a^{(-)} \phi_b | W | \phi_a \Delta^\beta \phi_b^{(+)} \rangle - \sum_{ab}^{occ} \langle \Delta^\alpha \phi_a^{(+)} \phi_b | W | \phi_a \Delta^\beta \phi_b^{(-)} \rangle \\ &- \sum_{ab}^{occ} \langle \phi_b \phi_a | W | \Delta^\beta \phi_b^{(+)} \Delta^{*\alpha} \phi_a^{(-)} \rangle - \sum_{ab}^{occ} \langle \phi_b \phi_a | W | \Delta^\beta \phi_b^{(-)} \Delta^{*\alpha} \phi_a^{(+)} \rangle \\ &+ \sum_{a}^{occ} \langle \Delta^\alpha \phi_a^{(-)} | V_x - v_x | \Delta^\beta \phi_a^{(+)} \rangle + \sum_{a}^{occ} \langle \Delta^\alpha \phi_a^{(+)} | V_x - v_x | \Delta^\beta \phi_a^{(-)} \rangle \\ &- \sum_{ab}^{occ} \left[\langle \Delta^\alpha \phi_a^{(-)} | \Delta^\beta \phi_b^{(+)} \rangle + \langle \Delta^\alpha \phi_a^{(+)} | \Delta^\beta \phi_b^{(-)} \rangle \right] \langle \phi_b | V_x - v_x | \phi_a \rangle \\ &+ \sum_{a}^{occ} \langle \delta\phi_a | \Delta^\alpha V^* | \Delta^\beta \phi_a^{(+)} + \Delta^\beta \phi_a^{(-)} \rangle + \sum_{a}^{occ} \langle \Delta^\alpha \phi_a^{(+)} + \Delta^\alpha \phi_a^{(-)} | \Delta^\beta V | \delta\phi_a \rangle \\ &- \sum_{ab}^{occ} \langle \delta\phi_a | \Delta^\beta \phi_b^{(+)} + \Delta^\beta \phi_b^{(-)} \rangle \langle \phi_b | \Delta^\alpha V^* | \phi_a \rangle - \sum_{ab}^{occ} \langle \Delta^\alpha \phi_a^{(-)} + \Delta^\alpha \phi_a^{(+)} | \delta\phi_b \rangle \langle \phi_b | \Delta^\beta V | \phi_a \rangle . \end{aligned} \tag{3.25}$$

where the sums run over the occupied single-particle KS states only and $|\Delta\phi_a^{(\pm)}\rangle$, $|\Delta^*\phi_a^{(\pm)}\rangle$ and $|\delta\phi_a\rangle$ are the (conduction-band projected) variations of the occupied single-particle states. They can be efficiently computed resorting to the linear-response techniques of density functional perturbation theory:

$$\begin{aligned} [H_{KS} + \gamma P_v - (\varepsilon_a \pm iu)] |\Delta\phi_a^{(\pm)}\rangle &= -(1 - P_v) \Delta V |\phi_a\rangle \\ [H_{KS} + \gamma P_v - (\varepsilon_a \pm iu)] |\Delta^*\phi_a^{(\pm)}\rangle &= -(1 - P_v) \Delta V^* |\phi_a\rangle \\ [H_{KS} + \gamma P_v - \varepsilon_a] |\delta\phi_a\rangle &= -(1 - P_v)[V_x - v_x] |\phi_a\rangle \end{aligned} \tag{3.26}$$

where V_x is the non-local exchange operator identical to the Hartree-Fock one but constructed from KS orbitals, $v_x = \delta E_x / \delta n$ is the local exchange potential, $P_v = \sum_a^{occ} |\phi_a\rangle\langle\phi_a|$ is the projector on the occupied manifold and γ is a positive constant larger than the valence bandwidth in order to ensure that the linear system is not singular even in the limit for $iu \to 0$. A detailed derivation of Eq. (3.25) from its many-body counterpart Eq. (3.24) is given in Appendix A. The first two lines are simply the Hartree contribution $h_H^{\alpha\beta} = \langle \Delta^\alpha V | \chi_0 v \chi_0 | \Delta^\beta V \rangle$ and the rest correspond therefore to $h_x^{\alpha\beta} = \langle \Delta^\alpha V | \chi_0 f_x \chi_0 | \Delta^\beta V \rangle$. The basic operations required for computing these matrix elements, and ultimately the RPAx correlation energy, are essentially DFPT calculations for different imaginary frequencies and trial potentials and are basically the same required for the calculation of RPA energies and potentials in the implementations proposed by Nguyen and de Gironcoli [58, 59] and Nguyen *et al.* [69, 70] respectively. Our implementation share therefore the same main advantages and in particular the possibility to avoid explicit cumbersome summations over unoccupied states and the possibility to use efficient iterative diagonalization technique to calculate valence state of the KS problem and low-lying eigenvalues of the generalized eigenvalue problem (3.9).

3.2.3 Implementation in plane wave basis set

The method presented in previous sections for the calculation of the RPAx correlation energy is very general and in principle applicable to all cases. In this section we will present some technical aspects of the implementation in the plane-wave basis set which is now part of a developer version of the QUANTUM ESPRESSO distribution [84].

In the plane-wave approach any system is treated as periodic, meaning that the response functions are block diagonal and can be classified by a vector $\mathbf{q}$ in the first Brilloiun zone. For each $\mathbf{q}$-vector the linear response of the system to pertubing potentials of the form $\Delta V(\mathbf{r}, t) = [\Delta v_{\mathbf{q}}(\mathbf{r}) e^{i\mathbf{q}\cdot\mathbf{r}} + \Delta v^*_{\mathbf{q}}(\mathbf{r}) e^{-i\mathbf{q}\cdot\mathbf{r}}] e^{ut}$, where $\Delta v_{\mathbf{q}}(\mathbf{r})$ is a lattice-periodic potential, is considered. The correlation energy E_c can therefore be computed solving N_q independent generalized eigenvalues problems, one for each $\mathbf{q}$ in the first Brilloiun zone, and then summing-up all the contributions:

$$E_c = -\frac{\hbar}{2\pi} \int_0^1 d\lambda \int_0^\infty du \, \frac{1}{N_q} \sum_{q=1}^{N_q} \mathrm{Tr} \left\{ v[\chi_\lambda^{\mathbf{q}}(iu) - \chi_0^{\mathbf{q}}(iu)] \right\}. \tag{3.27}$$

The RPAx approximation given in Eq. (3.13) becomes

$$E_c^{(2)} = -\frac{\hbar}{2\pi} \int_0^\infty du \, \frac{1}{N_q} \sum_{q=1}^{N_q} \sum_\alpha \frac{s_\alpha(\mathbf{q}, iu)}{a_\alpha(\mathbf{q}; iu)} \left\{ a_\alpha(\mathbf{q}; iu) + \ln[1 - a_\alpha(\mathbf{q}; iu)] \right\} \tag{3.28}$$

where $s_\alpha(\mathbf{q}, iu) = \langle \omega_\alpha^{\mathbf{q}} | \chi_0^{\mathbf{q}}(iu) v \chi_0^{\mathbf{q}}(iu) | \omega_\alpha^{\mathbf{q}} \rangle$ and $\{a_\alpha(\mathbf{q}; iu), |\omega_\alpha^{\mathbf{q}}\rangle\}$ are the eigenpairs solution of the generalized eigenvalues problem (3.9) for $h_{Hx}^{\mathbf{q}}(iu)$

$$- h_{Hx}^{\mathbf{q}}(iu) |\omega_\alpha^{\mathbf{q}}\rangle = a_\alpha(\mathbf{q}; iu)[-\chi_0^{\mathbf{q}}(iu)]|\omega_\alpha^{\mathbf{q}}\rangle. \tag{3.29}$$

The integration over the first Brillouin zone, represented by the sum over the regular grid of $\mathbf{q}$-vectors, can be efficiently computed resorting to the special point technique [85, 86, 87], thus reducing the number of $\mathbf{q}$ vectors needed to accurately approximate the integral. In the present work we have focused our attention on the study of atoms and simple diatomic molecules using the supercell approach; in this particular case we expect that the dependence on the $\mathbf{q}$-vector is negligible, meaning that just one $\mathbf{q}$-vector is enough for a good estimation of the correlation energy. Finally the integration over imaginary frequency iu can be done efficiently by Gauss-Legendre method since the correlation energy is a smooth function of this variable.

We can now turn to the solution of the generalized eigenvalues problem (3.29) for $h_{Hx}^{\mathbf{q}}(iu)$ with $\chi_0^{\mathbf{q}}(iu)$ as an overlap matrix. In principle an iterative diagonalization technique can be adopted to solve this eigenvalue problem (see Appendix B); however we found that this implementation suffers of numerical instability problems related to the inversion of the overlap matrix $\chi_0^{\mathbf{q}}(iu)$. It's likely that during the iterative procedure some of the trial eigenpotentials of $h_{Hx}^{\mathbf{q}}(iu)$ have components corresponding to very small eigenvalues of $\chi_0^{\mathbf{q}}(iu)$ leading to numerical instabilities when the latter is inverted. In order to overcome this problem we have not found any better solution than solve the generalized eigenvalues problem (3.9) on a fixed basis set where the representation of the overlap matrix $\chi_0^{\mathbf{q}}(iu)$ is always well behaved. For each value of the wave-vector $\mathbf{q}$ and imaginary frequency iu we choose the basis set defined by the eigenpotentials $\{|z_i^{\mathbf{q}}\rangle\}$ (imaginary frequency label is implicitly implied) associated to the low-lying eigenvalues of the RPA eigenvalues problem in Eq. (2.59) which for a periodic system reads

$$\chi_0^{\mathbf{q}}(iu)|z_i^{\mathbf{q}}\rangle = e_i(\mathbf{q}, iu) v^{-1} |z_i^{\mathbf{q}}\rangle. \tag{3.30}$$

On this basis set $\chi_0^{\mathbf{q}}(iu)$ is simply diagonal with matrix elements $\chi_0^{ij}(\mathbf{q}, iu) = \delta_{ij} e_i(\mathbf{q}, iu)$. Since only the low-lying eigenvalues (negative and different from zero) are considered we are guaranteed that the overlap matrix can be inverted without any numerical instability.

As pointed out the eigenvalue problem (3.30) defining the basis set is exactly the same problem one has to solve for computing the RPA correlation energy (see Sec. 2.3.3); its eigen-

values e_i define the RPA correlation via Eq. (2.58) which, for a periodic system, reads

$$E_c^{RPA} = \frac{\hbar}{2\pi}\int_0^\infty du\ \frac{1}{N_q}\sum_{q=1}^{N_q}\sum_i \left[e_i(\mathbf{q},iu) + \ln\left(1-e_i(\mathbf{q},iu)\right)\right], \tag{3.31}$$

while its eigenpotentials $\{|z_i^{\mathbf{q}}\rangle\}$ define the basis set for the solution of the RPAx eigenvalues problem (3.29) and hence the RPAx correlation energy. Therefore our implementation allows to compute both RPA and RPAx correlation energies at the same time and procede as follows:

1 RPA eigenvalues problem (3.30) is solved on a discrete grid of the wave-vector $\mathbf{q}$ and imaginary frequency iu, using an iterative diagonalization technique; the eigenvalues $e_i(\mathbf{q},iu)$ are kept in memory while the eigenpotentials $\{|z_i^{\mathbf{q}}\rangle\}$ are used as a basis set for the next step;

2 RPAx eigenvalues problem (3.29) is solved on the basis set defined by the RPA eigenvectors $\{|z_i^{\mathbf{q}}\rangle\}$; the eigenvalues $a^\alpha(\mathbf{q},iu)$ and the auxiliary quantities $s_\alpha(\mathbf{q},iu)$ are computed and kept in memory;

3 the RPA and RPAx correlation energy are calculated according to Eq. (3.31) and Eq. (3.28) respectively, summing all the contributions on the $\mathbf{q}$-vector and iu-frequency grids.

We will now describe in some detail each step of the implementation.

Step-1: RPA eigenvalue problem and basis set calculation. In order to find the eigenvectors $\{|z_i^{\mathbf{q}}\rangle\}$ corresponding to the lowest eigenvalues $e_i(\mathbf{q},iu)$ an iterative technique has been used. The basic operation involved in this is the application of the non-interacting response function to a trial potential $\Delta V(\mathbf{r},t) = [\Delta v_{\mathbf{q}}(\mathbf{r})e^{i\mathbf{q}\cdot\mathbf{r}} + \Delta v^*_{\mathbf{q}}(\mathbf{r})e^{-i\mathbf{q}\cdot\mathbf{r}}]e^{ut}$, that is the induced density response $\Delta n(\mathbf{r},t)$. Denoting with $\phi_{\mathbf{k},v}(\mathbf{r})$ and $\varepsilon_{\mathbf{k},v}$ the solution of the time-independent KS equations for an electron moving in a periodic potential

$$H_{KS}(\mathbf{r})\phi_{\mathbf{k},v}(\mathbf{r}) = \varepsilon_{\mathbf{k},v}\phi_{\mathbf{k},v}(\mathbf{r}), \tag{3.32}$$

and with $\psi_{\mathbf{k},v}(\mathbf{r},t) = \phi_{\mathbf{k},v}(\mathbf{r})e^{-i\varepsilon_{\mathbf{k},v}t}$ its time dependent counterpart, the density variation $\Delta n(\mathbf{r},t)$ can be written as

$$\Delta n(\mathbf{r},t) = \sum_{\mathbf{k},v}\psi^*_{\mathbf{k},v}(\mathbf{r},t)\Delta\psi_{\mathbf{k},v}(\mathbf{r},t) + \Delta\psi^*_{\mathbf{k},v}(\mathbf{r},t)\psi_{\mathbf{k},v}(\mathbf{r},t) \tag{3.33}$$

where the sum runs over occupied state and $\Delta\psi_{\mathbf{k},v}(\mathbf{r},t)$ is the wavefunction variation induced by the perturbation $\Delta V(\mathbf{r},t)$. Because of the linearity of the Schrödinger equation, the latter

can be written as

$$\Delta\psi_{\mathbf{k},v}(\mathbf{r},t) = [\Delta\phi_{\mathbf{k}+\mathbf{q},v}e^{i\mathbf{q}\cdot\mathbf{r}} + \Delta\phi_{\mathbf{k}-\mathbf{q},v}e^{-i\mathbf{q}\cdot\mathbf{r}}]e^{-i\varepsilon_{\mathbf{k},v}t}e^{ut}. \tag{3.34}$$

Substituting into Eq. (3.33) leads to

$$\begin{aligned}\Delta n(\mathbf{r},t) &= \left\{\sum_{\mathbf{k},v}[\phi^*_{\mathbf{k},v}(\mathbf{r})\Delta\phi_{\mathbf{k}+\mathbf{q},v}(\mathbf{r}) + \Delta\phi^*_{\mathbf{k}-\mathbf{q},v}(\mathbf{r})\phi_{\mathbf{k},v}(\mathbf{r})]e^{i\mathbf{q}\cdot\mathbf{r}} + c.c.\right\}e^{ut} \\ &= \left\{\Delta n_{\mathbf{q}}(\mathbf{r})e^{i\mathbf{q}\cdot\mathbf{r}} + \Delta n^*_{\mathbf{q}}(\mathbf{r})e^{-i\mathbf{q}\cdot\mathbf{r}}\right\}e^{ut}\end{aligned} \tag{3.35}$$

where the frequency dependence of $\Delta n_{\mathbf{q}}(\mathbf{r})$ is implicitly implied. Exploiting the fact that the Hamiltonian is real, $\phi_{\mathbf{k},v}(\mathbf{r})$ can always be chosen such that $\phi_{-\mathbf{k},v}(\mathbf{r}) = \phi^*_{\mathbf{k},v}(\mathbf{r})$; therefore changing $\mathbf{k} \leftrightarrow -\mathbf{k}$ in the second summation, it can be seen that $\Delta n_{\mathbf{q}}(\mathbf{r})$ is determined by $\Delta\phi_{\mathbf{k}+\mathbf{q},v}(\mathbf{r})$ and $\Delta\phi^*_{-\mathbf{k}-\mathbf{q},v}(\mathbf{r})$. Moreover it's easy to verify that contributions to $\Delta n_{\mathbf{q}}(\mathbf{r})$ coming from product of occupied state cancel out so that $\Delta\phi_{\mathbf{k}+\mathbf{q},v}(\mathbf{r})$ can be thought of as its own projection onto the empty-state manifold and it satisfies the linearized Schrödinger equation:

$$\begin{aligned}\left[H_{KS}(\mathbf{r}) + \gamma P_v^{\mathbf{k}+\mathbf{q}} - (\varepsilon_{\mathbf{k},v} + iu)\right]\Delta\phi_{\mathbf{k}+\mathbf{q},v}(\mathbf{r}) &= -(1 - P_v^{\mathbf{k}+\mathbf{q}})\Delta v_{\mathbf{q}}(\mathbf{r})\phi_{\mathbf{k},v}(\mathbf{r}) \\ \left[H_{KS}(\mathbf{r}) + \gamma P_v^{-\mathbf{k}-\mathbf{q}} - (\varepsilon_{-\mathbf{k},v} + iu)\right]\Delta\phi_{-\mathbf{k}-\mathbf{q},v}(\mathbf{r}) &= -(1 - P_v^{-\mathbf{k}-\mathbf{q}})\Delta v_{-\mathbf{q}}(\mathbf{r})\phi_{-\mathbf{k},v}(\mathbf{r}).\end{aligned} \tag{3.36}$$

where $P_v^{\mathbf{k}+\mathbf{q}}$ and $P_v^{-\mathbf{k}-\mathbf{q}}$ are the projectors onto occupied states of wave vector $\mathbf{k}+\mathbf{q}$ and $-\mathbf{k}-\mathbf{q}$, respectively, and γ is a positive constant larger than the valence bandwidth in order to ensure that the linear system is not singular even in the limit for $iu \to 0$. Tacking the complex conjugate of the second one and exploiting the fact that the Hamiltonian is real[1], leads to

$$\begin{aligned}\left[H_{KS}(\mathbf{r}) + \gamma P_v^{\mathbf{k}+\mathbf{q}} - (\varepsilon_{\mathbf{k},v} + iu)\right]\Delta\phi_{\mathbf{k}+\mathbf{q},v}(\mathbf{r}) &= -(1 - P_v^{\mathbf{k}+\mathbf{q}})\Delta v_{\mathbf{q}}(\mathbf{r})\phi_{\mathbf{k},v}(\mathbf{r}) \\ \left[H_{KS}(\mathbf{r}) + \gamma P_v^{\mathbf{k}+\mathbf{q}} - (\varepsilon_{\mathbf{k},v} - iu)\right]\Delta\phi^*_{-\mathbf{k}-\mathbf{q},v}(\mathbf{r}) &= -(1 - P_v^{\mathbf{k}+\mathbf{q}})\Delta v_{\mathbf{q}}(\mathbf{r})\phi_{\mathbf{k},v}(\mathbf{r}).\end{aligned} \tag{3.37}$$

Renaming $\Delta\phi^*_{-\mathbf{k}-\mathbf{q},v}(\mathbf{r})$ with $\Delta\phi^{(-)}_{\mathbf{k}+\mathbf{q},v}(\mathbf{r})$ and $\Delta\phi_{\mathbf{k}+\mathbf{q},v}(\mathbf{r})$ with $\Delta\phi^{(+)}_{\mathbf{k}+\mathbf{q},v}(\mathbf{r})$, the equations defining the linear density response at wave vector $\mathbf{q}$ and imaginary frequency iu can be written as

$$\begin{aligned}\Delta n_{\mathbf{q}}(\mathbf{r}) &= \sum_{\mathbf{k},v}\phi^*_{\mathbf{k},v}(\mathbf{r})[\Delta\phi^{(+)}_{\mathbf{k}+\mathbf{q},v}(\mathbf{r}) + \Delta\phi^{(-)}_{\mathbf{k}+\mathbf{q},v}(\mathbf{r})] \\ \left[H_{KS}(\mathbf{r}) + \gamma P_v^{\mathbf{k}+\mathbf{q}} - (\varepsilon_{\mathbf{k},v} \pm iu)\right]\Delta\phi^{(\pm)}_{\mathbf{k}+\mathbf{q},v}(\mathbf{r}) &= -(1 - P_v^{\mathbf{k}+\mathbf{q}})\Delta v_{\mathbf{q}}(\mathbf{r})\phi_{\mathbf{k},v}(\mathbf{r}).\end{aligned} \tag{3.38}$$

[1] For a real Hamiltonian $[H_{KS}(\mathbf{r})]^* = H_{KS}(\mathbf{r})$, $\Delta v^*_{-\mathbf{q}}(\mathbf{r}) = \Delta v_{\mathbf{q}}(\mathbf{r})$, $\phi^*_{-\mathbf{k},v}(\mathbf{r}) = \phi_{\mathbf{k},v}(\mathbf{r})$ and $\varepsilon_{-\mathbf{k},v} = \varepsilon_{\mathbf{k},v}$

The equations for $\Delta\phi^{(\pm)}_{\mathbf{k}+\mathbf{q},v}(\mathbf{r})$ are a generalization to the time-dependent domain of the static equations of DFPT which are routinely used, for instance, for phonon frequencies calculations. Note however that in this case there is no need to perform a self-consistent cycle over density responses and screened perturbing potentials, since we are dealing with the response of a non-interacting system. However several iterations are needed to obtain well-converged eigenvalues $e_i(\mathbf{q}, iu)$ and eigenpotentials $|z^i_{\mathbf{q}}\rangle$, making the computational cost of the two calculations more or less similar.

Step-2: RPAx eigenvalue problem solution. Once the RPA problem is solved for a given wave-vector $\mathbf{q}$ and imaginary frequency iu we use the RPA eigenpotentials $\{|z^i_{\mathbf{q}}\rangle\}$ as a basis set for the solution of the RPAx eigenvalue problem (3.29). The matrix element of $h^{\mathbf{q}}_{Hx}(iu)$ on this basis set are given by the general expression in Eq. (3.25) just specified for a periodic system. The Hartree contribution $h^{ij}_H(\mathbf{q}, iu)$ (first two line in Eq. (3.25)) and the exchange contribution $h^{ij}_x(\mathbf{q}, iu)$, are given by

$$
\begin{aligned}
h^{ij}_H(\mathbf{q}, iu) =& \langle z^{\mathbf{q}}_i|\chi^{\mathbf{q}}_0(iu)v\chi^{\mathbf{q}}_0(iu)|z^{\mathbf{q}}_j\rangle = \delta_{ij}e^2_i(\mathbf{q}, iu) \\
h^{ij}_x(\mathbf{q}, iu) =& -\sum_{\mathbf{k},v}^{occ}\sum_{\mathbf{p},v'}^{occ}\langle\Delta^i\phi^{(-)}_{\mathbf{k}+\mathbf{q},v}\phi_{\mathbf{p},v'}|W|\phi_{\mathbf{k},v}\Delta^j\phi^{(+)}_{\mathbf{p}+\mathbf{q},v'}\rangle - \sum_{\mathbf{k},v}^{occ}\sum_{\mathbf{p},v'}^{occ}\langle\Delta^i\phi^{(+)}_{\mathbf{k}+\mathbf{q},v}\phi_{\mathbf{p},v'}|W|\phi_{\mathbf{k},v}\Delta^j\phi^{(-)}_{\mathbf{p}+\mathbf{q},v}\rangle \\
&- \sum_{\mathbf{k},v}^{occ}\sum_{\mathbf{p},v'}^{occ}\langle\phi_{\mathbf{p},v'}\phi_{\mathbf{k},v}|W|\Delta^j\phi^{(+)}_{\mathbf{p}+\mathbf{q},v'}\Delta^{*i}\phi^{(-)}_{\mathbf{k}-\mathbf{q},v}\rangle - \sum_{\mathbf{k},v}^{occ}\sum_{\mathbf{p},v'}^{occ}\langle\phi_{\mathbf{p},v'}\phi_{\mathbf{k},v}|W|\Delta^j\phi^{(-)}_{\mathbf{p}+\mathbf{q},v'}\Delta^{*i}\phi^{(+)}_{\mathbf{k}-\mathbf{q},v}\rangle \\
&+ \sum_{\mathbf{k},v}^{occ}\langle\Delta^i\phi^{(-)}_{\mathbf{k}+\mathbf{q},v}|V_x - v_x|\Delta^j\phi^{(+)}_{\mathbf{k}+\mathbf{q},v}\rangle + \sum_{\mathbf{k},v}^{occ}\langle\Delta^i\phi^{(+)}_{\mathbf{k}+\mathbf{q},v}|V_x - v_x|\Delta^j\phi^{(-)}_{\mathbf{k}+\mathbf{q},v}\rangle \\
&- \sum_{\mathbf{k},v,v'}^{occ}\left[\langle\Delta^i\phi^{(-)}_{\mathbf{k}+\mathbf{q},v}|\Delta^j\phi^{(+)}_{\mathbf{k}+\mathbf{q},v'}\rangle + \langle\Delta^i\phi^{(+)}_{\mathbf{k}+\mathbf{q},v}|\Delta^j\phi^{(-)}_{\mathbf{k}+\mathbf{q},v'}\rangle\right]\langle\phi_{\mathbf{k},v'}|V_x - v_x|\phi_{\mathbf{k},v}\rangle \\
&+ \sum_{\mathbf{k},v}^{occ}\langle\delta\phi_{\mathbf{k},v}|\Delta^i v^*_{\mathbf{q}}|\Delta^j\phi^{(+)}_{\mathbf{k}+\mathbf{q},v} + \Delta^j\phi^{(-)}_{\mathbf{k}+\mathbf{q},v}\rangle + \sum_{\mathbf{k},v}^{occ}\langle\Delta^j\phi^{(+)}_{\mathbf{k}+\mathbf{q},v} + \Delta^j\phi^{(-)}_{\mathbf{k}+\mathbf{q},v}|\Delta^j v_{\mathbf{q}}|\delta\phi_{\mathbf{k},v}\rangle \\
&- \sum_{\mathbf{k},v,v'}^{occ}\langle\delta\phi_{\mathbf{k}+\mathbf{q},v}|\Delta^j\phi^{(+)}_{\mathbf{k}+\mathbf{q},v'} + \Delta^j\phi^{(-)}_{\mathbf{k}+\mathbf{q},v'}\rangle\langle\phi_{\mathbf{k},v'}|\Delta^i v^*_{\mathbf{q}}|\phi_{\mathbf{k}+\mathbf{q},v}\rangle \\
&- \sum_{\mathbf{k},v,v'}^{occ}\langle\Delta^i\phi^{(-)}_{\mathbf{k}+\mathbf{q},v} + \Delta^i\phi^{(+)}_{\mathbf{k}+\mathbf{q},v}|\delta\phi_{\mathbf{k}+\mathbf{q},v'}\rangle\langle\phi_{\mathbf{k}+\mathbf{q},v'}|\Delta^j v_{\mathbf{q}}|\phi_{\mathbf{k},v}\rangle. \qquad (3.39)
\end{aligned}
$$

The linear variations $\Delta\phi^{(\pm)}_{\mathbf{k}+\mathbf{q},v}(\mathbf{r})$ are the same computed in Step-1 for the solution of the RPA problem while $\Delta^*\phi^{(\pm)}_{\mathbf{k}-\mathbf{q},v}(\mathbf{r})$ is given by the solution of the linear problem

$$
\left[H_{KS}(\mathbf{r}) + \gamma P_v^{\mathbf{k}-\mathbf{q}} - (\varepsilon_{\mathbf{k},v} \pm iu)\right]\Delta^*\phi^{(\pm)}_{\mathbf{k}-\mathbf{q},v}(\mathbf{r}) = -(1 - P_v^{\mathbf{k}-\mathbf{q}})\Delta v^*_{\mathbf{q}}(\mathbf{r})\phi_{\mathbf{k}+\mathbf{q},v}(\mathbf{r}); \qquad (3.40)
$$

however it can be shown that for a real Hamiltonian $\Delta^*\phi^{(\pm)}_{-\mathbf{k}-\mathbf{q},v}(\mathbf{r}) = \left[\Delta\phi^{(\mp)}_{\mathbf{k}+\mathbf{q},v}(\mathbf{r})\right]^*$, thus

changing $\mathbf{k} \rightarrow -\mathbf{k}$ in the second line of the expression for $h_x^{ij}(\mathbf{q}, iu)$ and using this identity the solution of the linear systems for $\Delta^* \phi^{(\pm)}_{\mathbf{k}-\mathbf{q},v}(\mathbf{r})$ can be avoided.

The only yet unknown quantity in Eq. (3.39) is $\delta\phi_{\mathbf{k},v}(\mathbf{r})$ which is given by the solution of equation (3.26) just restated for the particular case of an electron moving in a periodic potential:

$$[H_{KS}(\mathbf{r}) - \varepsilon_{\mathbf{k},v}]\delta\phi_{\mathbf{k},v}(\mathbf{r}) = -[\hat{V}_x - v_x(\mathbf{r})]\phi_{\mathbf{k},v}(\mathbf{r}) \tag{3.41}$$

In order to solve this equation we need to compute first the local exchange potential $v_x(\mathbf{r}) = \delta E_x[\{\phi_{\mathbf{k},v}(\mathbf{r})\}]/\delta n(\mathbf{r})$. This has to be done using an OEP approach since the exact KS exchange energy

$$E_x[\{\phi_{\mathbf{k},v}\}] = -\frac{e^2}{2}\int d\mathbf{r}\int d\mathbf{r}'\ \frac{|\sum_{\mathbf{k},v}^{occ}\phi^*_{\mathbf{k},v}(\mathbf{r})\phi_{\mathbf{k},v}(\mathbf{r}')|^2}{|\mathbf{r}-\mathbf{r}'|} \tag{3.42}$$

is an implicit functional of the density via the single-particle KS orbitals $\phi_{\mathbf{k},v}$. Its functional derivative with respect to the density can be written as

$$v_x(\mathbf{r}) = \frac{\delta E_x}{\delta n(\mathbf{r})} = \int d\mathbf{r}_1\ \frac{\delta E_x}{\delta v_{KS}(\mathbf{r}_1)}\frac{\delta v_{KS}(\mathbf{r}_1)}{\delta n(\mathbf{r})} \tag{3.43}$$

where $\delta v_{KS}(\mathbf{r}_1)/\delta n(\mathbf{r})$ is formally the inverse of the non-interacting response function $\chi_0(\mathbf{r}, \mathbf{r}_1)$ meaning that the solution of the problem, $v_x(\mathbf{r})$, is such that

$$\int d\mathbf{r}\ \chi_0(\mathbf{r}_1, \mathbf{r})v_x(\mathbf{r}) = \frac{\delta E_x}{\delta v_{KS}(\mathbf{r}_1)} = \delta n_x(\mathbf{r}_1). \tag{3.44}$$

This integral equation can be solved using an iterative approach; starting from a guess solution, $v_x^{(0)}(\mathbf{r})$, and applying the non-interacting response function the induced density response $\chi_0(\mathbf{r}, \mathbf{r}')|v_x^{(0)}(\mathbf{r}')\rangle$ is computed. Comparing with the target density response $\delta n_x(\mathbf{r})$ a correction can be estimated for the trial potential $v_x^{(0)}(\mathbf{r})$, improving the initial guess and leading to a new trial solution. More generally, assuming that at a given iteration, i^{th}, the approximate effective potential is $v_x^{(i)}(\mathbf{r})$, the residual quantity

$$S^{(i)}(\mathbf{r}) = \chi_0(\mathbf{r}, \mathbf{r}')|v_x^{(i)}(\mathbf{r}')\rangle - \frac{\delta E_x}{\delta v_{KS}(\mathbf{r})} \tag{3.45}$$

can be efficiently calculated using DFPT. This quantity vanishes everywhere if and only if the potential is the solution of our OEP problem. Otherwise $S^{(i)}(\mathbf{r})$ can be used, together with the residual vectors of the previous iterations, to update the trial potential as:

$$v_x^{(i+1)}(\mathbf{r}) = v_x^{(0)}(\mathbf{r}) + \sum_{m=1}^{i}\beta_m S^{(m)}(\mathbf{r}), \tag{3.46}$$

where the β_m coefficients are re-optimized at each step in order to minimize the new residuum $||S^{(i+1)}(\mathbf{r})|| = \int dr[S^{(i+1)}(\mathbf{r})]^2$. The iterative process could be terminated when a given threshold, typically of the order of 10^{-6}, is reached.

We can now turn to the target density variation $\delta n_x(\mathbf{r})$. It is defined as the variation of the exact KS exchange energy with respect to the variation of the KS potential and can be written as

$$\delta n_x(\mathbf{r}) = \frac{\delta E_x}{\delta v_{KS}(\mathbf{r})} = \int d\mathbf{r}' \sum_{\mathbf{k},v} \frac{\delta E_x}{\delta \phi_{\mathbf{k},v}(\mathbf{r}')} \cdot \frac{\delta \phi_{\mathbf{k},v}(\mathbf{r}')}{\delta v_{KS}(\mathbf{r})} + \int d\mathbf{r}' \sum_{\mathbf{k},v} \frac{\delta E_x}{\delta \phi^*_{\mathbf{k},v}(\mathbf{r}')} \cdot \frac{\delta \phi^*_{\mathbf{k},v}(\mathbf{r}')}{\delta v_{KS}(\mathbf{r})}; \tag{3.47}$$

where $\delta\phi_{\mathbf{k},v}(\mathbf{r}')/\delta v_{KS}(\mathbf{r})$ can be easily derived from standard time-independent perturbation theory (a similar equation holds true for $\delta\phi^*_{\mathbf{k},v}(\mathbf{r}')/\delta v_{KS}(\mathbf{r})$)

$$\delta\phi_{\mathbf{k},v}(\mathbf{r}') = \sum_{\mathbf{p},u} \phi_{\mathbf{p},u}(\mathbf{r}') \frac{\langle \phi_{\mathbf{p},u} | v_{KS} | \phi_{\mathbf{k},v} \rangle}{\varepsilon_{\mathbf{p},u} - \varepsilon_{\mathbf{k},v}} \quad \Rightarrow \quad \frac{\delta\phi_{\mathbf{k},v}(\mathbf{r}')}{\delta v_{KS}(\mathbf{r})} = \sum_{\mathbf{p},u} \phi_{\mathbf{p},u}(\mathbf{r}') \frac{\phi^*_{\mathbf{p},u}(\mathbf{r})\phi_{\mathbf{k},v}(\mathbf{r})}{\varepsilon_{\mathbf{p},u} - \varepsilon_{\mathbf{k},v}} \tag{3.48}$$

while $\delta E_x/\delta\phi_{\mathbf{k},v}(\mathbf{r}')$ and $\delta E_x/\delta\phi^*_{\mathbf{k},v}(\mathbf{r}')$ can be written as the non local exchange operator V_x acting from the right on $\langle\phi_{\mathbf{k},v}(\mathbf{r}')|$ and from the left on $|\phi_{\mathbf{k},v}(\mathbf{r}')\rangle$ respectively. Putting all together we get

$$\delta n_x(\mathbf{r}) = \sum_{\mathbf{k},v}\sum_{\mathbf{p},u} \langle \phi_{\mathbf{k},v} | V_x | \phi_{\mathbf{p},u} \rangle \frac{\phi^*_{\mathbf{p},u}(\mathbf{r})\phi_{\mathbf{k},v}(\mathbf{r})}{\varepsilon_{\mathbf{p},u} - \varepsilon_{\mathbf{k},v}} + c.c. = \sum_{\mathbf{k},v} \phi^*_{\mathbf{k},v}(\mathbf{r}) \delta^{NL}\phi_{\mathbf{k},v}(\mathbf{r}) + c.c. \tag{3.49}$$

where $\delta^{NL}\phi_{\mathbf{k},v}(\mathbf{r})$ is given by the solution of the linear problem

$$[H_{KS} - \varepsilon_{\mathbf{k},v}]\delta^{NL}\phi_{\mathbf{k},v}(\mathbf{r}) = -V_x\phi_{\mathbf{k},v}(\mathbf{r}). \tag{3.50}$$

The OEP approach described above allows to compute the local exchange potential $v_x(\mathbf{r})$ which determines the vectors $\delta\phi_{\mathbf{k},v}(\mathbf{r})$ and $\delta\phi_{\mathbf{k}+\mathbf{q},v}(\mathbf{r})$ via Eq. (3.41) and hence contributes to completely define the matrix elements of the exchange kernel matrix $h^{\mathbf{q}}_x(iu)$ in Eq. (3.39).

Step-3: Integration over imaginary frequency and sampling of the Brillouin zone. The last step of our implementation consists of summing up all the contribution for each $\mathbf{q}$-vector and imaginary frequency iu. As already pointed out the integral over $\mathbf{q}$-vector can be efficiently done using special point technique for the sampling of the first Brilloiun zone. Integration over imaginary frequency can be done efficiently by Gauss-Legendre method since the correlation energy is a smooth function of this variable.

Compared to the RPA correlation energy calculation, the only additional operations required for the RPAx correlation energy calculation are that needed in Step-2. They are essentially the solution of the linear systems for $\delta\phi_{\mathbf{k},v}(\mathbf{r})$ and $\delta\phi_{\mathbf{k}+\mathbf{q},v}(\mathbf{r})$ via DFPT and the calculation of the matrix elements $h^{ij}_{Hx}(\mathbf{q}, iu)$ in Eq. (3.39). Considering that the equations defining $\delta\phi_{\mathbf{k},v}(\mathbf{r})$ and $\delta\phi_{\mathbf{k}+\mathbf{q},v}(\mathbf{r})$ do not depend on iu, they can be solved once for every fixed values of the

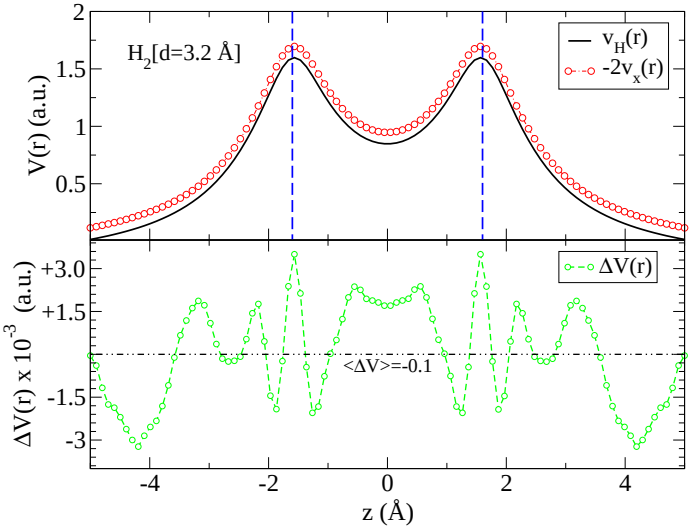

Figure 3.1: Comparison between the Hartree potential and the local exchange potential of the Hydrogen molecule at interatomic distance $d = 3.2$ Å. In the top panel the potentials are plotted along the molecule axis. The blue dashed lines indicate the positions of the Hydrogen atoms. In the lower panel the difference between the the Hartree and the exchange potential is plotted having set the zero to the mean value of the difference $\langle \Delta V(\mathbf{r}) \rangle$.

q-vector outside the loop over the imaginary frequencies. Also the local exchange potential $v_x(\mathbf{r})$, which enters in the definition of these vectors and of the matrix elements $h^{ij}_{Hx}(\mathbf{q}, iu)$, can be computed once for all outside the **q**-vector and imaginary frequency loops. The matrix elements calculation, although requires Coulomb integrals in real space, can be efficiently done thanks to FFT algorithm. The only time-consuming operation remains the iterative solution of the RPA eigenvalues problem. Therefore the workload increase passing from RPA to RPAx correlation energy calculation is restrained and accounted for by a small multiplicative prefactor in front of the RPA computational cost.

3.2.4 Testing the implementation

In order to check the correctness of the implementation some simple tests have been conducted over 2-electrons systems. For this kind of systems the local exchange potential $v_x(\mathbf{r})$ and the exact-exchange kernel $f_x(\mathbf{r}, \mathbf{r}'; iu)$ are simply related to the Hartree potential and kernel. In particular $v_x(\mathbf{r}) = -v_H(\mathbf{r})/2$ (a part from a trivial shift) and consequently $f_x(\mathbf{r}, \mathbf{r}'; iu) = -v(\mathbf{r}, \mathbf{r}')/2$. Both these relations simply come from the fact that the exact KS energy for 2-electrons systems is just half of the Hartree energy (with a minus sign in front). Taking the

functional derivative with respect to the density leads to the relation between the exchange and Hartree potentials; one more functional derivative leads to the relation between the corresponding kernels [2]. Thanks to these simple relations all the properties of a 2-electron system at the RPAx level can be easily related to the corresponding properties in the RPA. This kind of systems therefore represents a perfect testing case to validate the RPAx implementation by simply comparing the results from the new approximation with the well-established RPA calculations.

We started testing our OEP implementation for the local exchange potential. In Fig. 3.1 we report the Hartree and the local exchange potential (multiplied by a factor -2 for a easier comparison), plotted along the molecular axis of the H_2 molecule at bond-length $d = 3.2$ Å. The calculation has been performed with the supercell approach using a simple-cubic cell with size length $a = 22$ bohr and placing the atoms along the diagonal of the simulation box. Norm-conserving pseudopotentials[3] have been used with a kinetic-energy cut-off of 50 Ry.

As expected, a part from an irrelevant constant, the two potentials essentially coincide; a rigid shift of $\langle \Delta V(\mathbf{r}) \rangle \sim 0.1$ a.u. aligns the two curves within an error of $\sim 10^{-3}$; this can be seen from the lower panel of the figure, where the difference between the two potential, $\Delta V(\mathbf{r}) = v_H(\mathbf{r}) + 2v_x(\mathbf{r})$, is plotted along the molecular axis setting its mean value, $\langle \Delta V(\mathbf{r}) \rangle$, as a reference.

For a 2-electrons system also the RPAx eigenvalues problem greatly simplify; the matrix h_{Hx} becomes $h_{Hx} = \chi_0(v/2)\chi_0$ since the exchange kernel is just half of the Hartree kernel (with a minus sign); therefore the RPAx eigenvalue problem

$$-\chi_0^{\mathbf{q}}(iu)[v + f_x(iu)]\chi_0^{\mathbf{q}}(iu)|\omega_\alpha^{\mathbf{q}}\rangle = a_\alpha(\mathbf{q}, iu)[-\chi_0^{\mathbf{q}}(iu)]|\omega_\alpha^{\mathbf{q}}\rangle \tag{3.51}$$

simply reduce to the RPA eigenvalue problem

$$v\chi_0^{\mathbf{q}}(iu)|\omega_\alpha^{\mathbf{q}}\rangle = 2a_\alpha(\mathbf{q}, iu)|\omega_\alpha^{\mathbf{q}}\rangle, \tag{3.52}$$

showing that, for 2-electrons systems, the RPAx eigenpotentials coincide withe the RPA ones and a simple relation exists between the RPAx and RPA eigenvalues: $a_\alpha(\mathbf{q}, iu) = e_\alpha(\mathbf{q}, iu)/2$. Therefore in order to validate the expression derived for the matrix $h_{Hx}^{\mathbf{q}}(iu)$, we computed and compared the lowest 20 eigenvalues of the RPA and RPAx response functions of the

[2] Actually this way of deriving the kernel as the second functional derivative of the energy, is rigorous just for the static case; however the relation holds true also for the time dependent kernels and can be rigorously derived from Eq. (3.25) considering that $\delta\phi_a = 0$ and $[V_x - v_x]|\phi_a\rangle = 0$ for a 2-electron system in a spin-restricted configuration.

[3] We used the pseudopotential H.pbe-mt_fhi.UPF from the http://www.quantum-espresso.org webpage

Index	RPA	RPAx	Δ ($\times 10^{-4}$)	Index	RPA	RPAx	Δ ($\times 10^{-4}$)
1	-5.5598	-2.7799	+0.00	11	-0.0836	-0.0418	+14.96
2	-0.5315	-0.2657	-2.01	12	-0.0811	-0.0404	-22.90
3	-0.3889	-0.1944	-1.76	13	-0.0639	-0.0320	+0.53
4	-0.3485	-0.1743	+1.00	14	-0.0639	-0.0320	+0.50
5	-0.3485	-0.1743	+1.00	15	-0.0590	-0.0295	+18.04
6	-0.2838	-0.1419	+0.13	16	-0.0584	-0.0292	-2.19
7	-0.2838	-0.1419	+0.13	17	-0.0584	-0.0292	-2.19
8	-0.2670	-0.1335	+1.50	18	-0.0570	-0.0285	+10.61
9	-0.1641	-0.0821	+1.02	19	-0.0570	-0.0285	+10.56
10	-0.0836	-0.0418	+14.96	20	-0.0564	-0.0282	-7.07

Table 3.1: Eigenvalues of the RPA and RPAx response function at $\mathbf{q} = (0,0,0)$ and $iu = 0.1Ry$ for the hydrogen molecule at bond length $d = 3.2$ Å.

H_2 molecule at an interatomic distance $d = 3.2$ Å. The calculation has been performed for $\mathbf{q} = (0,0,0)$ and $iu = 0.1$ Ry using well-converged PBE density and orbitals. In Tab 3.1 the RPA and RPAx eigenvalues are listed together with the quantity $\Delta = 1 - 2a_\alpha/e_\alpha$ which indicates how much the calculations are close to the exact relation $e_\alpha = 2a_\alpha$ and therefore gives and estimation of the correctness of our implementation. The mean values of Δ over the 20 eigenvalues is about 10^{-4}, thus indicating that the general expression for h_{Hx} in Eq. (3.25) and its plane-wave implementation in Eq. (3.39) are both correct.

As already pointed out, in the present work we focused on the study of simple diatomic molecules using the supercell approach. It's therefore important to check the convergence of the calculations with respect to the kinetic energy cut-off, supercell size and number of eigenvalues used for computing the RPA and RPAx correlation energies. While important in general the convergence issue becomes crucial, for instance, for a system with very small binding energy where a not converged calculations could lead to a qualitatively wrong description of the physical property of the system. We chose the beryllium dimer as an example of such situations and in the following we describe and discuss all the test carried out to carefully check how the exact-exchange and correlation energy depends on the parameters mentioned before. It's understood that this kind of analysis has to be carried out for any system under

study.

As a starting estimation for the kinetic energy cut-off and supercell size we used the values of 30 Ry and 22 bohr respectively which has been verified to give well converged results for the PBE total energy (less than 1 meV). Keeping fixed the size of the simulation box we increased the cut-off up to 60 Ry and check the changes in all the different contributions to the total energy. While the RPA correlation energy change by less than 0.5 meV passing from 30 to 60 Ry, the exact-exchange and RPAx correlation energies are more sensitive and a cut-off of 40 Ry is needed to ensure the same degree of accuracy.

The dependence of the exact-exchange and RPA correlation energy of the Be dimer on the supercell size has been already carefully analyzed by Nguyen and de Gironcoli [58]. In their calculations the sampling of the RPA correlation energy on the first Brillouin zone was computed on a shifted mesh of $\mathbf{q}$ point since for $\mathbf{q} \to 0$ both the leading matrix elements of $\chi_0(\mathbf{q} \to 0)$ and v^{-1} goes to zero as $|\mathbf{q}|^2$ making the RPA eigenvalue problem (3.30) ill defined. Here we use a different strategy and compute the RPA and RPAx correlation energy for $\mathbf{q} = \mathbf{0}$ but using a modified coulomb interaction. The long range tail of the coulomb interaction in real space is truncated after a distance of the order of half of the supercell size making its Fourier transformation going to a finite values for $\mathbf{q} \to 0$ thus leading to a well defined problem even in this limit. The idea of using a modified coulomb interaction relies on the assumption that the truncation does not affect the properties of the system under study. The approximation becomes exact in the limit of infinite supercell meaning that a carefully check of the convergence with respect to the supercell size is needed. In Fig. 3.2 we report the result for the RPA and RPAx correlation energies of the Be dimer at equilibrium distance ($d = 2.45$ Å) as a function of the volume of the simulation box calculated within different approximations. Simply setting to zero the $|\mathbf{q} + \mathbf{G}| = 0$ component ($G_0 = 0$ in the figure), leads to a slowly convergent behavior for the correlation energies that eventually goes to a limiting value (extrapolated with a fit of the $G_0 = 0$ data) represented by the dashed black lines in Fig. 3.2. For the RPA correlation energy (top panel) we also report the result from a calculation with a shifted $\mathbf{q}$ mesh (in particular we setted $\mathbf{q} = (0, 0, 0.01)$) and notice that a much faster convergence toward the same limit of the $G_0 = 0$ calculation is obtained thus validating this strategy. We then tested two different modified Coulomb interactions implemented in the QUANTUM ESPRESSO distribution [84]. The first one, referred to as "Spherical cut" in the figure, is an abrupt truncation of the coulomb interaction for distances greater than half of the supercell size. In the second one, "WS cut", the coulomb interaction is unchanged inside the Wigner-Seitz cell and periodically repeated outside. Both these two approximation

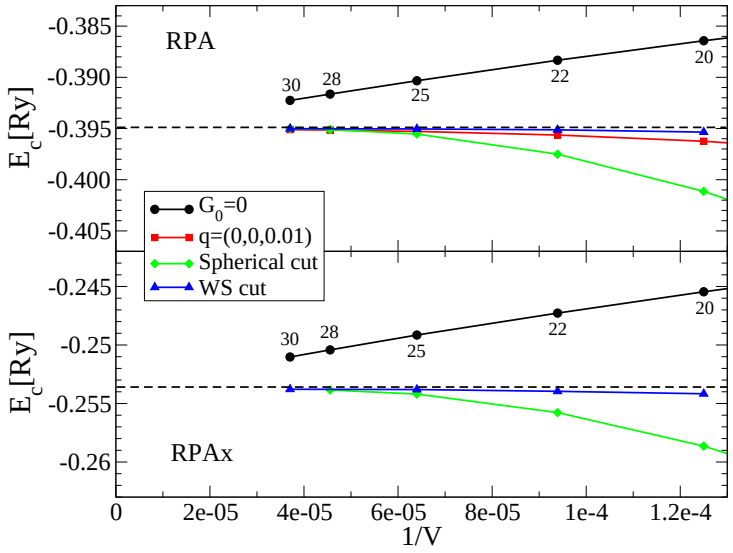

Figure 3.2: Convergence of the RPA (top panel) and RPAx (bottom panel) correlation energy E_c of the Be_2 molecule at an interatomic distance $d = 2.45$ Å , with respect to the size of the supercell. The numbers close to the black circles indicate the size in bohr of the cubic supercell. Different schemes for treating the $\mathbf{q} \to \mathbf{0}$ limit are compared. See text for details.

converge fast and to the correct limit increasing the simulation box volume. In particular the Wigner-Seitz truncation is the most effective and already for a supercell lattice size of 20 bohr gives very well converged results for both RPA and RPAx correlation energies.

The same analysis has been carried out for the exact-exchange energy and the result are shown in Fig. 3.3. The slow convergence of the exact-exchange energy with respect to the Brillouin zone sampling in a plane-wave implementation is a well known problem and originate from an integrable divergence in the expression for the exact-exchange energy. Using the scheme proposed by Gygi-Baldereschi (GB) [88], one adds and subtracts a reference term which has the same singularity and whose integral on the Brilloiun zone can be evaluated analytically. One is therefore left with the integral of a smooth function that can be evaluated numerically with standard sampling technique. Using the GB scheme one gets a convergence behavior (black circle in Fig. 3.3) that is proportional to the inverse of the simulation box volume and eventually goes to the infinite volume limit represented by the dashed black lines in Fig. 3.3. Nguyen and de Gironcoli [58, 59], argued that this error proportional to $1/V$ is due to a finite contribution for $\mathbf{q} = \mathbf{0}$ that cannot be computed numerically in $\mathbf{q} = 0$ since it's a $0/0$ limit. They proposed an extrapolation scheme that allows to efficiently estimate this contribution leading to a much faster convergence (brown square in Fig. 3.3) to the correct value.

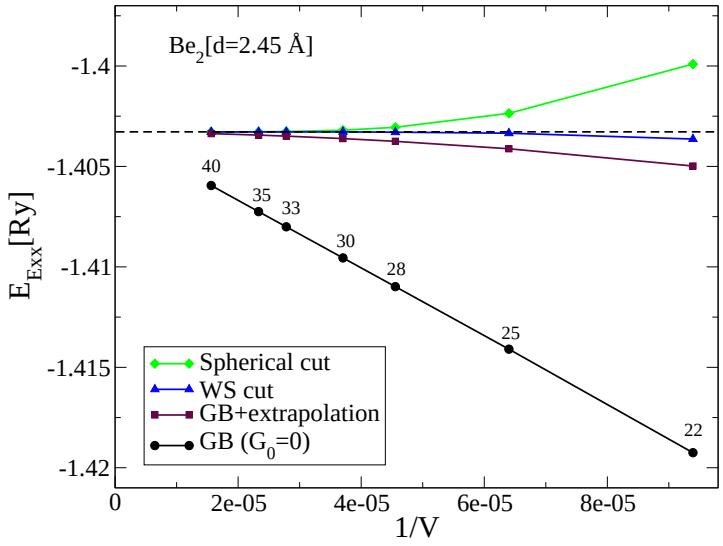

Figure 3.3: Convergence of exact-exchange energy E_x of the Be_2 molecule at an interatomic distance $d = 2.45$ Å , with respect to the size of the supercell. The numbers close to the black circles indicate the size in bohr of the cubic supercell. Different schemes for treating the integrable divergence in the exact-exchange expression are compared. See text for details.

Also in this case, both modified coulomb interactions recover the same limit and in particular the Wigner-Seitz renormalization gives converged results within few tenths of meV already for a supercell lattice size of $a = 25$ bohr.

We therefore expect that using the "Wigner-Seitz prescription" for the coulomb interaction truncation, together with a kinetic energy cut-off of 40 Ry and a supercell lattice size of 25 bohr is the best set-up for the Be_2 simulation and should give results within an error estimated to be of the order of 1 meV.

It's worth mentioning that using a modified coulomb interaction is an approximation that can be used for isolated system only, when a supercell approach is needed. For extended system, instead, using the GB approach plus the extrapolation scheme for the exact-exchange energy, and a shifted mesh of $\mathbf{q}$ point for the calculation of the RPA/RPAx correlation energies is probably the best strategy one can choose since it does not require the analytic evaluation of the ill-defined limit for $\mathbf{q} \to 0$ and still gives good results.

Finally the convergence with respect to the number of eigenvalues N_{eig} has also been checked. In Fig. 3.4 we report the RPA and RPAx correlation energy of the Be_2 molecule at equilibrium as a function of N_{eig} for two different values of the simulation box size. In all the cases the convergence is achieved with a relative small number of eigenvalues showing that

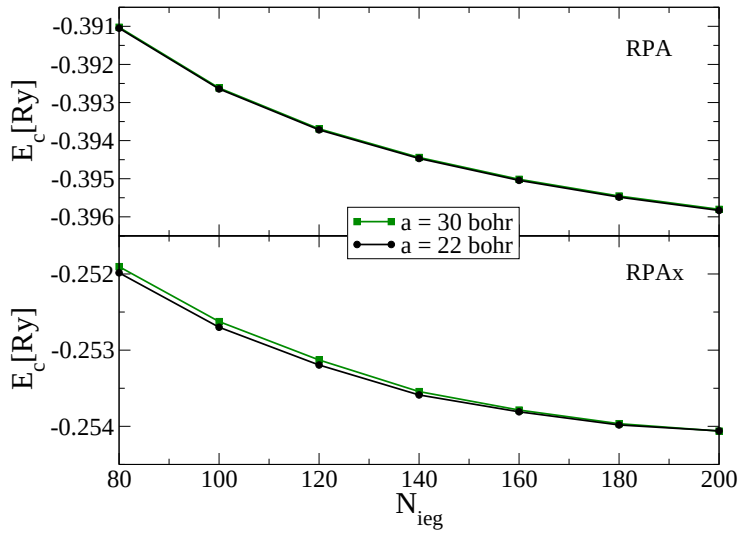

Figure 3.4: Convergence of RPA (top panel) and RPAx (bottom panel) correlation energy of the Be_2 molecule at an interatomic distance $d = 2.45$ Å bohr, with respect to the number of eigenvalues N_{eig}.

E_c is a rapidly converging function of N_{eig}; truncating the sum at $N_{eig} = 160$ already ensure a convergence within few meV for the absolute correlation energies and one could expect an even smaller error if energy differences are considered.

Chapter 4

Application to selected systems

In this Chapter we will assess the performance of the RPAx approximation in some test cases. We will first analyze in some detail the homogeneous electron gas computing the correlation energies and its spin magnetization dependence for different values of the density. We then move to realistic systems studying the dissociation curves of small molecules. We found that a sensible improvement in the total energy description is disturbed by a pathological behavior of the RPAx response function which ultimately leads to a break-down of the method. We propose here two simple modifications of the original RPAx approximation which are able to overcome its deficiency without compromising the overall accuracy of the approach.

4.1 The homogeneous electron gas

As a test of the accuracy of the RPAx approximation we choose the simple homogeneous electron gas. The homogeneous electron gas is an idealized system of electrons moving in a uniform neutralizing background. At zero temperature it is characterized by two parameters only, i.e. the number density $n = 1/(4\pi r_s^3 a_B^3/3)$, or equivalently the Wigner-Seitz radius r_s, and the spin polarization $\zeta = |n^\uparrow - n^\downarrow|/(n^\uparrow + n^\downarrow)$, where $n^{\uparrow(\downarrow)}$ is the density of spin up (down) electrons and $n = n^\uparrow + n^\downarrow$. Despite its simplicity, (i) the HEG model represents the first approximation to metals where the valence electrons are weakly bound to the ionic cores (see for instance Ref. [34]), (ii) the system is found to display a complex phase diagram including magnetic ordering and transition to the Wigner crystal [89] with lowering the density and in addition (iii) it provides the basic ingredient of any practical density functional calculation. As described in Sec. 2.2.4, the most widely used approximations for the unknown xc-energy functional are based on properties of the HEG.

For this model system the Hartree energy exactly cancel out the sum of the electron-background and background-background interaction; therefore the total energy per particle $\epsilon(r_s)$ (let us forget about the spin dependence for the moment) can be decomposed as

$$\epsilon(r_s) = t(r_s) + \epsilon_{xc}(r_s) \tag{4.1}$$

where $t(r_s)$ is the kinetic energy per particle of the non-interacting system and $\epsilon_{xc}(r_s)$ is the exchange and correlation energy per particle. By symmetry the KS potential must be constant and we can always take it to be zero; imposing periodic boundary condition on a cubic box of volume Ω, the single particle KS orbitals are then plane-waves, $|\mathbf{k}\rangle = \exp(i\mathbf{k}\cdot\mathbf{r})/\sqrt{\Omega}$, with wave-vector $\mathbf{k}$ and energy $\varepsilon_{\mathbf{k}} = \hbar^2k^2/(2m_e)$. The kinetic and exchange energy per particle can be exactly calculated [73] and are given by

$$\begin{aligned} t(r_s) &= \frac{3}{5}\frac{\hbar^2 k_F^2(r_s)}{2m_e} \\ \epsilon_x(r_s) &= -\frac{3}{4}\frac{e^2 k_F(r_s)}{\pi} \end{aligned} \tag{4.2}$$

where $k_F(r_s)$ is the Fermi wave-vector defined by $k_F(r_s) = (3\pi^2 n(r_s))^{1/3}$.

The generalization to the spin-polarized case for the kinetic and exchange energy is very simple since the up and down components of the gas contribute independently to the total energy. One can therefore define two Fermi wave-vectors $k_F^{\uparrow}$ and $k_F^{\downarrow}$ associated to the corresponding up and down densities and compute each spin component contribution to the kinetic and exchange energy simply replacing the k_F vector in Eq. (4.2) with its spin counterparts k_F^{σ} (with $\sigma = \uparrow, \downarrow$). It's then easy to show that

$$\begin{aligned} t(r_s,\zeta) &= t(r_s)\frac{(1+\zeta)^{5/3} + (1-\zeta)^{5/3}}{2} \\ \epsilon_x(r_s,\zeta) &= \epsilon_x(r_s)\frac{(1+\zeta)^{4/3} + (1-\zeta)^{4/3}}{2} \end{aligned} \tag{4.3}$$

The correlation energy ϵ_c is defined as the difference between the total energy of the system and the kinetic plus exchange contributions. In the limit for $r_s \to 0$ an asymptotic expansion for ϵ_c can be derived from the RPA correlation energy which is exact in the high density limit. In the opposite limit the Coulomb potential energy, decreasing like $1/r_s$, eventually becomes much greater that the average kinetic energy, meaning that, as a starting point, the kinetic contribution to the Hamiltonian of the system can be neglected. The ground state of this system is close to the equilibrium state of a system of N classical point charges distributed on a uniform background and it's believed to be crystalline. This hypothesis was first suggested by Wigner [89] and the state is now know as "Wigner crystal".

More insight on the phase diagram of the electron liquid has been achieved thanks to Quantum Monte Carlo (QMC) methods. The exact correlation energy of the paramagnetic phase as well as that of magnetic ordered phases and Wigner crystal (with different lattice) for a wide range of densities, has been calculated [39, 90]. Accurate parametrizations of these results [8, 38, 37] provide the basic ingredients used to construct LDA and GGA functionals for non-homogeneous electronic systems and will be used in the next section as a reference for our RPAx correlation energy calculations.

4.1.1 The RPAx correlation energy of the unpolarized HEG

While the solution of Dyson equation is demanding in general, it becomes trivial in the case of the HEG; the response functions and the kernels are all diagonal in momentum space and the RPAx Dyson equation can be easily solved as

$$\chi_\lambda^{RPAx}(q,iu) = \frac{\chi_0(q,iu)}{1-\lambda[v(q)+f_x(q,iu)]\chi_0(q,iu)} \tag{4.4}$$

where $v_c(q) = 4\pi e^2/q^2$ and $f_x(q,iu)$ is the exchange kernel at a given momentum and imaginary frequency. The RPAx correlation energy per electron ϵ_c^{RPAx} follows from the general expression in Eq. (2.44) where the interacting response function is approximated by χ_λ^{RPAx}, the trace is replaced by an integral over momentum $\mathbf{q}$[1] and the integration over λ is done analytically

$$\epsilon_c^{RPAx} = \frac{\hbar}{2\pi^2 n}\int_0^\infty q^2 dq \int_0^\infty du\; v_c(q)\chi_0(q,iu)\left[1+\frac{\ln[1-K(q,iu)]}{K(q,iu)}\right]. \tag{4.5}$$

Here $K(q,iu)$ has been defined as

$$K(q,iu) = [v(q)+f_x(q,iu)]\chi_0(q,iu) = v(q)\chi_0(q,iu) + \frac{h_x(q,iu)}{\chi_0(q,iu)} \tag{4.6}$$

While the Lindhard function $\chi_0(q,iu)$ at imaginary frequency iu is known exactly [73]

$$\chi_0(q,iu) = \frac{mk_F}{2(\hbar\pi)^2}\left\{-1+\frac{Q^2-\tilde{u}^2-1}{4Q}\ln\left[\frac{(1+Q)^2+\tilde{u}^2}{(1-Q)^2+\tilde{u}^2}\right] + \alpha\left[\arctan\left(\frac{1+Q}{\tilde{u}}\right)+\arctan\left(\frac{1-Q}{\tilde{u}}\right)\right]\right\} \tag{4.7}$$

[1] In the thermodynamic limit the discrete sum over the momenta $\mathbf{q}$ imposed by the periodic boundary condition, can be replaced by the integral

$$Tr = \sum_{\mathbf{q}} \to \frac{\Omega}{(2\pi)^3}\int d\mathbf{q}$$

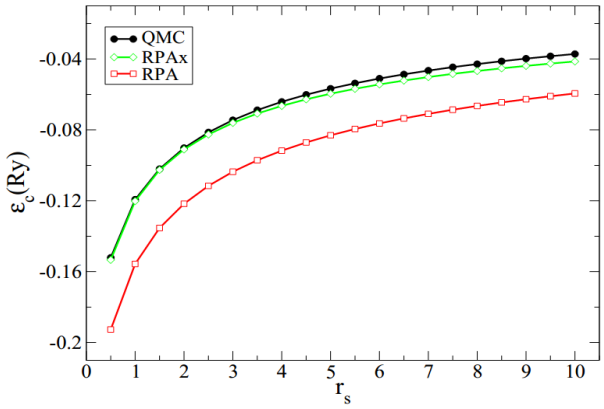

r_s	RPA	RPAx	QMC
0.5	-0.194	-0.154	-0.153
1.0	-0.157	-0.121	-0.119
2.0	-0.122	-0.092	-0.089
3.0	-0.105	-0.077	-0.074
5.0	-0.084	-0.060	-0.056
8.0	-0.068	-0.047	-0.043
10.0	-0.061	-0.042	-0.037
11.0	-0.058	--	-0.035

Figure 4.1: Correlation Energy per particle in the homogeneous electron gas as a function of the Wigner-Seitz radius evaluated with different kernels: RPA (red squares), RPAx (green diamonds) and QMC calculation (black circles).

with $Q = q/(2k_F)$ and $\tilde{u} = mu/(\hbar q k_F)$, the function $h_x(q, iu)$ can be directly derived from the general expression given in Eq. (3.25) replacing the generic single particle orbitals ϕ_a with the plane-waves $|\mathbf{k}\rangle$ and removing the generic perturbing potentials $\Delta^{\alpha,\beta}V$. After a straightforward manipulation $h_x(q, iu)$ can be rewritten as a six-fold integral over crystal momenta. Its static values was computed first numerically by several author [91, 92, 93] and later analytically by Engel and Vosko [94, 95].The frequency dependence of h_x has been calculated by Brosens, Lemmens and Devreese [96, 97] for real frequencies and by Richardson and Ashcroft [98] for imaginary frequencies. Following Brosens *et al.* four integrations can be done analytically using cylindrical coordinates; we used numerical quadrature for the two remaining integrations. Our numerical integration is able to recover the analytic results of Engel and Vosko [94, 95] in the limit $u \to 0$. Finally the integration over momentum q and imaginary frequency u in Eq. (4.5) has been computed numerically. The results are shown and listed in Fig. 4.1. RPA can be easily obtained from Eq. (4.5) and Eq. (4.6) with $h_x = 0$ and can be seen to seriously overestimate the correlation energy at all densities. Including the exact exchange kernel greatly improves over simple RPA and the RPAx correlation energy per particle is close to the accurate Quantum Monte Carlo (QMC) results [39].

As expected RPAx works well for small values of r_s with very good results for typical metallic density regime ($r_s = 3 - 6$) and becomes less accurate when r_s increases. According to our calculation, within RPAx for $r_s > 10.6$ there is a charge density instability with

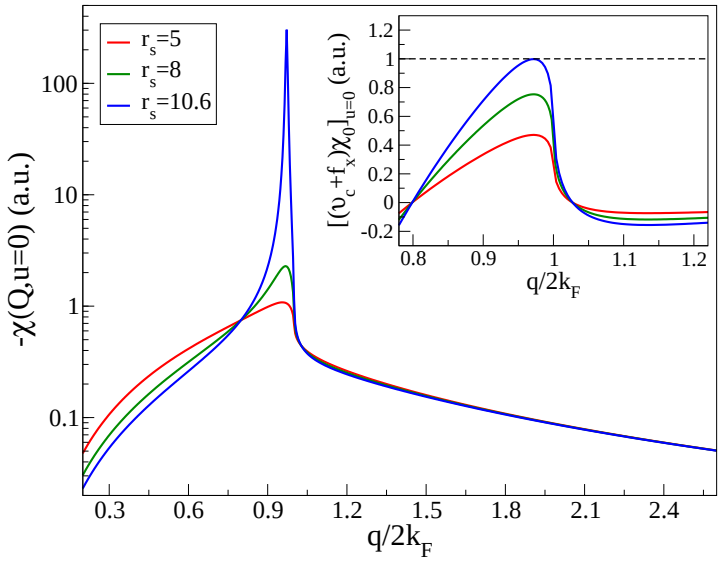

Figure 4.2: Critical behavior of the static density-density RPAx response function when the density decreases. For $r_s > 10.6$ the system becomes unstable respect to charge modulation with wavevector $\approx 2k_F$.

wave-vector $q \approx 2k_F$. In Fig. 4.2 the critical behavior of the static density-density RPAx response function is shown for the full interacting system (Eq. (4.4), $\lambda = 1$). When the density decreases a pronounced peak appears at $q \approx 2k_F$ indicating the instability with respect to charge modulations with this wave-vector. As can be seen from the inset in Fig. (4.2), for sufficient large values or r_s, $K = (v + f_x)\chi_0$ approaches unity and the denominator in Eq. (4.4) tends to vanish leading to the appearance of the peak. Beyond $r_s = 10.6$, K exceeds unity and RPAx approximation breaks down as the density-density response function χ_λ is not anymore negative definite.

This instability resembles the charge density wave instability, already observed at the Hartree-Fock level by Overhauser [99, 73] and is an artifact of the truncation of the kernel expansion to first order in the interacting strength. A full treatment of correlation in the QMC calculations moves the density instability toward the Wigner crystal to much smaller densities [39] corresponding to $r_s \approx 80$.

4.1.2 Alternative RPAx resummations

In Sect. 3.1 we have established a strategy for a systematic inclusion of higher order terms in the kernel expansion. However, because of the complexity of the procedure, before proceed-

ing along this way we propose here two simple modifications to the original RPAx approximation which are able to fix the instability problem and, at the same time, to give correlation energies on the same level of accuracy as RPAx.

We notice that i) the RPA response function is negative defined for any values of r_s and also that ii) the RPAx response function is exact up to first order in the coupling strength λ, meaning that the instability observed at the RPAx level must be due to the re-summation up to infinite order of the "bare" exact-exchange kernel contributions, that is without any correlation corrections. Therefore, in order to mitigate the instability problem, we can either include higher order contributions to the kernel (rigorous but expensive) or truncate the re-summation of the exact-exchange kernel (approximate but inexpensive) mimicking the effect of the missing correlation kernel as discussed below.

Introducing the irreducible polarizability P_λ, the Dyson equation Eq. (2.56) for the interacting response function χ_λ can be written as $\chi_\lambda = P_\lambda + \lambda P_\lambda v_c \chi_\lambda$, where the polarizability itself is the solution of the Dyson equation $P_\lambda = \chi_0 + \chi_0[\lambda f_x + f_c(\lambda)]P_\lambda$. Neglecting the unknown $f_c(\lambda)$ leads to the original RPAx approximation, while just truncating the power expansion of P_λ to first order in the coupling strength gives a new approximation, here named tRPAx, for the interacting response function:

$$\chi_\lambda^{tRPAx} = P_\lambda^{(1)} + \lambda P_\lambda^{(1)} v_c \chi_\lambda^{tRPAx} \tag{4.8}$$

with $P_\lambda^{(1)} = \chi_0 + \lambda \chi_0 f_x \chi_0$. A similar idea has also been proposed in Ref. [100] where the authors suggest to expand the full interacting response function χ_λ in a power series of the RPA response function (instead of the non-interacting one), and then to truncate this expansion to first order. This amounts to have an other approximation, here named t'RPAx, for the interacting response function:

$$\chi_\lambda^{t'RPAx} = \chi_\lambda^{\mathrm{RPA}} + \lambda \chi_\lambda^{\mathrm{RPA}} f_x \chi_\lambda^{\mathrm{RPA}} \tag{4.9}$$

We notice that the only quantity entering in the definitions of the tRPAx and t'RPAx response functions is $\chi_0 f_x \chi_0 = h_x$, which is nothing but the first-order exchange contribution to the response function χ_λ and does not require any explicite reference to f_x in order to be defined. While the Dyson-like equation for the original RPAx approximation requires a formal definition of the exchange kernel, the alternatives resummations only need h_x in order to be defined and therefore are simply based on standard many-body perturbation theory.

Up to first order these two alternative response functions coincide with the original RPAx one, while they have different power expansions starting from the λ^2 term, meaning that

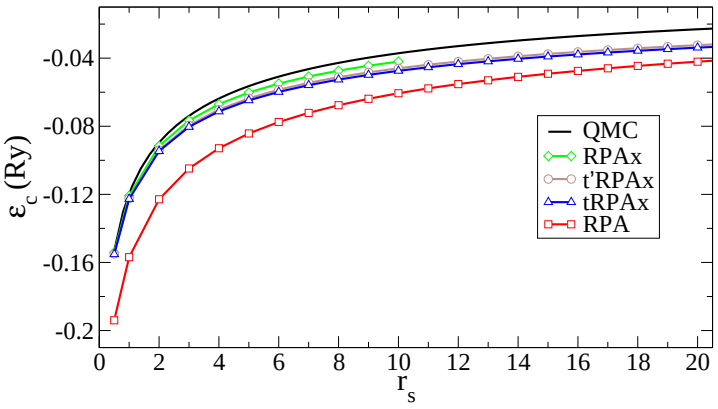

Figure 4.3: Correlation energies per particle as a function of r_s evaluated from the RPA, original and modified RPAx response functions and compared to accurate QMC calculations.

only contributions already approximated at the RPAx level are affected by these alternative re-summations. Moreover we notice that the tRPAx and t'RPAx response functions can be obtained from the TDDFT Dyson-like Eq. (2.56) setting $f_{xc}^{\lambda} = \lambda f_x/(1+\lambda\chi_0 f_x)$ and $f_{xc}^{\lambda} = \lambda f_x/(1+\lambda\chi_{\lambda}^{\mathrm{RPA}} f_x)$ respectively, explaining how the truncations mimic the correlation contributions that are missing at RPAx level.

Fig. 4.3 shows the correlation energies per particle obtained starting from the alternative RPAx approximations of the response function. As expected, for high density electron gases (small values of r_s) the correlation energies are essentially identical to the original one, since the underlying response functions are the same in the limit for $\lambda \to 0$. At the same time they are well behaved also where the original RPAx approximation breaks down.

In Fig. 4.4 we compare the corresponding static density response functions (calculated at full interaction strength $\lambda = 1$) with the exact one, obtained from QMC calculation [101], for a density corresponding to $r_s = 5$. The difference between RPA and QMC results reveals that exchange and correlation effects in the kernel are important already at this density; including the exact-exchange kernel (original RPAx) overcorrects the RPA deficiency, in particular between k_F and $2k_F$, while both the alternative RPAx approximations give a much better agreement with accurate QMC calculations. Thus despite the fact that the RPAx energy is better at this value of r_s the static response function is worse suggesting that the RPAx results are subjected to a cancellation of errors when integrated over the frequency. In addition the plots in Fig. 4.5 confirms the effectiveness of truncating the re-summations in fixing the instability problem. The static tRPAx and t'RPAx response functions (evaluated at full interaction $\lambda = 1$), plotted

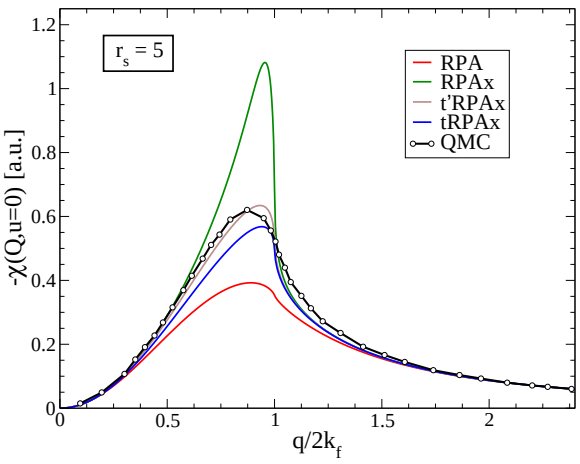

Figure 4.4: Comparison between all the approximate static response functions of the HEG at $r_s = 5$ with the exact response function from QMC [101] .

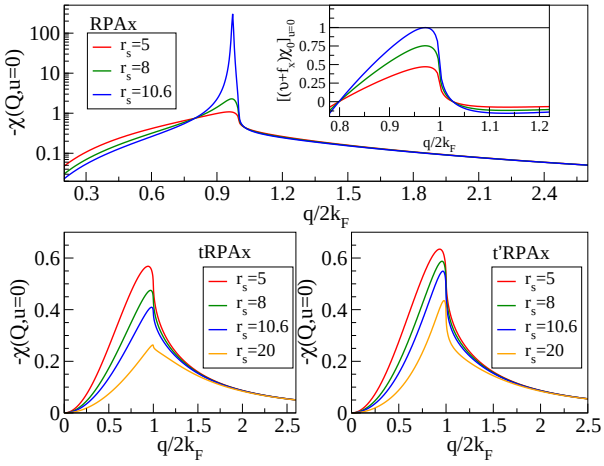

Figure 4.5: tRPAx and t′RPAx static response functions for different values of r_s. No critical behavior is found even in the low density regime.

in the lower panel of Fig. 4.5, do not show any critical behavior in the range of density analyzed (r_s up to 20); moreover when the density decreases a trend opposite to the one found for the RPAx response function is observed with a reduction (instead of the enhancement shown in the top panel of Fig. 4.5) of the height of the peak near $2k_F$, suggesting no divergence would appear even for smaller densities.

4.1.3 The RPAx correlation energy of the spin-polarized HEG

We continue our analysis of the HEG at the RPAx level by studying the spin magnetization dependence of the correlation energy of the system. We start noticing that for the non-interacting system the spin-up and spin-down components of the gas are independent so that a simple scaling relation between the non-interacting density-density response functions of the polarized and unpolarized gas can be derived:

$$\chi_0^{\uparrow\uparrow}[n^\uparrow] = \frac{1}{2}\chi_0[2n^\uparrow]$$
$$\chi_0^{\downarrow\downarrow}[n^\downarrow] = \frac{1}{2}\chi_0[2n^\downarrow] \tag{4.10}$$

while $\chi_0^{\uparrow\downarrow} = \chi_0^{\downarrow\uparrow} = 0$[2].

[2] These results can be derived from the fact that the kinetic energy functional of a arbitrarily spin-polarized system $T[n^\uparrow, n^\downarrow]$ can be written in terms of the kinetic energy functional of the spin-unpolarized system $T[n]$

The spin-up and spin-down components behave as independent constituents of the system at the exchange level too and a scaling relation similar to Eq (4.10) holds true also for the exchange energy [102] and, accordingly, for the exchange potential and kernel:

$$\begin{cases} v_x^{\uparrow}[n^{\uparrow}] = v_x[2n^{\uparrow}] \\ v_x^{\downarrow}[n^{\downarrow}] = v_x[2n^{\downarrow}] \end{cases} \qquad \begin{cases} f_x^{\uparrow\uparrow}[n^{\uparrow}] = 2f_x[2n^{\uparrow}] \\ f_x^{\downarrow\downarrow}[n^{\downarrow}] = 2f_x[2n^{\downarrow}] \end{cases} \tag{4.11}$$

while $f_x^{\uparrow\downarrow} = f_x^{\downarrow\uparrow} = 0$. Thus at the RPAx level the interaction between the spin-up and spin-down components of the system is only mediated by the Coulomb kernel v. Eq. (4.10) and (4.11) show that the non-interacting spin-dependent response function and the spin-dependent exchange kernel can be written in term of their spin-unpolarized counterparts already introduced and computed in the previous section.

We can now derive the generalization of the RPAx Dyson equation for the spin-polarized gas. Applying a spin-independent perturbing potential ΔV_0, the induced self-consistent field Δv_{KS}^{σ} is such that $\Delta n^{\sigma} = \sum_{\sigma'} \chi_0^{\sigma\sigma'} \Delta v_{KS}^{\sigma}$ and can be written as $\Delta v_{KS}^{\sigma} = \Delta V_0 + \Delta v_H + \Delta v_x^{\sigma} + \Delta v_c^{\sigma}$ where

$$\begin{aligned} \Delta v_H &= v(\Delta n^{\uparrow} + \Delta n^{\downarrow}) \\ \Delta v_x^{\sigma} &= f_x^{\sigma\sigma}[n^{\sigma}]\Delta n^{\sigma} \\ \Delta v_c^{\sigma} &= \sum_{\sigma'} f_c^{\sigma\sigma'}[n]\Delta n^{\sigma'} \end{aligned} \tag{4.12}$$

are the Hartree, exchange and correlation contributions to the induced KS potential Δv_{KS}^{σ}. At the RPAx level the correlation contribution is neglected and the density variations for the up and down component read

$$\begin{aligned} \Delta n^{\uparrow} &= \frac{1}{2}\chi_0(2n^{\uparrow}) \left[\Delta V_0 + v\Delta n + 2f_x[2n^{\uparrow}]\Delta n^{\uparrow}\right] \\ \Delta n^{\downarrow} &= \frac{1}{2}\chi_0(2n^{\downarrow}) \left[\Delta V_0 + v\Delta n + 2f_x[2n^{\downarrow}]\Delta n^{\downarrow}\right] \end{aligned} \tag{4.13}$$

where we have used Eq. (4.10) and (4.11). Solving for $\Delta n^{\uparrow}$ in the first and for $\Delta n^{\downarrow}$ in the second and then summing up the results we get

$$\begin{aligned} \Delta n = &\frac{1}{2}\left[\frac{\chi_0(2n^{\uparrow})}{1-\chi_0(2n^{\uparrow})f_x(2n^{\uparrow})} + \frac{\chi_0(2n^{\downarrow})}{1-\chi_0(2n^{\downarrow})f_x(2n^{\downarrow})}\right]\Delta V_0 \\ &+ \frac{1}{2}\left[\frac{\chi_0(2n^{\uparrow})}{1-\chi_0(2n^{\uparrow})f_x(2n^{\uparrow})} + \frac{\chi_0(2n^{\downarrow})}{1-\chi_0(2n^{\downarrow})f_x(2n^{\downarrow})}\right] v\Delta n. \end{aligned} \tag{4.14}$$

as [102]:

$$T[n^{\uparrow}, n^{\downarrow}] = \frac{1}{2}T[2n^{\uparrow}] + \frac{1}{2}T[2n^{\downarrow}].$$

Taking the functional derivative with respect to the external perturbation shows that the non-interacting response function is made up of the two separate contributions, given in Eq. (4.10).

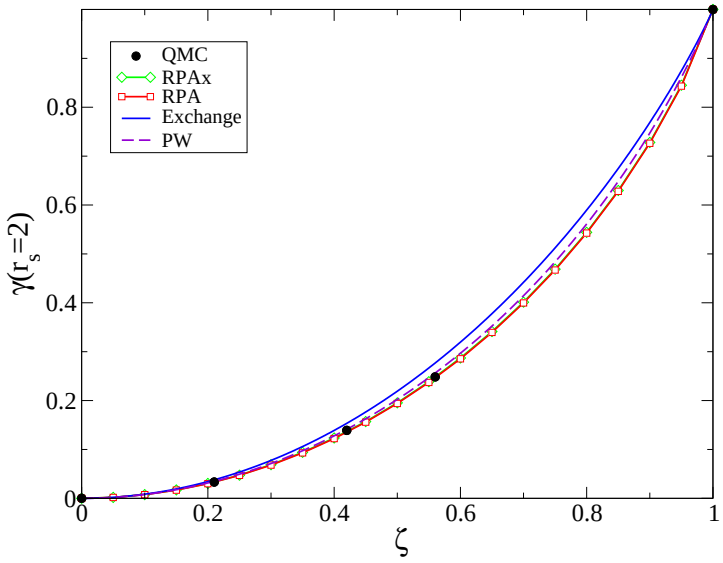

Figure 4.6: Spin polarization function γ for $r_s = 2$ from RPA (red squares), RPAX (green diamonds), Perdew-Zunger parametrization [8] (blue solid line), Perdew-Wang parametrization [38] (brown dashed line) and Quantum Monte Carlo calculation [90] (black circles).

Comparing this expression with the definition of the response function $\Delta n = \chi \Delta V_0$ and inserting the scaling factor λ, we obtain the final result

$$\chi_\lambda = \frac{\frac{1}{2}\left\{\left[\frac{\chi_0}{1-\lambda\chi_0 f_x}\right]_{2n^\uparrow} + \left[\frac{\chi_0}{1-\lambda\chi_0 f_x}\right]_{2n^\downarrow}\right\}}{1 - \frac{1}{2}\left[\frac{\lambda\chi_0 v}{1-\lambda\chi_0 f_x}\right]_{2n^\uparrow} - \frac{1}{2}\left[\frac{\lambda\chi_0 v}{1-\lambda\chi_0 f_x}\right]_{2n^\downarrow}} \tag{4.15}$$

where χ_0 and f_x are the same functions already used for the unpolarized case but evaluated at density $2n^\uparrow$ or $2n^\downarrow$.

Integrating the ACFD formula in Eq. (2.44) with the new definition of χ_λ in Eq. (4.15) and χ_0 in Eq. (4.10), gives the correlation energy per particle, ϵ_c, as a function of $n^\uparrow$ and $n^\downarrow$ or, equivalently, as a function of r_s and ζ. At the RPA level the dependence of the correlation energy on the spin magnetization has been already calculated long time ago by Von Barth and Hedin [103] and more recently by Vosko, Wilk, and Nusair [37]. Our RPA results, simply obtained by setting $f_x = 0$ in Eq. (4.15), are, within the numerical accuracy, in perfect agreement with both the above mentioned calculations. Fig. 4.6 shows the spin-polarization function γ defined as

$$\gamma(r_s, \zeta) = \frac{\epsilon_c(r_s, \zeta) - \epsilon_c(r_s, 0)}{\epsilon_c(r_s, 1) - \epsilon_c(r_s, 0)} \tag{4.16}$$

for the case $r_s = 2$ evaluated at the RPA and RPAx level, and compares it with the exchange-only dependence that is the one assumed in the Perdew-Zunger parametrization [8] of Spin

Local Density Approximation (LSDA) and with the Perdew-Wang parametrization [38], that is based on the more physically motivated spin-interpolation expression proposed by Vosko, Wilk, and Nusair [37]. While within RPAx the correlation energy significantly improves with respect to RPA results, there is essentially no difference between the RPA and RPAx spin-polarization functions. Calculations done with the alternative re-summations (tRPAx and t′RPAx) give essentially the same results as the original RPAx and are not shown in Fig. (4.6). Thus for this property of the system RPA and all the RPAx (original and alternative) approximations give results in very good agreement with accurate Quantum Monte Carlo calculations[90] performing much better than the Perdew-Zunger parametrization and slightly better than the more sophisticated Perdew-Wang parametrization.

4.1.4 Summary

We have tested the accuracy of the RPAx approximation on the homogeneous electron gas. RPAx correlation energies greatly improve RPA results and are in very good agreement with accurate QMC calculations. The spin magnetization dependency of the RPA and RPAx correlation energies has been calculated as well, showing a big improvement if compared to standard parametrizations and a nearly perfect agreement with QMC calculations.

These encouraging results are however disturbed by the break-down of the approximation for large values of r_s where the RPAx density-density response function unphysically changes sign thus indicating that correlation contributions to the kernel are needed to obtain accurate results for the HEG at low densities. Although combining higher order GLPT with the systematic approach proposed here could give access to the needed higher order contributions to the kernel, we have suggested two simpler and inexpensive modifications of the RPAx approximation which are able to mimic the missing correlation contributions leading to a good description of the correlation energy of the system even in the limit of small densities.

4.2 Dissociation of small molecules

As already pointed out in Section 2.2.4, one of the most serious problems of present KS methods is their inability to describe dispersion interaction between non overlapping molecular fragments, and weakly bound systems such as molecules about to break during a chemical reaction. Both these drawbacks are due to the intrinsic local or semi-local nature of these approximations which are obviously not able to give a correct description of systems with important long-ranged correlation effects. These limitations reflect in a wrong description of all

sparsely packed systems, ranging from the simple noble-gas dimers to bio-molecule and in a poor characterization of processes such as, for instance, adsorption on surfaces and chemical reactions.

Also system with a significant static correlation[3] are poorly described within LDA, GGAs and by hybrid functionals as well. This limitation leads, for instance, to a dramatic failure of standard KS method when studying the dissociation of open shell systems whose simplest and paradigmatic example is the stretched hydrogen molecule.

The poor performances of standard Density Functional Approximations (DFAs) in very simple systems, reflect those of much larger and complex systems. It's therefore of primary importance to understand the origin of these inadequacies and to develop functionals which are able to correctly describe simple physical situations before claiming them to be suitable for much complicated problems.

In particular in order to achieve a more complete description of chemistry, DFAs are asked to perform well for molecules beyond their equilibrium geometries and above all to correctly describe molecular dissociation, starting from that of very simple ones.

4.2.1 Van der Waals dimers

Although one of the weakest, dispersion (or van der Waals) interaction is of primary importance to an accurate understanding of, for instance, biological processes as well as adsorption on surfaces and chemical reactions. Dispersion forces originate from the response of an electron in one region to instantaneous charge-density fluctuations in another one. The leading contribution arises from dipole-induced dipole interaction and leads to an attractive energy with the well-known $-1/R^6$ decaying behavior with the interatomic separation R. Standard xc functionals only consider local properties in order to calculate the xc energy and cannot obviously describe these kinds of interactions. They give binding or repulsion only when there is an overlap of density charges of the individual components of the system, and since the overlap decay exponentially with the interatomic separation so does the binding energy too. In Fig. 4.7 this wrong behavior is shown for the Kr_2 molecule.

In order to recover the correct $-1/R^6$ decay at large interatomic separation, the simplest approach proposed was to add an extra energy term which accounts for the long-range attraction. Within these new method, usually called "DFT-D" (Density Functional Theory plus

[3] In terms of "hand-waving" arguments dynamic correlation is roughly associated to "simple" correlations due to Coulomb repulsion, while static correlation appears in situations where multiple determinants associated with degeneracy or near degeneracy are needed.

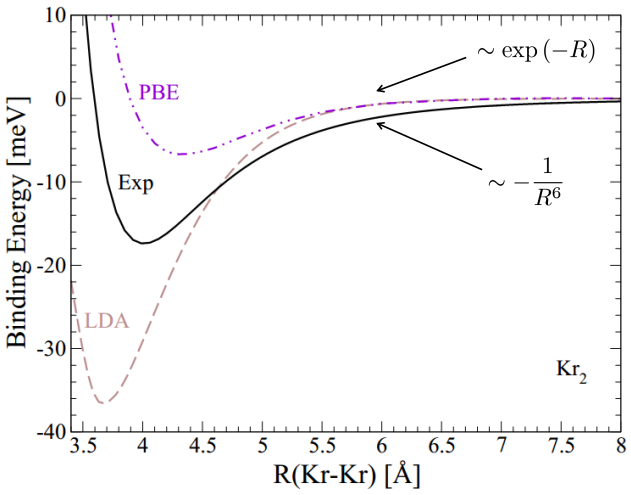

Figure 4.7: LDA and PBE binding energy for the Kripton dimer compared to an accurate model potential [104]. The $-1/R^6$ decay is not reproduced by standard functionals which instead give an exponential behavior originating from the overlap of the atomic charge densities.

Dispersion), the total energy reads

$$E_{tot} = E_{DFT} - \sum_{ij} \frac{C_6^{ij}}{R_{ij}^6} f_{damp}(R_{ij}) \tag{4.17}$$

where the sum in the dispersion term run over all pairs of atoms i and j, and a damping function f_{damp} has to be introduced in order to remove the short-range divergence of the extra energy term. The major question in the application of these methods is the origin of the C_6 coefficients. One possibility is to derive them from experimental information or calculate them using *ab-initio* method. Using an extended data-base for the C_6 coefficient and appropriate damping functions allows the application of the equation above to a large range of interesting chemical application. However the C_6 coefficient can vary considerably depending on the different chemical states of the atom and the influence of its environment and it's unclear how one should assign the chemical environment to apply the correct C_6 coefficient. Although some progres has been made in order to capture the environmental dependence of the C_6 coefficients [105, 106, 107, 108, 109], all the DFT-D methods required anyway, to a lesser or greater extent, predetermined input parameters.

Truly non-local and parameter-free functionals have been introduced in 1990s, but in their original formulation, they were restricted to non-overlapping fragments. New ideas by Lan-

greth *et al.* [13] removed this limitation renewing the community interest in the area of non-local correlation functionals and leading to a new class of functionals called vdW-DF [13, 15]. They are usually defined as an additional correction

$$E_c^{nl} = \int d\mathbf{r} \int d\mathbf{r}' \; n(\mathbf{r})\Phi(\mathbf{r},\mathbf{r}')n(\mathbf{r}'), \tag{4.18}$$

to the local or semilocal approximation $E_{xc}^{LDA/GGA}$ for exchange-correlation energy. In the general expression for E_c^{nl}, $n(\mathbf{r})$ is the electron density and the integral kernel $\Phi(\mathbf{r},\mathbf{r}')$ is derived starting from the exact ACFD formula (2.44) for the correlation energy followed by several approximations. For this reason it automatically recover the correct $O(|\mathbf{r}-\mathbf{r}'|^{-6})$ asymptotic behavior and therefore correctly describe long-range correlation interactions. The total exchange-correlation energy in this approach is then given by $E_{xc} = E_{xc}^{LDA/GGA} + E_c^{nl}$ with $E_{xc}^{LDA/GGA}$ taking into account for the exchange and short-range correlation effects. However it is a difficult task to find the best xc functional to go with the non-local piece; the interplay between the short-range part and the non-local one is still a matter of active research. While the long-range limit of these functionals is designed to recover exact expressions for weakly-interacting fragments, in the overlapping regime double-counting could produce sensible errors in the energy and reduce the predictive power of the total functional.

As already pointed out in Sec. 2.3 correlation energy functionals derived within the ACFD formalism are fully non-local and therefore include automatically and seamlessly dispersion interactions (see, for instance, Ref. [51] for a detailed proof). Moreover they perfectly combine with exact-exchange energy calculation thus removing the ambiguity, present in almost any other approach to van der Waals systems, in the choice of the combination of exchange, short-range correlation and non-local correlation contributions.

In order to assess the performace of the RPAx approximation for van der Waals system we computed the binding energy of two simple noble-gas dimers, i.e. the Ar_2 and Kr_2 molecules, and compare our results with,vdW-DF methods, well established RPA calculations and accurate model potential-energy-surfaces fitted on experimental data.

Noble-gas dimers have binding energies (BEs) of the order of tens of meV and represent an interesting testing case to investigate the accuracy of RPA and RPAx methods. Most of the RPA calculations for realistic system in general and for noble-gas in the specific case have been performed in a non self-consistent-field (non-scf) fashion, namely, exact-exchange and RPA correlation energies were computed using single particle orbitals obtained from a local or semi-local self-consistent DFT calculation. For convenience we will indicate these kinds of calculations as RPA@DFA, and similarly RPAx@DFA, specifying any time the density functional

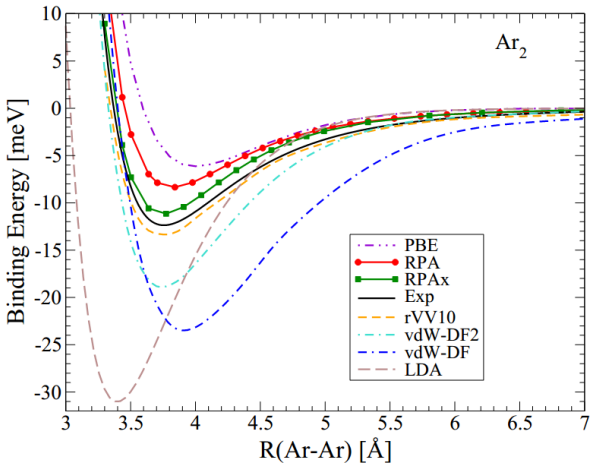

Ar_2	R_0(Å)	BE(meV)	ω(cm^{-1})
PBE	3.99	6.1	23.4
RPA	3.84	8.3	26.8
RPAx	3.75	11.1	30.8
rVV10	3.75	13.4	32.3
vdW-DF2	3.74	18.6	38.6
vdW-DF	3.91	23.4	34.1
LDA	3.39	31.0	58.3
Exp	**3.76**	**12.4**	**31.2**

Figure 4.8: Dissociation curve of Argon dimer obtained with different xc functionals. LDA (brown dashed line) and PBE (violet dashed-dotted line) functionals give very poor results. RPA@PBE(red circle) perform better than vdW-DF [13] (blue dashed-dotted line) and its revised version vdW-DF2 [15] (turquoise dotted-dashed line). RPAx@PBE further improve and gives results comparable to the the one obtained from the recent rVV10 [110] functional.

approximation (LDA, GGAs etc...) used to compute the input orbitals.

Only recently we [69] have performed for the first time a fully scf calculation for Ar_2 and Kr_2 at the RPA level revealing a close agreement between the scf-RPA and the RPA@PBE dissociation curves. This indicates that the PBE density is rather close to the scf-RPA density and thus justifies the use of this density in non-scf calculations instead of performing a full scf-RPA one. According to these finding and in absence of a scf-RPAx method, we performed our RPAx correlation energy calculation starting from well converged PBE orbitals.

The dimers and the corresponding isolated atoms have been simulated using a simple-cubic supercell with a size length $a = 25$ bohr. The electron ion interactions have been described by conventional norm-conserving pseudopotentials [35]; a kinetic energy cut-off of 80 Ry and 50 Ry for Ar and Kr, respectively, has been used. Finally we used up to 400 low-lying eigenvalues of $v\chi_0$ in order to calculate RPA correlation energy according to Eq. (3.31) and the corresponding 400 eigenvectors as a basis set for the solution of the RPAx problem (3.29). Extensive tests have been conducted to ensure that these parameters give well converged binding energy with errors estimated to be less than 1meV.

In Fig. 4.8 we report our results for the RPAx@PBE dissociation curve or Ar dimer (green squares) together with those of several DFA and compare with an accurate model potential

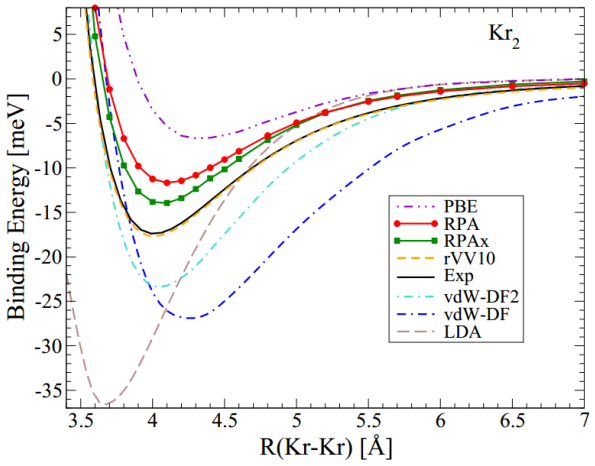

Kr_2	R_0(Å)	BE(meV)	ω(cm^{-1})
PBE	4.33	6.7	15.4
RPA	4.11	11.7	20.1
RPAx	4.06	14.0	22.8
rVV10	4.01	17.7	23.8
vdW-DF2	4.05	23.2	26.8
vdW-DF	4.24	27.0	22.6
LDA	3.67	36.6	39.8
Exp	**4.01**	**17.4**	**23.6**

Figure 4.9: Dissociation curve of Kripton dimer obtained with different xc functionals. See text an Fig. 4.8 for details.

fitted on experimental data [104] (black solid line). The RPAx and RPA binding energies have been calculated using well converged PBE orbitals as input while all the other density functional calculations are fully self-consistent.

As expected LDA and PBE (and GGAs in general) give very poor results predicting either too large or too small binding energies and equilibrium distances. The non-local vdW-DF functional proposed by Langreth *et al.* [13] and briefly described at the beginning of this section, overestimates binding energy and bond-length by about 90% and 4% respectively. Its revised version vdW-DF2 [15], although giving a better description of the whole dissociation curve, still greately overestimates the binding energy. Including the exact-exchange kernel leads to an overall improvement of the RPA performance. Compared to the binding energy (12.4 meV), bond-length (3.76 Å) and vibrational frequency (31.2 cm^{-1}) obtained from a model potential fitted to experimental data [104], our RPAx results of 11.1 meV, 3.75 Å and 30.8 cm^{-1} show an impressive agreement. The RPAx dissociation curve turns out to be as good as the newly developed vdW functional rVV10 [110] which is a a simple revision of the VV10 non-local density functional by Vydrov and Van Voorhis [111], specifically designed for molecular systems.

Similar results are also observed for Kripton dimer and reported in Fig. 4.9. Although comparison with dissociation energy curve obtained from an accurate model potential fitted to experimental data [104] shows that RPAx scheme underestimate the binding energy by about 20%, the structural properties at the RPAx level show an improvement if compared to

the RPA and vdW-DF counterparts; our RPAx results for the bond length and the vibrational frequency differ only by 1% and −3% from the experimental values, respectively, and compare better than RPA (3%, −15%), vdW-DF (6%, −5%) and vdW-DF2 (1%, 13%) bond lengths and vibrational frequencies. Only the rVV10 functional outshines the RPAx and gives result essentially identical to the experiments.

We end this section mentioning that the alternative RPAx re-summation proposed in the previous section give, for the cases of Ar_2 and Kr_2, essentially the same results as the original RPAx and are therefore not shown in Figs. 4.8 and 4.9.

4.2.2 Covalent dimers

Besides their inability to describe dispersion interaction, another limitation of standard DFA is their very poor performance in systems with a significant static correlation. This becomes particularly problematic for the dissociation of electron pair bonds in situations where multiple determinants associated with degeneracy or near degeneracy are needed. The simplest and paradigmatic example is the dissociation of the H_2 molecule. While around the equilibrium position standard DFAs gives reasonable results, the proper (singlet) KS ground state at large interatomic separations has too high total energy, as shown in Fig. 4.10. Hartree-Fock energies are too high both around the equilibrium position and at dissociation; GGAs improve the description of the whole dissociation curve but still give wrong total energies for the stretched molecule. Not surprisingly hybrid functional calculations (HSE [9, 112] in Fig 4.10), which admix HF exchange with explicit density xc functionals, lead to an intermediate behavior. A better agreement with the accurate potential energy curve can be achieved resorting to spin-polarized calculations (not shown in Fig. 4.10) which give good energies, however at the price of a qualitatively wrong spin-density. Beyond a certain bond-length, the spin-up and spin-down electron densities are no longer equal leading to a solution which is no more a singlet as it should. These limitations, illustrated for the paradigmatic case of the H_2 molecules, are intrinsic of standard local or semi-local DFAs and appears for any covalent bond breaking.

Also in this case, like for van der Waals systems, fully non-local functionals derived form the ACFD theory have been shown to be a promising way to overcome standard DFA deficiencies. The behavior of RPA for breaking covalent bonds was examined in its early day by Furche [20] who argued that most of the strong static correlation in the N_2 dimer at large interatomic distances can be recovered at the RPA level. Soon after Fuchs *et al.* [21] have shown that RPA is size-consistent and can correctly describe bond dissociation in H_2 without

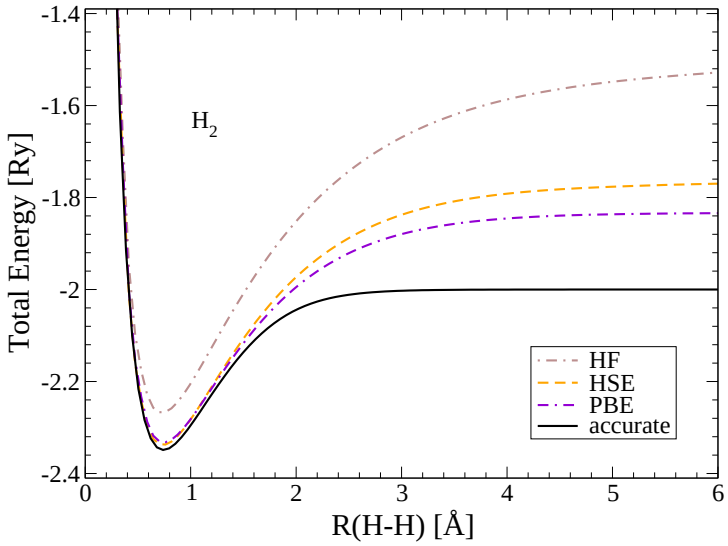

Figure 4.10: Dissociation curve of H_2 from PBE, HF and Hybrid-functional (HSE) spin-restricted calculations.

resorting to any artificial spin-symmetry breaking. However the RPA total energy is far too negative because of the well know overestimation of the correlation energy [55]; moreover an erroneous repulsion hump happears in the dissociation curve of covalent bonded systems at intermediate distances. Recently Heßelmann *et al.* [52] reported the H_2 dissociation curve within the RPAx approximation showing very good result for the total energy both around the equilibrium position R_0 and at dissociation but still the problem of the unphysical bump at intermediate bond-lengths remains. We are not aware of any dissociation curve for N_2 at the RPAx level.

Here we have assessed the performance of the RPAx, the original one and the alternative re-summations introduced in Section 4.1.2, for covalent bonded system beyond their equilibrium geometries studying the dissociation curves of H_2 and N_2. The dimers atoms have been simulated using a simple-cubic super cell with a size length $a = 22$ and $a = 25$ bohr, respectively. A kinetic energy cut-off of 50 Ry has been used for both systems and up to 200 lowest-lying eigenpairs of the generalized-eigenvalue problem in Eq. (3.9) has been used to compute the RPA and RPAx correlation energies. All the calculations have been done starting from well converged PBE orbitals.

In Figs. 4.11 we report our results for the dissociation curves of H_2 and the structural parameters extracted from it. Comparison with accurate calculations [113] illustrates the aforementioned deficiencies of PBE and RPA dissociation curves: standard DFAs give too high total

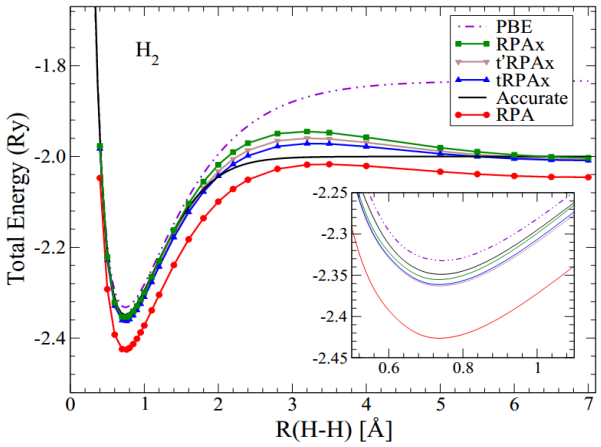

H_2	R_0(Å)	BE(eV)	ω(cm^{-1})
PBE	0.755	6.78	4219
RPA	0.740	4.85	4520
RPAx	0.738	4.41	4560
tRPAx	0.742	4.48	4506
t'RPAx	0.738	4.45	4406
Accurate	**0.741**	**4.75**	**4529**

Figure 4.11: Dissociation curve of H_2 from PBE, RPA and RPAx (original and alternative) spin-restricted calculations compared with accurate calculation [113].

energies in the dissociation limit while the simple RPA severely overestimates the correlation energy leading to a curve well below the reference one. Including the exact-exchange kernel leads to a sensible improvement in the total energy description; as can be seen from the inset in Fig. 4.11 the RPAx total energies around the equilibrium position is in very good agreement with accurate quantum chemistry calculations. The alternative re-summations while essentially giving the same energy as the original RPAx in the minimum region, have a positive effect on the dissociation curve at intermediate distances reducing the height of the repulsive hump. Finally we notice that at large interatomic separations all the RPAx approximation drops below the exact dissociation limit of 2 Ry in agreement with the analysis reported in Ref. [21].

With the simple H_2 example in mind we can turn to analyze the more interesting case of the N_2 molecule. In Fig. 4.12 we report our results for the dissociation curve and the structural parameters obtained from them. As already observed for the H dimer also in this case the whole RPA dissociation curve lies far below all the other curves. Nevertheless the structural parameters at the RPA level are in very good agreement with results from accurate quantum chemistry calculations [114]. Including the exact-exchange contribution to the kernel corrects for the RPA overestimation of the correlation energy shifting the RPAx dissociation curve upward. At the same time, the good performance for the equilibrium bond length and the vibrational frequency already obtained at the RPA level is maintained. However, unlike what happens for the H_2 molecule, in this case the original RPAx approximation breaks-down when

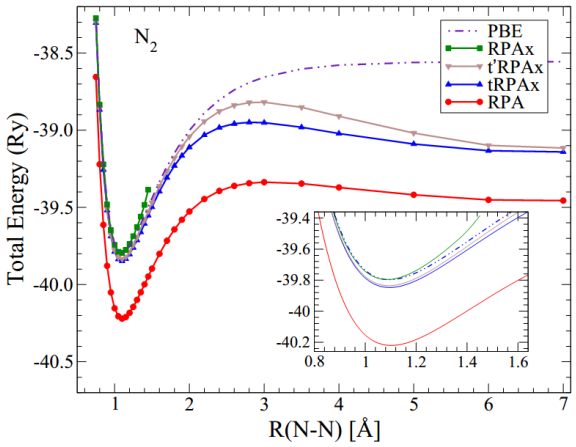

N_2	R_0(Å)	BE(eV)	ω(cm^{-1})
PBE	1.102	16.86	2274
RPA	1.100	9.92	2322
RPAx	1.085	--	2569
tRPAx	1.090	9.22	2430
t'RPAx	1.085	9.07	2482
Accurate	**1.095**	**9.91**	**2383**

Figure 4.12: Dissociation curve of N_2 from PBE, RPA and RPAx (original and alternative) spin-restricted calculations. The table shows structural parameter obtained from the curves compared with accurate calculation results [114].

the nitrogen atoms are separated. For bond lengths greater than $R = 1.45$Å the RPAx response function is no more negative-definite leading to an instability which is very similar to the one observed in the low-density homogeneous electron gas and, ultimately, causes the breakdown of the approximation. The alternative re-summations proposed to fix the pathological behavior of the RPAx response function in the HEG, turn out to be effective also in this very different situation. The tRPAx and t'RPAx dissociation curves are close to the RPAx one in the equilibrium region (see the inset in Fig. 4.12) but they are well-behaved also for bond lengths greater that $R = 1.45$Å overcoming, also in this case, what appears to be an intrinsic inadequacy of the original RPAx approximation.

4.2.3 The beryllium dimer

As an interesting example of a mixed covalent-vdW system we studied the challenging case of beryllium dimer. Be_2 represents a more complex situation in which both long-range van der Waals interaction and static correlation play an important role. Several theoretical investigations have been devoted to this simple molecule using different *ab initio* methods ranging from standard DFT calculations with local or semi-local functionals, which predict bond lengths rather close to the experimental value but E_b about 500% too large (see, e.g., Ref. [16]), to quantum Monte Carlo (QMC) techniques [115, 116], to high accuracy quantum chemistry methods such as the second-order Møller-Plesset perturbation theory [117], the couple-cluster

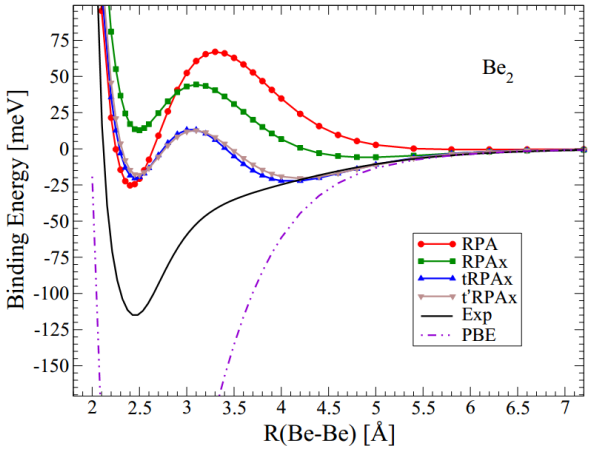

Be_2	R_0(Å)	BE(meV)	ω(cm^{-1})
PBE	2.456	399.4	336
RPA	2.405	25.1	293
RPAx	2.493	-13.1	221
tRPAx	2.460	20.0	231
t'RPAx	2.470	18.8	239
Exp	**2.454**	**115.3**	**276**

Figure 4.13: Dissociation curve of Be_2 from PBE, RPA and RPAx (original and alternative) spin-restricted calculations. The table shows structural parameter obtained from the cureves compared with experimental results [119].

approach [117] and the configuration interaction (CI) method [118]. In addition, the study of dissociation energy curve and structure of Be dimer using RPA technique has also been carried out [16, 19, 58, 69]. Although nscf-RPA can predict R_0 and ω_0 in rather good agreement with experiment, E_b is severely underestimated. Moreover in Ref. [19] the presence of an unphysical maximum in the nscf-RPA dissociation curve was found and the whole curve was shown to be very sensitive to the input orbitals used. The authors suggested the full self-consistent treatment of the RPA density and potential as a possible solution for the hump puzzle. Recently Nguyen *et al.* [69] have performed such a calculation for this systems and pointed out that the scf treatment is indeed important and significantly lower the total energy of the system, yet it is not enough to fix the unphysical maximum problem and even leads to the metastability of the Be dimer since the energy at the minimum of the potential energy surface is higher than the one at the dissociation limit. These finding, as already pointed out in the original work, indicate a real limitation of the RPA that call for the inclusion of correlation contributions beyond the simple Coulomb kernel.

In Fig. 4.13 we report our results for the binding energy curve of Be_2 and structural parameters from standard PBE, RPA and RPAx calculations and compare them with an accurate model potential-energy-surface fitted on experimental data [119]. The dimer and the corresponding isolated atom have been simulated using a simple-cubic super cell with a size length $a = 25$ bohr and a kinetic energy cut-off of 40 Ry. Up to 200 lowest-lying eigenpairs

of the generalized-eigenvalue problem in Eq. (3.9) have been used to compute the RPA and RPAx correlation energies. All the RPA and RPAx calculations have been performed starting from well converged PBE orbitals.

The PBE calculation predicts a bond length rather close to the experimental value but too large a binding energy (400% overestimate). At the RPA level the dissociation curve exhibit an unphysical hump for intermediate values of the bond length very similar to the one observed for covalent bonded systems. The RPA severely underestimate the binding energy but still gives equilibrium bond length and vibrational frequency in good agreement with experimental data. Passing from RPA to RPAx leads to a worse description of the dissociation curve near the equilibrium position and even to the metastability of the Be dimer. However we notice that in the dissociation region the RPAx curve approaches the experimental potential energy surface faster than the RPA one. The results obtained from the alternative resummations tRPAx and t′RPAx, recover the RPA performance near the minimum, reduce the height of the hump for intermediate values of the bond length and approach the correct asymptotic behavior of the Be-Be interaction potential much faster then all the other DFA.

Compared to the previous results for the dissociation curve of covalent bond and vdW systems, not surprisingly Be_2 shows similarity with both. In the range of intermediate interatomic separation, where the bond is expected to be mostly covalent in nature, an hump similar to the one observed for the H_2 and N_2 molecules appears in the dissociation curve. In the dissociation region instead, where the vdW interaction between the atoms becomes important, RPAx approximations and in particular the alternative resummation give results in very good agreement with experimental data, illustrating the effectiveness of ACFD-derived functional in describing long-range interactions.

Given the sensitivity of the results on the input orbital already reported in literature [19] we decided to investigate this issue. Although we do not have an scf RPAx method we can still indirectly infer how a fully self-consistent treatment of the density and potential would modify the dissociation curve by performing calculations similar to the one reported before but starting with different input densities. Therefore we repeated the dissociation curve calculations starting from LDA, exact-exchange (EXX) and RPA orbitals. While for the former a standard DFT calculation is needed, EXX and RPA orbitals have been determined using the efficient OEP approach recently implemented by Nguyen *et al.* [69, 70] in a developper version of QUANTUM ESPRESSO. In Fig. 4.14 we report our results. Each panel of the figure shows the potential energy surface of the Be dimer calculated within different total energy scheme: RPA (top left panel), RPAx (top right panel) tRPAx (bottom left panel) and t′RPAx (bottom

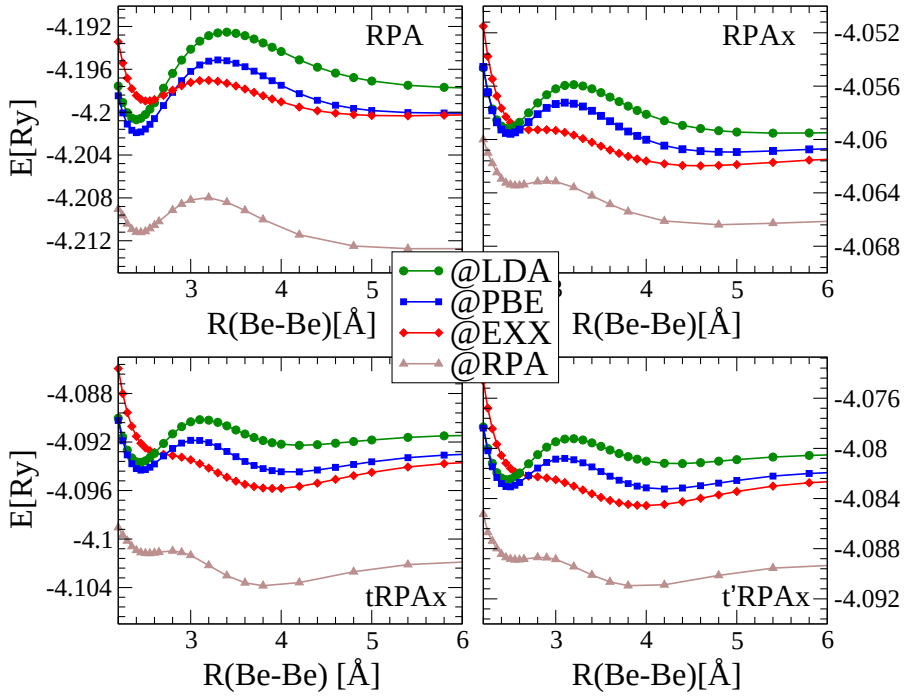

Figure 4.14: Total energies of Be_2 within different schemes: RPA (top left panel), RPAx (top right panel) tRPAx (bottom left panel) and t'RPAx (bottom right panel). Different colors correspond to different input densities: LDA (green), PBE (blue), EXX(red) RPA (brown).

right panel). In each panel the results obtained using different input orbitals are represented with different colors. The plots clearly indicate that a scf treatment could significantly lowers the total energy of the system since using the RPA orbitals as input shifts the whole curves downwards by about $\sim$ 100 meV which is a significant change if compared to the binding energy of this system.

Further the dissociation curves change also qualitatively using different input densities. In particular using EXX and RPA orbitals, instead of PBE ones, leads to a much pronounced metastable behavior as can be seen from the binding energy plots in Fig. 4.15. For the RPA calculations, reported in the top left panel of Fig. 4.14 and Fig. 4.15, it can be seen that the energy gain obtained passing from non scf densities to the scf RPA one is higher at large interatomic separation than near the equilibrium position, leading to the metastability of the dimer. This seems to be an intrinsic limitation of the RPA itself that calls for the inclusion of correlation contributions beyond the simple Coulomb kernel. However, despite some improvements in the description of the molecule in its stretched geometry, the RPAx approximations (original and alternative) does not seem to be sufficiently accurate for the challenging case of Be dimer.

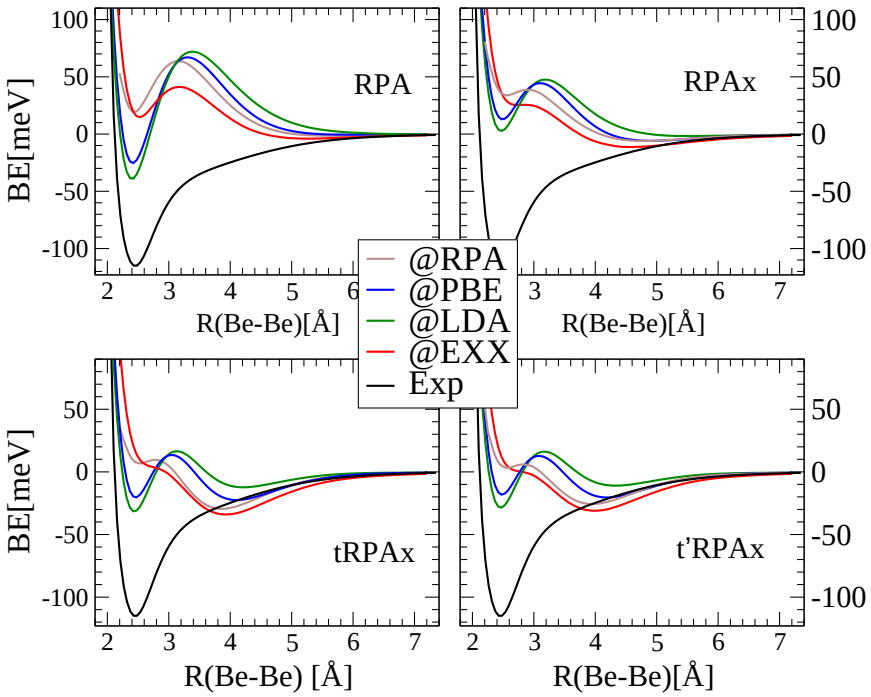

Figure 4.15: Binding energies of Be_2 within different schemes: RPA (left top panel), RPAx (right top panel) tRPAx (left bottom panel) and t′RPAx (right bottom panel). Different colors correspond to different input densities: LDA (green), PBE (blue), EXX(red) RPA (brown). An accurate model potential-energy-surface fitted on experimental data [119] (black) is also shown.

Nevertheless the fact that for large interatomic distances the binding energy obtained starting from different densities are close one to each others and to the experimental data, may indicate that in this region the density is close to the real one and a self consistent calculation at the RPAx level would not change much the results. Instead near the equilibrium position we could expect much bigger changes given the strong dependence of the results on the input orbitals in this region. Therefore, before a final conclusion can be drown for the RPAx approximation in the delicate case of Be dimer, a fully self-consistent calculation is certainly needed.

4.2.4 Summary

We have assessed the performance of the RPAx approximation and its modifications tRPAx and t′RPAx for purely van der Waal, covalent and mixed van der Waals covalent systems. The binding energy and structural properties of Ar and Kr dimers computed at the RPAx

level (the original and alternative re-summations perform identically in these cases) improve compared to standard DFAs and RPA results. The study of covalent molecules dissociation within the RPAx approximation, reveal the same virtues and vices already observed in the HEG case. A sensible improvement of the total energy description is however disturbed by a pathological behavior of the response function. The alternative re-summations, tRPAx and t'RPAx, proposed here, have been shown to be simple and inexpensive modifications to the original one and able to fix RPAx inadequacy without compromising its virtues. For the challenging case of Be_2 dimer, although not improving upon RPA in the equilibrium region the alternative RPAx re-summations have been shown to give results in perfect agreement with the experiments for the molecule in its stretched geometry.

Chapter 5

Conclusion

In this work we described a general and systematic scheme aiming at computing increasingly accurate correlation energy in the ACFD framework. It is based on a many-body perturbative approach along the adiabatic connection path that allows to practically define an expansion for the exchange-correlation kernel of TDDFT in the coupling strength tuning the electron-electron interaction. Within this general scheme the simple RPA is an "incomplete" approximation. If the exact-exchange kernel is correctly taken into account one obtains a consistent description to first order in the interaction strength and recover the so called RPAx approximation for the correlation energy for which a novel and efficient implementation has been proposed. It is based on an eigenvalue decomposition of the time-dependent response function of the many body system in the limit of vanishing coupling constant, efficiently evaluated resorting to the linear response technique of DFPT. We verified that a relative small number of its eigenvalues and eigenvectors are sufficient to obtain an accurate representation of the RPAx response function and, ultimately, well converged results for the RPAx correlation energy. The additional workload needed in order to pass from RPA correlation energies calculations to their exact-exchange corrected counterparts is limited and accounted for by a small multiplicative prefactor in front of the RPA computational cost. Technical details of the method as implemented in the plane-wave pseudopotential approach were discussed at some level.

The accuracy of the RPAx approximation has been first tested on the homogeneous electron gas revealing a great improvement over RPA results and a very good agreement with accurate QMC calculations. The well-known overestimation of the correlation energy at the RPA level is indeed almost completely corrected by including the exact-exchange contribution

to the kernel. The spin magnetization dependency of the RPA and RPAx correlation energies has been calculated as well, showing a big improvement if compared to standard parametrizations and a perfect agreement with QMC calculation. These encouraging results are however disturbed by the break-down of the procedure for values of $r_s \gtrsim 10$ where the RPAx density-density response function unphysically changes sign. In this density regime the full treatment of the contributions coming from the exchange kernel, induces the observed instability and would require large correlation contributions to compensate for it and move the density instability toward the Wigner crystal to much smaller densities of the order of $r_s \approx 80$ [39]. Staying within an exact first order approximation to the particle-hole interaction we have suggested two simple and inexpensive modifications of the RPAx approximation which lead to a good description of the correlation energy of the system even in the limit of small densities. The rationale of the proposed approximate resummations is indeed to prevent the instability at low density by removing the higher order contributions from the exchange kernel, and therefore the need for compensating higher-order correlation ones, keeping the expansion accurate at high density.

As a second and more stringent test for the RPAx approximation, we investigated the dissociation of simple molecules. Indeed one of the most serious problems of present KS methods is their inability to describe dispersion interaction between non overlapping molecular fragments, and weakly bound systems such as molecules about to break during a chemical reaction. Already at their lowest level of approximation, i.e. RPA methods, ACFD-derived functionals have been shown to be a promising way to overcome these deficiencies. However also the RPA and its modifications are not without limitations. We found that including the exact-exchange contribution to the kernel leads to an improvement of the binding energies and structural properties of noble gas dimers. We reported a sensible improvement of the total energy description within the RPAx approximation also for H_2 and N_2 molecule. However examining the dissociation of N_2, we discovered the same virtues and vices already observed in the HEG case. The good description of the total energy is disturbed by a pathological behavior of the response function which thus appears to be an intrinsic features of the RPAx itself and ultimately poses doubts on the broad applicability of this approximation. Also in this very different situation the alternative re-summations, tRPAx and t'RPAx, have been shown to be able to fix the RPAx inadequacy without compromising its virtues and thus emerge as promising and stable alternatives to the original RPAx approximation. We believe the success of these two alternative resummation in overcoming the limitations of the original RPAx approximations lies in a reduction of the strength of the contributions coming from the

exact-exchange kernel and thus indicates a proper renormalization of the exchange terms as a possible route to follow.

Beside the improvements obtained taking into account the exchange contribution to the kernel, some questions are still open. The hump problem already observed at RPA level for covalent bonded system is still not solved and deserves further investigation. The extensive calculations on the Be dimer indicate that correlation effects in the kernel may play a major role for this very delicate system. However we can not completely rule out a possible role of a fully self-consistent treatment at the RPAx level.

In conclusion, a general and systematic scheme for the calculation of increasingly accurate correlation energies in the ACFDT has been formally introduced and practically applied to first order. Our efficient implementation for the calculation of RPAx correlation energies has been presented and used to study selected systems representative of well know drawbacks of standard density functional approximations. We found that the inclusion of the exact-exchange contribution to the kernel plays a crucial role for a correct and accurate description of the total energy of an electronic system without compromising the achievements of the original RPA functional. An intrinsic pathological behavior of the RPAx response function, not reported before, has been successfully treated by introducing two inexpensive modifications of the original RPAx Dyson-like equation. Staying within an exact first order approximation to the many-body response function, these slight redefinitions of RPAx fix the instability in total energy calculations without compromising the overall accuracy of the approach.

Appendix A

EXX-kernel

We give here the detailed derivation of Eq. (3.25). For convinience we rewrite here the starting point of our derivation, i.e. Eq. (3.24):

$$\begin{aligned} h^{\alpha\beta}_{Hx} = &+ \langle \delta\Phi_0 | \Delta^\alpha V^* | \Delta^\beta \Phi_0^{(+)} + \Delta^\beta \Phi_0^{(-)} \rangle + \langle \Delta^\alpha \Phi_0^{(-)} + \Delta^\alpha \Phi_0^{(+)} | \Delta^\beta V | \delta\Phi_0 \rangle \\ &+ \langle \Delta^\alpha \Phi_0^{(+)} | \delta V | \Delta^\beta \Phi_0^{(-)} \rangle + \langle \Delta^\alpha \Phi_0^{(-)} | \delta V | \Delta^\beta \Phi_0^{(+)} \rangle. \\ &- \left[\langle \Delta^\alpha \Phi_0^{(+)} | \Delta^\beta \Phi_0^{(-)} \rangle + \langle \Delta^\alpha \Phi_0^{(-)} | \Delta^\beta \Phi_0^{(+)} \rangle \right] \langle \Phi_0 | \delta V | \Phi_0 \rangle \end{aligned} \tag{A.1}$$

This equation can be recast in a more symmetric form explicitely separating the ground state contribution to $|\Delta\Phi_0^{(\pm)}\rangle$:

$$|\Delta\Phi_0^{(\pm)}\rangle = |\widetilde{\Delta}\Phi_0^{(\pm)}\rangle + |\Phi_0\rangle \frac{\langle \Phi_0 | \Delta V | \Phi_0 \rangle}{\pm iu} = |\widetilde{\Delta}\Phi_0^{(\pm)}\rangle + |\Phi_0\rangle \frac{\langle \Delta V \rangle}{\pm iu}. \tag{A.2}$$

Replacing into Eq. (A.1) and considering that $\langle \Phi_0 | \widetilde{\Delta}\Phi_0^{(\pm)} \rangle = 0$ we get

$$\begin{aligned} h^{\alpha\beta}_{Hx} = &+ \langle \delta\Phi_0 | \Delta^\alpha V^* | \widetilde{\Delta}^\beta \Phi_0^{(+)} + \widetilde{\Delta}^\beta \Phi_0^{(-)} \rangle + \langle \widetilde{\Delta}^\alpha \Phi_0^{(-)} + \widetilde{\Delta}^\alpha \Phi_0^{(+)} | \Delta^\beta V | \delta\Phi_0 \rangle \\ &- \frac{\langle \Delta^\alpha V^* \rangle}{iu} \left[\langle \Phi_0 | \delta V | \widetilde{\Delta}^\beta \Phi_0^{(-)} \rangle - \langle \Phi_0 | \delta V | \widetilde{\Delta}^\beta \Phi_0^{(+)} \rangle \right] \\ &- \left[\langle \widetilde{\Delta}^\alpha \Phi_0^{(+)} | \delta V | \Phi_0 \rangle - \langle \widetilde{\Delta}^\alpha \Phi_0^{(-)} | \delta V | \Phi_0 \rangle) \right] \frac{\langle \Delta^\beta V \rangle}{iu} \\ &+ \langle \widetilde{\Delta}^\alpha \Phi_0^{(+)} | \delta V | \widetilde{\Delta}^\beta \Phi_0^{(-)} \rangle + \langle \widetilde{\Delta}^\alpha \Phi_0^{(-)} | \delta V | \widetilde{\Delta}^\beta \Phi_0^{(+)} \rangle. \\ &- \left[\langle \widetilde{\Delta}^\alpha \Phi_0^{(+)} | \widetilde{\Delta}^\beta \Phi_0^{(-)} \rangle + \langle \widetilde{\Delta}^\alpha \Phi_0^{(-)} | \widetilde{\Delta}^\beta \Phi_0^{(+)} \rangle \right] \langle \Phi_0 | \delta V | \Phi_0 \rangle. \end{aligned} \tag{A.3}$$

Multipying the h.c. of Eq (3.16) on the right by $|\delta\Phi_0\rangle$ and Eq. (3.20) on the left by $\langle\widetilde{\Delta}\Phi_0^{(\pm)}|$, the following identities can be easily derived

$$\begin{aligned}\langle\widetilde{\Delta}\Phi_0^{(\pm)}|H_0 - E_0|\delta\Phi_0\rangle &= -\langle\widetilde{\Delta}\Phi_0^{(\pm)}|\delta V|\Phi_0\rangle \\ \langle\widetilde{\Delta}\Phi_0^{(\pm)}|H_0 - E_0|\delta\Phi_0\rangle &= -\langle\Phi_0|\Delta V^*|\delta\Phi_0\rangle \mp iu\langle\widetilde{\Delta}\Phi_0^{(\pm)}|\delta\Phi_0\rangle\end{aligned} \tag{A.4}$$

where again we have splitted $|\Delta\Phi_0^{(\pm)}\rangle$ according to Eq. (A.2) and we have exploited the fact that $\langle\Phi_0|\widetilde{\Delta}\Phi_0^{(\pm)}\rangle = 0$. Comparing these identities leads to

$$\langle\widetilde{\Delta}\Phi_0^{(\pm)}|\delta V|\Phi_0\rangle = \langle\Phi_0|\Delta V^*|\delta\Phi_0\rangle \pm iu\langle\widetilde{\Delta}\Phi_0^{(\pm)}|\delta\Phi_0\rangle. \tag{A.5}$$

A similar expression can be derived for $\langle\Phi_0|\delta V|\widetilde{\Delta}\Phi_0^{(\pm)}\rangle$ in the same way. Replacing into Eq. (A.3) we find a symmetric expression for $h_{Hx}^{\alpha\beta}$:

$$\begin{aligned}h_{Hx}^{\alpha\beta} = &+ \langle\delta\Phi_0|\Delta^\alpha V^*|\widetilde{\Delta}^\beta\Phi_0^{(+)} + \widetilde{\Delta}^\beta\Phi_0^{(-)}\rangle + \langle\widetilde{\Delta}^\alpha\Phi_0^{(-)} + \widetilde{\Delta}^\alpha\Phi_0^{(+)}|\Delta^\beta V|\delta\Phi_0\rangle \\ &- \langle\Delta^\alpha V^*\rangle\langle\delta\Phi_0|\widetilde{\Delta}^\beta\Phi_0^{(-)} + \widetilde{\Delta}^\beta\Phi_0^{(+)}\rangle - \langle\widetilde{\Delta}^\alpha\Phi_0^{(-)} + \widetilde{\Delta}^\alpha\Phi_0^{(+)}|\delta\Phi_0\rangle\langle\Delta^\beta V\rangle \\ &+ \langle\widetilde{\Delta}^\alpha\Phi_0^{(+)}|\delta V|\widetilde{\Delta}^\beta\Phi_0^{(-)}\rangle + \langle\widetilde{\Delta}^\alpha\Phi_0^{(-)}|\delta V|\widetilde{\Delta}^\beta\Phi_0^{(+)}\rangle. \\ &- \left[\langle\widetilde{\Delta}^\alpha\Phi_0^{(+)}|\widetilde{\Delta}^\beta\Phi_0^{(-)}\rangle + \langle\widetilde{\Delta}^\alpha\Phi_0^{(-)}|\widetilde{\Delta}^\beta\Phi_0^{(+)}\rangle\right]\langle\Phi_0|\delta V|\Phi_0\rangle\end{aligned} \tag{A.6}$$

We can now turn to the expression of the many-body wave-functions in terms of single particle KS orbitals $|\phi_i\rangle$. In the following the subscripts a, b, c will refer to occupied states, the subscripts s, t, u to unoccupied states and the subscripts k, l, m, n to both occupied and unoccupied states. In second quantization the single particle perturbation $\Delta V = \sum_i \Delta V(\mathbf{r}_i)$ can be written as

$$\Delta V = \sum_{kl}\langle k|\Delta V|l\rangle c_k^\dagger c_l \qquad \text{with} \qquad \langle k|\Delta V|l\rangle = \int d\mathbf{r}\, \phi_k^*(\mathbf{r})\Delta V(\mathbf{r})\phi_l(\mathbf{r}). \tag{A.7}$$

where $c_i^\dagger$ and c_i are the fermion creation and annihilation operators for the single-particle KS orbital $|\phi_i\rangle$. Since ΔV is a one-body operator the perturbed wave-functions $|\widetilde{\Delta}\Phi_0^{(\pm)}\rangle$ only have contributions from single exitations (we destroy a particle in the occupied state "a" and create a particle in the empty state "t") and precisely are

$$\boxed{|\widetilde{\Delta}\Phi_0^{(\pm)}\rangle = \sum_{atkl}|c_t^\dagger c_a\rangle\frac{\langle k|\Delta V|l\rangle}{\varepsilon_{at}\pm iu}\langle c_a^\dagger c_t c_k^\dagger c_l\rangle = +\sum_{atkl}|c_t^\dagger c_a\rangle\frac{\langle k|\Delta V|l\rangle}{\varepsilon_{at}\pm iu}\delta_{al}\delta_{tk} = +\sum_{at}|c_t^\dagger c_a\rangle\frac{\langle t|\Delta V|a\rangle}{\varepsilon_{at}\pm iu}}} \tag{A.8}$$

where $|c_t^\dagger c_a\rangle$ is a short notation for $c_t^\dagger c_a|\Phi_0\rangle$ and $\langle\dots\rangle$ is the average over the ground-state $|\Phi_0\rangle$ that can be easily computed using the Wick's theorem (see for instance Ref. [120] or Ref. [73]).

The variation $\delta\Phi_0$ is instead determined by the static perturbation

$$\begin{aligned}
\delta V &= \sum_{klmn} \frac{\langle kl|W|mn\rangle}{2} c_k^\dagger c_l^\dagger c_m c_n + \sum_{kl} \langle k| - v_H - v_x|l\rangle c_k^\dagger c_l \\
\langle kl|W|mn\rangle &= \int d\mathbf{r} \int d\mathbf{r}'\ \phi_k^*(\mathbf{r})\phi_l^*(\mathbf{r}')W(|\mathbf{r}-\mathbf{r}'|)\phi_m(\mathbf{r}')\phi_n(\mathbf{r}) \\
\langle k| - v_H - v_x|l\rangle &= \int d\mathbf{r}\ \phi_k^*(\mathbf{r})[-v_H(\mathbf{r}) - v_x(\mathbf{r})]\phi_l(\mathbf{r})
\end{aligned} \tag{A.9}$$

which has both a two-body and a one-body part. Correspondingly $|\delta\Phi_0\rangle$ has a single-exitations contribution $|\delta\Phi_0^S\rangle$ and a double-exitations contribution $|\delta\Phi_0^D\rangle$. While the latter is only determined by the Coulomb interaction W, the former has contribution both from W and the one-body operator $-v_H - v_x$:

$$|\delta\Phi_0^S\rangle = \sum_{atklmn} |c_t^\dagger c_a\rangle \frac{1}{\varepsilon_{at}} \frac{\langle kl|W|mn\rangle}{2} \langle c_a^\dagger c_t c_k^\dagger c_l^\dagger c_m c_n\rangle + \sum_{atkl} |c_t^\dagger c_a\rangle \frac{1}{\varepsilon_{at}} \langle k| - v_H - v_x|l\rangle \langle c_a^\dagger c_t c_k^\dagger c_l\rangle \tag{A.10}$$

If we compute all the contractions and exploit the symmetry of the Coulomb interaction when $\mathbf{r} \leftrightarrow \mathbf{r}'$ we find

$$\begin{aligned}
\sum_{atklmn} |c_t^\dagger c_a\rangle \frac{1}{\varepsilon_{at}} \frac{\langle kl|W|mn\rangle}{2} \langle c_a^\dagger c_t c_k^\dagger c_l^\dagger c_m c_n\rangle &= +\sum_{atc} |c_t^\dagger c_a\rangle \frac{1}{\varepsilon_{at}} \langle ct|W|ac\rangle - \sum_{atc} |c_t^\dagger c_a\rangle \frac{1}{\varepsilon_{at}} \langle tc|W|ac\rangle \\
&= +\sum_{at} |c_t^\dagger c_a\rangle \frac{\langle t|v_H + V_x|a\rangle}{\varepsilon_{at}} \\
\sum_{atkl} |c_t^\dagger c_a\rangle \frac{1}{\varepsilon_{at}} \langle k| - v_H - v_x|l\rangle \langle c_a^\dagger c_t c_k^\dagger c_l\rangle &= +\sum_{at} |c_t^\dagger c_a\rangle \frac{\langle t| - v_H - v_x|a\rangle}{\varepsilon_{at}}
\end{aligned} \tag{A.11}$$

The sum of these two contribution gives the single-exitations variation $|\delta\Phi_0^S\rangle$:

$$|\delta\Phi_0^S\rangle = +\sum_{at} |c_t^\dagger c_a\rangle \frac{\langle t|V_x - v_x|a\rangle}{\varepsilon_{at}}. \tag{A.12}$$

The double-exitations contribution is instead given by

$$\begin{aligned}
|\delta\Phi_0^D\rangle &= \sum_{a<bs<t} \sum_{klmn} |c_t^\dagger c_s^\dagger c_b c_a\rangle \frac{1}{\varepsilon_{at} + \varepsilon_{bs}} \frac{\langle kl|W|mn\rangle}{2} \langle c_a^\dagger c_b^\dagger c_s c_t c_k^\dagger c_l^\dagger c_m c_n\rangle \\
&= \sum_{a<bs<t} |c_t^\dagger c_s^\dagger c_b c_a\rangle \frac{1}{\varepsilon_{at} + \varepsilon_{bs}} \langle st|W|ab\rangle - \sum_{a<bs<t} |c_t^\dagger c_s^\dagger c_b c_a\rangle \frac{1}{\varepsilon_{at} + \varepsilon_{bs}} \langle st|W|ba\rangle \\
&= \sum_{abst} |c_t^\dagger c_s^\dagger c_b c_a\rangle \frac{1}{\varepsilon_{at} + \varepsilon_{bs}} \frac{\langle st|W|ab\rangle - \langle st|W|ba\rangle}{4}
\end{aligned} \tag{A.13}$$

where the restriction on the sum is needed to correctly identify a Fock state of indistinguishable particle thus avoiding any double counting of equivalent[1] states. At the end the restric-

[1] Here "equivalent states" means states that differ only by a phase factor.

tion can be relaxed multiplying by a factor $1/4$. Summing up the single and double contribution we get the perturbed wave-function

$$\boxed{|\delta\Phi_0\rangle = |\delta\Phi_0^S\rangle + |\delta\Phi_0^D\rangle = \sum_{at} |c_t^\dagger c_a\rangle \frac{\langle t|V_x - v_x|a\rangle}{\varepsilon_{at}} + \sum_{abst} |c_t^\dagger c_s^\dagger c_b c_a\rangle \frac{\langle st|W|ab\rangle - \langle st|W|ba\rangle}{4(\varepsilon_{at}+\varepsilon_{bs})}.} \tag{A.14}$$

We have now all the ingredients ($\Delta\Phi_0^{(\pm)}$, $\delta\Phi_0$, $\delta V = W - v_H - v_x$) we need in order to express Eq. (A.6) in term of single-particle wave-functions. Let us start with the third and forth lines in Eq. (A.6).

Evaluation of $\left[\langle\widetilde{\Delta}^\alpha\Phi_0^{(-)}|\delta V|\widetilde{\Delta}^\beta\Phi_0^{(+)}\rangle - \langle\widetilde{\Delta}^\alpha\Phi_0^{(-)}|\widetilde{\Delta}^\beta\Phi_0^{(+)}\rangle\langle\Phi_0|\delta V|\Phi_0\rangle\right]$.

The static perturbation δV is made up of a 2-body, i.e. W, and a 1-body, i.e. $-v_H - v_x$, operators. The contribution form the latter is as follows

$$\begin{aligned}
\langle\widetilde{\Delta}^\alpha\Phi_0^{(-)}| - v_H - v_x|\widetilde{\Delta}^\beta\Phi_0^{(+)}\rangle &= \sum_{atbskl} \frac{\langle a|\Delta^\alpha V^*|t\rangle}{\varepsilon_{at}+iu}\langle k| - V_H - v_x|l\rangle\frac{\langle s|\Delta^\beta V|b\rangle}{\varepsilon_{bs}+iu}\langle c_a^\dagger c_t c_k^\dagger c_l c_s^\dagger c_b\rangle \\
&= -\sum_{ab}\left[\sum_t \frac{\langle a|\Delta^\alpha V^*|t\rangle}{\varepsilon_{at}+iu}\langle t|\right]\left[\sum_s |s\rangle\frac{\langle s|\Delta^\beta V|b\rangle}{\varepsilon_{bs}+iu}\right]\langle b| - v_H - v_x|a\rangle \\
&\quad + \sum_a\left[\sum_t \frac{\langle a|\Delta^\alpha V^*|t\rangle}{\varepsilon_{at}+iu}\langle t|\right][-v_H - v_x]\left[\sum_s |s\rangle\frac{\langle s|\Delta^\beta V|b\rangle}{\varepsilon_{bs}+iu}\right] \\
&\quad + \sum_a\left[\sum_t \frac{\langle a|\Delta^\alpha V^*|t\rangle}{\varepsilon_{at}-iu}\langle t|\right]\left[\sum_s |s\rangle\frac{\langle s|\Delta^\beta V|b\rangle}{\varepsilon_{bs}+iu}\right]\sum_k\langle k| - v_H - v_x|k\rangle
\end{aligned}$$

$$\begin{aligned}
\langle\widetilde{\Delta}^\alpha\Phi_0^{(-)}|\widetilde{\Delta}^\beta\Phi_0^{(+)}\rangle &= \sum_{atbs}\frac{\langle a|\Delta^\alpha V^*|t\rangle}{\varepsilon_{at}+iu}\frac{\langle s|\Delta^\beta V|b\rangle}{\varepsilon_{bs}+iu}\langle c_a^\dagger c_t c_s^\dagger c_b\rangle \\
&= \sum_a\left[\sum_t\frac{\langle a|\Delta^\alpha V^*|t\rangle}{\varepsilon_{at}+iu}\langle t|\right]\left[\sum_s|s\rangle\frac{\langle s|\Delta^\beta V|b\rangle}{\varepsilon_{bs}+iu}\right]
\end{aligned}$$

$$\langle\Phi_0| - v_H - v_x|\Phi_0\rangle = \sum_{kl}\langle k| - v_H - v_x|l\rangle\langle c_k^\dagger c_l\rangle = \sum_k\langle k| - v_H - v_x|k\rangle. \tag{A.15}$$

where again we have evaluated all the contractions and used a resolution of the identity as needed. Notice that the term $\langle\widetilde{\Delta}^\alpha\Phi_0^{(-)}|\widetilde{\Delta}^\beta\Phi_0^{(+)}\rangle\langle\Phi_0| - v_h - v_x|\Phi_0\rangle$ excatly cancel out the last contribution of $\langle\widetilde{\Delta}^\alpha\Phi_0^{(-)}| - v_H - v_x|\widetilde{\Delta}^\beta\Phi_0^{(+)}\rangle$. For the sake of clearness in the expressions above we have highlighted in the square brackets the (conduction-band projected) variations of oc-

cupied KS orbital which are the given by the solutions of the following linear problems

$$|\Delta\phi_a^{(\pm)}\rangle = \sum_t |t\rangle \frac{\langle t|\Delta V|a\rangle}{\varepsilon_{at} \pm iu} \quad \Leftrightarrow \quad [H_{KS} + \gamma P_v - (\varepsilon_a \pm iu)]|\Delta\phi_a^{(\pm)}\rangle = -(1-P_v)\Delta V|\phi_a\rangle. \tag{A.16}$$

Sustituting the definitions above in Eq. (A.15) and putting all the pieces together, we get the final result for the 1-body contribution to $\left[\langle\widetilde{\Delta}^\alpha\Phi_0^{(-)}|\delta V|\widetilde{\Delta}^\beta\Phi_0^{(+)}\rangle - \langle\widetilde{\Delta}^\alpha\Phi_0^{(-)}|\widetilde{\Delta}^\beta\Phi_0^{(+)}\rangle\langle\Phi_0|\delta V|\Phi_0\rangle\right]$

$$\text{1-Body} = \sum_{ab}\langle\Delta^\alpha\phi_a^{(-)}|\Delta^\beta\phi_b^{(+)}\rangle\langle\phi_b|v_H + v_x|\phi_a\rangle - \langle\Delta^\alpha\phi_a^{(-)}|v_H + v_x|\Delta^\beta\phi_b^{(+)}\rangle \tag{A.17}$$

The term deriving from the 2-body contribution (W) to the perturbation δV is instead

$$\begin{aligned}
\langle\widetilde{\Delta}^\alpha\Phi_0^{(-)}|W|\widetilde{\Delta}^\beta\Phi_0^{(+)}\rangle &= \sum_{atbsklmn}\frac{\langle a|\Delta V|t\rangle}{\varepsilon_{at}+iu}\frac{\langle kl|W|mn\rangle}{2}\frac{\langle s|\Delta V|b\rangle}{\varepsilon_{bs}+iu}\langle c_a^\dagger c_t c_k^\dagger c_l^\dagger c_m c_n c_s^\dagger c_b\rangle \\
&= -\sum_{abst}\frac{\langle a|\Delta^\alpha V^*|t\rangle}{\varepsilon_{at}+iu}\langle bt|W|sa\rangle\frac{\langle s|\Delta^\beta V|b\rangle}{\varepsilon_{bs}+iu} + \sum_{abst}\frac{\langle a|\Delta^\alpha V^*|t\rangle}{\varepsilon_{at}+iu}\langle bt|W|as\rangle\frac{\langle s|\Delta^\beta V|b\rangle}{\varepsilon_{bs}+iu} \\
&\quad -\sum_{abtk}\frac{\langle a|\Delta^\alpha V^*|t\rangle}{\varepsilon_{at}+iu}\langle bk|W|ka\rangle\frac{\langle t|\Delta^\beta V|b\rangle}{\varepsilon_{bt}+iu} + \sum_{abtk}\frac{\langle a|\Delta^\alpha V^*|t\rangle}{\varepsilon_{at}+iu}\langle bk|W|ak\rangle\frac{\langle t|\Delta^\beta V|b\rangle}{\varepsilon_{bt}+iu} \\
&\quad -\sum_{astk}\frac{\langle a|\Delta^\alpha V^*|t\rangle}{\varepsilon_{at}+iu}\langle tk|W|sk\rangle\frac{\langle s|\Delta^\beta V|a\rangle}{\varepsilon_{as}+iu} + \sum_{astk}\frac{\langle a|\Delta^\alpha V^*|t\rangle}{\varepsilon_{at}+iu}\langle tk|W|ks\rangle\frac{\langle s|\Delta^\beta V|a\rangle}{\varepsilon_{as}+iu} \\
&\quad -\sum_{atkl}\frac{\langle a|\Delta^\alpha V^*|t\rangle}{\varepsilon_{at}+iu}\frac{\langle kl|W|kl\rangle}{2}\frac{\langle t|\Delta^\beta V|a\rangle}{\varepsilon_{at}+iu} + \sum_{atkl}\frac{\langle a|\Delta^\alpha V^*|t\rangle}{\varepsilon_{at}+iu}\frac{\langle kl|W|lk\rangle}{2}\frac{\langle t|\Delta^\beta V|a\rangle}{\varepsilon_{at}+iu} \\
&= -\sum_{ab}\langle\phi_b\Delta^\alpha\phi_a^{(-)}|W|\Delta^\beta\phi_b^{(+)}\phi_a\rangle + \sum_{ab}\langle\phi_b\Delta^\alpha\phi_a^{(-)}|W|\phi_a\Delta^\beta\phi_b^{(+)}\rangle \\
&\quad -\sum_{ab}\langle\Delta^\alpha\phi_a^{(-)}|\Delta^\beta\phi_b^{(+)}\rangle\langle\phi_b|v_H + V_x|\phi_a\rangle + \sum_a\langle\Delta^\alpha\phi_a^{(-)}|v_H + V_x|\Delta^\beta\phi_a^{(+)}\rangle \\
&\quad +\sum_a\langle\Delta^\alpha\phi_a^{(-)}|\Delta^\beta\phi_a^{(+)}\rangle(E_H + E_x).
\end{aligned}$$

$$\langle\widetilde{\Delta}^\alpha\Phi_0^{(-)}|\widetilde{\Delta}^\beta\Phi_0^{(+)}\rangle = \sum_{atbs}\frac{\langle a|\Delta^\alpha V^*|t\rangle}{\varepsilon_{at}+iu}\frac{\langle s|\Delta^\beta V|b\rangle}{\varepsilon_{bs}+iu}\langle c_a^\dagger c_t c_s^\dagger c_b\rangle = \sum_a\langle\Delta^\alpha\phi_a^{(-)}|\Delta^\beta\phi_a^{(+)}\rangle.$$

$$\langle\Phi_0|W|\Phi_0\rangle = \sum_{klmn}\frac{\langle kl|W|mn\rangle}{2}\langle c_k^\dagger c_l^\dagger c_m c_n\rangle = -\sum_{kl}\frac{\langle kl|W|kl\rangle}{2} + \sum_{kl}\frac{\langle kl|W|lk\rangle}{2} = E_H + E_x. \tag{A.18}$$

Summing up all the three terms we get for the 2-body contribution

$$\begin{aligned}
\text{2-Body} &= -\sum_{ab}\langle\phi_b\Delta^\alpha\phi_a^{(-)}|W|\Delta^\beta\phi_b^{(+)}\phi_a\rangle + \sum_{ab}\langle\phi_b\Delta^\alpha\phi_a^{(-)}|W|\phi_a\Delta^\beta\phi_b^{(+)}\rangle \\
&\quad -\sum_{ab}\langle\Delta^\alpha\phi_a^{(-)}|\Delta^\beta\phi_b^{(+)}\rangle\langle\phi_b|v_H + V_x|\phi_a\rangle + \sum_a\langle\Delta^\alpha\phi_a^{(-)}|v_H + V_x|\Delta^\beta\phi_a^{(+)}\rangle.
\end{aligned} \tag{A.19}$$

After summing the 1- and 2-body contribution we get the final result:

$$\begin{aligned}\langle\widetilde{\Delta}^{\alpha}\Phi_0^{(-)}|\delta V|\widetilde{\Delta}^{\beta}\Phi_0^{(+)}\rangle - \langle\widetilde{\Delta}^{\alpha}\Phi_0^{(-)}|\widetilde{\Delta}^{\beta}\Phi_0^{(+)}\rangle\langle\Phi_0|\delta V|\Phi_0\rangle = \\ = \sum_{ab}\langle\phi_b\Delta^{\alpha}\phi_a^{(-)}|W|\phi_a\Delta^{\beta}\phi_b^{(+)}\rangle - \sum_{ab}\langle\phi_b\Delta^{\alpha}\phi_a^{(-)}|W|\Delta^{\beta}\phi_b^{(+)}\phi_a\rangle \\ \sum_{a}\langle\Delta^{\alpha}\phi_a^{(-)}|V_x - v_x|\Delta^{\beta}\phi_a^{(+)}\rangle. - \sum_{ab}\langle\Delta^{\alpha}\phi_a^{(-)}|\Delta^{\beta}\phi_b^{(+)}\rangle\langle\phi_b|V_x - v_x|\phi_a\rangle.\end{aligned} \tag{A.20}$$

the expression for $\langle\widetilde{\Delta}^{\alpha}\Phi_0^{(+)}|\delta V|\widetilde{\Delta}^{\beta}\Phi_0^{(-)}\rangle - \langle\widetilde{\Delta}^{\alpha}\Phi_0^{(+)}|\widetilde{\Delta}^{\beta}\Phi_0^{(-)}\rangle\langle\Phi_0|\delta V|\Phi_0\rangle$ is obtained from the equation above just changing $+ \leftrightarrow -$.

Evaluation of $\left[\langle\delta\Phi_0|\Delta^{\alpha}V^*|\widetilde{\Delta}^{\beta}\Phi_0^{(+)}\rangle - \langle\Phi_0|\Delta^{\alpha}V^*|\Phi_0\rangle\langle\delta\Phi_0|\widetilde{\Delta}^{\beta}\Phi_0^{(+)}\rangle\right]$.
For convenience and better understanding $|\delta\Phi_0\rangle$ is splitted into its single and double-exitations contributions $|\delta\Phi_0^S\rangle$ and $|\delta\Phi_0^D\rangle$:

$$\begin{aligned}\langle\delta\Phi_0^D|\Delta^{\alpha}V^*|\widetilde{\Delta}^{\beta}\Phi_0^{(+)}\rangle &= \sum_{abstcukl}\frac{\langle ba|W|ts\rangle - \langle ab|W|ts\rangle}{4(\varepsilon_{at}+\varepsilon_{bs})}\langle k|\Delta^{\alpha}V^*|l\rangle\frac{\langle u|\Delta^{\beta}V|c\rangle}{\varepsilon_{cu}+iu}\langle c_a^{\dagger}c_b^{\dagger}c_sc_tc_k^{\dagger}c_lc_u^{\dagger}c_c\rangle \\ &= -\sum_{abst}\frac{\langle ba|W|ts\rangle - \langle ab|W|ts\rangle}{4(\varepsilon_{at}+\varepsilon_{bs})}\langle s|\Delta^{\alpha}V^*|a\rangle\frac{\langle t|\Delta^{\beta}V|b\rangle}{\varepsilon_{bt}+iu} \\ &\quad + \sum_{abst}\frac{\langle ba|W|ts\rangle - \langle ab|W|ts\rangle}{4(\varepsilon_{at}+\varepsilon_{bs})}\langle t|\Delta^{\alpha}V^*|a\rangle\frac{\langle s|\Delta^{\beta}V|b\rangle}{\varepsilon_{bs}+iu} \\ &\quad + \sum_{abst}\frac{\langle ba|W|ts\rangle - \langle ab|W|ts\rangle}{4(\varepsilon_{at}+\varepsilon_{bs})}\langle s|\Delta^{\alpha}V^*|b\rangle\frac{\langle t|\Delta^{\beta}V|a\rangle}{\varepsilon_{at}+iu} \\ &\quad - \sum_{abst}\frac{\langle ba|W|ts\rangle - \langle ab|W|ts\rangle}{4(\varepsilon_{at}+\varepsilon_{bs})}\langle t|\Delta^{\alpha}V^*|b\rangle\frac{\langle s|\Delta^{\beta}V|a\rangle}{\varepsilon_{as}+iu} \\ &= +\sum_{abst}\frac{\langle ba|W|ts\rangle - \langle ab|W|ts\rangle}{\varepsilon_{at}+\varepsilon_{bs}}\langle t|\Delta^{\alpha}V^*|a\rangle\frac{\langle s|\Delta^{\beta}V|b\rangle}{\varepsilon_{bs}+iu}\end{aligned}$$

$$\begin{aligned}\langle\delta\Phi_0^S|\Delta^{\alpha}V^*|\widetilde{\Delta}^{\beta}\Phi_0^{(+)}\rangle &= \sum_{atbskl}\frac{\langle a|V_x - v_x|t\rangle}{\varepsilon_{at}}\langle k|\Delta^{\alpha}V^*|l\rangle\frac{\langle s|\Delta^{\beta}V|b\rangle}{\varepsilon_{bs}+iu}\langle c_a^{\dagger}c_tc_k^{\dagger}c_lc_s^{\dagger}c_b\rangle \\ &= +\sum_{ats}\frac{\langle a|V_x - v_x|t\rangle}{\varepsilon_{at}}\langle t|\Delta^{\alpha}V^*|s\rangle\frac{\langle s|\Delta^{\beta}V|a\rangle}{\varepsilon_{as}+iu} \\ &\quad - \sum_{abt}\frac{\langle a|V_x - v_x|t\rangle}{\varepsilon_{at}}\frac{\langle t|\Delta^{\beta}V|b\rangle}{\varepsilon_{bt}+iu}\langle b|\Delta^{\alpha}V^*|a\rangle \\ &\quad + \sum_{atk}\frac{\langle a|V_x - v_x|t\rangle}{\varepsilon_{at}}\langle k|\Delta^{\alpha}V^*|k\rangle\frac{\langle t|\Delta^{\beta}V|a\rangle}{\varepsilon_{at}+iu}\end{aligned}$$

$$\langle\delta\Phi_0^D|\widetilde{\Delta}^{\beta}\Phi_0^{(+)}\rangle = \sum_{abstcu}\frac{\langle ba|W|ts\rangle - \langle ab|W|ts\rangle}{4(\varepsilon_{at}+\varepsilon_{bs})}\frac{\langle u|\Delta^{\beta}V|c\rangle}{\varepsilon_{cu}+iu}\langle c_a^{\dagger}c_b^{\dagger}c_sc_tc_u^{\dagger}c_c\rangle = 0$$

$$\langle \delta\Phi_0^S | \widetilde{\Delta}^\beta \Phi_0^{(+)} \rangle = \sum_{atbs} \frac{\langle a|V_x - v_x|t\rangle}{\varepsilon_{at}} \frac{\langle s|\Delta^\beta V|b\rangle}{\varepsilon_{bs}+iu} \langle c_a^\dagger c_t c_s^\dagger c_b\rangle = \sum_{at} \frac{\langle a|V_x - v_x|t\rangle}{\varepsilon_{at}} \frac{\langle t|\Delta^\beta V|a\rangle}{\varepsilon_{at}+iu}$$

$$\langle \Phi_0|\Delta^\alpha V^*|\Phi_0\rangle = \sum_{kl} \langle k|\Delta^\alpha V^*|l\rangle \langle c_k^\dagger c_l\rangle = \sum_k \langle k|\Delta^\alpha V^*|k\rangle$$

where in the first term in the last identity we have exchanged the index as needed. Summing up all the contributions and introducing the conduction-band-projected variation $|\delta\phi_a\rangle$ of the occupied single particle state

$$|\delta\phi_a\rangle = \sum_t |t\rangle \frac{\langle t|V_x - v_x|a\rangle}{\varepsilon_{at} \pm iu} \quad \Leftrightarrow \quad [H_{KS} + \gamma P_v - \varepsilon_a]|\delta\phi_a\rangle = -(1-P_v)[V_x - v_x]|\phi_a\rangle \tag{A.21}$$

beside the variations already introduced in Eq. (A.16), we find the final result

$$\begin{aligned} &\langle \delta\Phi_0|\Delta^\alpha V^*|\widetilde{\Delta}^\beta\Phi_0^{(+)}\rangle - \langle\Phi_0|\Delta^\alpha V^*|\Phi_0\rangle\langle\delta\Phi_0|\widetilde{\Delta}^\beta\Phi_0^{(+)}\rangle \\ &\qquad = + \sum_{abst} \frac{\langle ba|W|ts\rangle - \langle ab|W|ts\rangle}{\varepsilon_{at}+\varepsilon_{bs}} \langle t|\Delta^\alpha V^*|a\rangle \frac{\langle s|\Delta^\beta V|b\rangle}{\varepsilon_{bs}+iu} \\ &\qquad\quad + \sum_a \langle \delta\phi_a|\Delta^\alpha V^*|\Delta^\beta \phi_a^{(+)}\rangle - \sum_{ab} \langle\delta\phi_a|\Delta^\beta\phi_b^{(+)}\rangle\langle\phi_b|\Delta^\alpha V^*|\phi_a\rangle. \end{aligned} \tag{A.22}$$

For all the other terms like the one above similar expression can be found in the same way.

Final expression for $h_{Hx}^{\alpha\beta}$.

Form Eq. (A.20) and Eq. (A.22) all the terms appearing in Eq. (A.6) can be derived carefully playing with the frequency signs $\pm$ and with the indeces α and β of the perturbing potentials.

Summing all the contribution lead to

$$
\begin{aligned}
h_{Hx}^{\alpha\beta} = &+\sum_{ab}^{occ}\langle\Delta^\alpha\phi_a^{(-)}\phi_b|W|\Delta^\beta\phi_b^{(+)}\phi_a\rangle+\sum_{ab}^{occ}\langle\Delta^\alpha\phi_a^{(+)}\phi_b|W|\Delta^\beta\phi_b^{(-)}\phi_a\rangle\\
&-\sum_{ab}^{occ}\langle\Delta^\alpha\phi_a^{(-)}\phi_b|W|\phi_a\Delta^\beta\phi_b^{(+)}\rangle-\sum_{ab}^{occ}\langle\Delta^\alpha\phi_a^{(+)}\phi_b|W|\phi_a\Delta^\beta\phi_b^{(-)}\rangle\\
&+\sum_{abst}\frac{\langle ba|W|ts\rangle-\langle ab|W|ts\rangle}{\varepsilon_{at}+\varepsilon_{bs}}\langle t|\Delta^\alpha V^*|a\rangle\frac{\langle s|\Delta^\beta V|b\rangle}{\varepsilon_{bs}+iu}\\
&+\sum_{abst}\frac{\langle ba|W|ts\rangle-\langle ab|W|ts\rangle}{\varepsilon_{at}+\varepsilon_{bs}}\langle t|\Delta^\alpha V^*|a\rangle\frac{\langle s|\Delta^\beta V|b\rangle}{\varepsilon_{bs}-iu}\\
&+\sum_{abst}\frac{\langle st|W|ab\rangle-\langle st|W|ba\rangle}{\varepsilon_{at}+\varepsilon_{bs}}\langle a|\Delta^\beta V|t\rangle\frac{\langle b|\Delta^\alpha V^*|s\rangle}{\varepsilon_{bs}-iu}\\
&+\sum_{abst}\frac{\langle st|W|ab\rangle-\langle st|W|ba\rangle}{\varepsilon_{at}+\varepsilon_{bs}}\langle a|\Delta^\beta V|t\rangle\frac{\langle b|\Delta^\alpha V^*|s\rangle}{\varepsilon_{bs}+iu}\\
&+\sum_{a}^{occ}\langle\Delta^\alpha\phi_a^{(-)}|V_x-v_x|\Delta^\beta\phi_a^{(+)}\rangle+\sum_{a}^{occ}\langle\Delta^\alpha\phi_a^{(+)}|V_x-v_x|\Delta^\beta\phi_a^{(-)}\rangle\\
&-\sum_{ab}^{occ}\left[\langle\Delta^\alpha\phi_a^{(-)}|\Delta^\beta\phi_b^{(+)}\rangle+\langle\Delta^\alpha\phi_a^{(+)}|\Delta^\beta\phi_b^{(-)}\rangle\right]\langle\phi_b|V_x-v_x|\phi_a\rangle\\
&+\sum_{a}^{occ}\langle\delta\phi_a|\Delta^\alpha V^*|\Delta^\beta\phi_a^{(+)}+\Delta^\beta\phi_a^{(-)}\rangle+\sum_{a}^{occ}\langle\Delta^\alpha\phi_a^{(+)}+\Delta^\alpha\phi_a^{(-)}|\Delta^\beta V|\delta\phi_a\rangle\\
&-\sum_{ab}^{occ}\langle\delta\phi_a|\Delta^\beta\phi_b^{(+)}+\Delta^\beta\phi_b^{(-)}\rangle\langle\phi_b|\Delta^\alpha V^*|\phi_a\rangle-\sum_{ab}^{occ}\langle\Delta^\alpha\phi_a^{(-)}+\Delta^\alpha\phi_a^{(+)}|\delta\phi_b\rangle\langle\phi_b|\Delta^\beta V|\phi_a\rangle
\end{aligned}
\tag{A.23}
$$

Changing $a \leftrightarrow b$ and $t \leftrightarrow s$ in the 5$^{\text{th}}$ and 6$^{\text{th}}$ lines and exploiting the fact that for a real Hamiltonian one can send $(\phi_a, \phi_t^*) \to (\phi_a^*, \phi_t)$ and similarly $(\phi_b, \phi_s^*) \to (\phi_b^*, \phi_s)$ as needed, we find for the sum of 3$^{\text{th}}$ and 5$^{\text{th}}$ lines and for the 4$^{\text{th}}$ and 6$^{\text{th}}$ lines

$$
\begin{aligned}
3^{\text{th}}+5^{\text{th}} &= \sum_{abst}\langle ba|W|ts\rangle-\langle ab|W|ts\rangle\frac{\langle t|\Delta^\alpha V^*|a\rangle}{\varepsilon_{at}-iu}\frac{\langle s|\Delta^\beta V|b\rangle}{\varepsilon_{bs}+iu}\\
&= \sum_{ab}\langle\phi_b\Delta^\alpha\phi_a^{(+)}|W|\phi_a\Delta^\beta\phi_b^{(+)}\rangle-\sum_{ab}^{occ}\langle\phi_b\phi_a|W|\Delta^\beta\phi_b^{(+)}\Delta^{\alpha *}\phi_a^{(-)}\rangle\\
4^{\text{th}}+6^{\text{th}} &= \sum_{abst}\langle ba|W|ts\rangle-\langle ab|W|ts\rangle\frac{\langle t|\Delta^\alpha V^*|a\rangle}{\varepsilon_{at}+iu}\frac{\langle s|\Delta^\beta V|b\rangle}{\varepsilon_{bs}-iu}\\
&= \sum_{ab}\langle\phi_b\Delta^\alpha\phi_a^{(-)}|W|\phi_a\Delta^\beta\phi_b^{(-)}\rangle-\sum_{ab}^{occ}\langle\phi_b\phi_a|W|\Delta^\beta\phi_b^{(-)}\Delta^{\alpha *}\phi_a^{(+)}\rangle.
\end{aligned}
\tag{A.24}
$$

where we have introduced the variation $|\Delta^* \phi_a^{(\pm)}\rangle$ which is given by

$$|\Delta^* \phi_a^{(\pm)}\rangle = \sum_t |t\rangle \frac{\langle t|\Delta V^*|a\rangle}{\varepsilon_{at} \pm iu} \quad \Leftrightarrow \quad [H_{KS} + \gamma P_v - (\varepsilon_a \pm iu)]|\Delta^* \phi_a^{(\pm)}\rangle = -(1 - P_v)\Delta V^*|\phi_a\rangle \tag{A.25}$$

Replacing in the privious expression, changing the index a and b in the sums and exploiting the simmetry of the Coulomb integral when $\mathbf{r} \leftrightarrow \mathbf{r}'$ as needed, we get the final result of the derivation

$$\begin{aligned}
h_{Hx}^{\alpha\beta} = &+ \sum_{ab}^{occ} \langle \Delta^\alpha \phi_a^{(-)} \phi_b | W | \Delta^\beta \phi_b^{(+)} \phi_a \rangle + \sum_{ab}^{occ} \langle \Delta^\alpha \phi_a^{(+)} \phi_b | W | \Delta^\beta \phi_b^{(-)} \phi_a \rangle \\
&+ \sum_{ab}^{occ} \langle \Delta^\alpha \phi_a^{(-)} \phi_b | W | \Delta^\beta \phi_b^{(-)} \phi_a \rangle + \sum_{ab}^{occ} \langle \Delta^\alpha \phi_a^{(+)} \phi_b | W | \Delta^\beta \phi_b^{(+)} \phi_a \rangle \\
&- \sum_{ab}^{occ} \langle \Delta^\alpha \phi_a^{(-)} \phi_b | W | \phi_a \Delta^\beta \phi_b^{(+)} \rangle - \sum_{ab}^{occ} \langle \Delta^\alpha \phi_a^{(+)} \phi_b | W | \phi_a \Delta^\beta \phi_b^{(-)} \rangle \\
&- \sum_{ab}^{occ} \langle \phi_b \phi_a | W | \Delta^\beta \phi_b^{(+)} \Delta^{*\alpha} \phi_a^{(-)} \rangle - \sum_{ab}^{occ} \langle \phi_b \phi_a | W | \Delta^\beta \phi_b^{(-)} \Delta^{*\alpha} \phi_a^{(+)} \rangle \\
&+ \sum_{a}^{occ} \langle \Delta^\alpha \phi_a^{(-)} | V_x - v_x | \Delta^\beta \phi_a^{(+)} \rangle + \sum_{a}^{occ} \langle \Delta^\alpha \phi_a^{(+)} | V_x - v_x | \Delta^\beta \phi_a^{(-)} \rangle \\
&- \sum_{ab}^{occ} \left[\langle \Delta^\alpha \phi_a^{(-)} | \Delta^\beta \phi_b^{(+)} \rangle + \langle \Delta^\alpha \phi_a^{(+)} | \Delta^\beta \phi_b^{(-)} \rangle \right] \langle \phi_b | V_x - v_x | \phi_a \rangle \\
&+ \sum_{a}^{occ} \langle \delta\phi_a | \Delta^\alpha V^* | \Delta^\beta \phi_a^{(+)} + \Delta^\beta \phi_a^{(-)} \rangle + \sum_{a}^{occ} \langle \Delta^\alpha \phi_a^{(+)} + \Delta^\alpha \phi_a^{(-)} | \Delta^\beta V | \delta\phi_a \rangle \\
&- \sum_{ab}^{occ} \langle \delta\phi_a | \Delta^\beta \phi_b^{(+)} + \Delta^\beta \phi_b^{(-)} \rangle \langle \phi_b | \Delta^\alpha V^* | \phi_a \rangle - \sum_{ab}^{occ} \langle \Delta^\alpha \phi_a^{(-)} + \Delta^\alpha \phi_a^{(+)} | \delta\phi_b \rangle \langle \phi_b | \Delta^\beta V | \phi_a \rangle .
\end{aligned} \tag{A.26}$$

Appendix B

Iterative Diagonalization

Having in mind to use an efficient iterative technique for solving the eigenvalue problem in Eq. (3.9), the matrix elements of h_{Hx} alone are not sufficient and we need also the action of the operator on a generic vector, i.e. $h_{Hx}|\Delta V\rangle$, in order to compute correction vectors needed in any iterative diagonalization technique. This implies we should be able to remove the potential $\Delta^\alpha V^*$ everywhere in Eq. (3.25) so that we are left with the desidered quantity $h_{Hx}|\Delta^\beta V\rangle$. This can be easily done for the Hartree term (first two lines of Eq. (3.25)) and for some of the exchange terms (first contributions in line 7 and 8 of Eq. (3.25)) which are already in the appropriate form explicitely exposing the dependence on $\Delta^\alpha V^*$. For all the other terms the dependence $\Delta^\alpha V^*$ is hidden inside the vectors $|\Delta^\alpha \phi_a^{(\pm)}\rangle$ and further manipulations are needed to expose this dependence. To this end we can replace $|\Delta^\alpha \phi_a^{(\pm)}\rangle$ with its formal solution

$$|\Delta^\alpha \phi_a^{(\pm)}\rangle = \sum_t^{vir} |\phi_t\rangle \frac{\langle \phi_t|\Delta^\alpha V|\phi_a\rangle}{\varepsilon_{at} \pm iu} \tag{B.1}$$

easily derived form Eq. (3.26), where the sum runs over unoccupied states only because of the presence of the projector over the unoccupied states manifold $(1 - P_v)$. This definition for $|\Delta^\alpha \phi_a^{(\pm)}\rangle$ has to be inserted in every terms of Eq. (3.25) in which it appears. We show how the derivation continues just for one of these terms, say the two contributions in line 3 of Eq. (3.25), being essentially the same for all the other. Denoting these two particular contributions with

$\widetilde{h}_x^{\alpha\beta}$ we have

$$\begin{aligned}\widetilde{h}_x^{\alpha\beta} &= -\sum_{ab}^{occ}\langle\Delta^\alpha\phi_a^{(-)}\phi_b|W|\phi_a\Delta^\beta\phi_b^{(+)}\rangle - \sum_{ab}^{occ}\langle\Delta^\alpha\phi_a^{(+)}\phi_b|W|\phi_a\Delta^\beta\phi_b^{(-)}\rangle \\ &= +\sum_{\sigma=\pm1}\left\{+\sum_a\langle\phi_a|\Delta^\alpha V^*|\sum_t\frac{|\phi_t\rangle\langle\phi_t|}{(\varepsilon_{at}+\sigma iu)}\left[-\sum_b\int d\mathbf{r}'\phi_b^*(\mathbf{r}')\frac{e^2}{|\mathbf{r}-\mathbf{r}'|}\phi_a(\mathbf{r}')\Delta^\beta\phi_b^{(\sigma)}(\mathbf{r})\right]\rangle\right\} \\ &= +\sum_a^{occ}\langle\phi_a|\Delta^\alpha V^*|\psi_{\beta,a}^{(+)}+\psi_{\beta,a}^{(-)}\rangle \end{aligned} \tag{B.2}$$

where the auxiliary vectors $|\psi_{\beta,a}^{(\pm)}\rangle$ solutions of the linear problem

$$\begin{aligned}&[H_0+\gamma P_v-(\varepsilon_a\pm iu)]|\psi_{\beta,a}^{(\pm)}\rangle = -(1-P_v)|t_{\beta,a}^{(\pm)}\rangle \\ &t_{\beta,a}^{(\pm)}(\mathbf{r}) = -\sum_b\int d\mathbf{r}'\phi_b^*(\mathbf{r}')\frac{e^2}{|\mathbf{r}-\mathbf{r}'|}\phi_a(\mathbf{r}')\Delta^\beta\phi_b^{(\pm)}(\mathbf{r})\end{aligned} \tag{B.3}$$

have been introduced. The potential $\Delta^\alpha V^*$ now appears expicitely in Eq. (B.2) and can be removed leading to the desidered expression for the action of the operator $\widetilde{h}_x$ on a generic potential $|\Delta^\beta V\rangle$:

$$\widetilde{h}_x|\Delta^\beta V\rangle = \sum_a^{occ}\phi_a^*(\mathbf{r})[\psi_{\beta,a}^{(-)}(\mathbf{r})+\psi_{\beta,a}^{(+)}(\mathbf{r})]. \tag{B.4}$$

with $\psi_{\beta,a}^{(\pm)}(\mathbf{r})$ difined by Eq. (B.3). Applying the same precedure to all the terms in Eq. (3.25) that require it, leads to the final expression

$$\begin{aligned}\delta\Delta^\beta n_x(\mathbf{r}) = h_x|\Delta^\beta V\rangle = &+\sum_a^{occ}\phi_a^*(\mathbf{r})[\psi_{\beta,a}^{(-)}(\mathbf{r})+\psi_{\beta,a}^{(+)}(\mathbf{r})]+\sum_a^{occ}[\widetilde{\psi}_{\beta,a}^{(-)}(\mathbf{r})+\widetilde{\psi}_{\beta,a}^{(+)}(\mathbf{r})]^*\phi_a(\mathbf{r}) \\ &+\sum_a^{occ}\delta\phi_a^*(\mathbf{r})[\Delta^\beta\phi_a^{(+)}(\mathbf{r})+\Delta^\beta\phi_a^{(-)}(\mathbf{r})] \\ &-\sum_{ab}^{occ}\langle\delta\phi_a|\Delta^\beta\phi_a^{(+)}+\Delta^\beta\phi_a^{(-)}\rangle\phi_b^*(\mathbf{r})\phi_a(\mathbf{r})\end{aligned} \tag{B.5}$$

with $\Delta^\beta\phi_a^{(\pm)}(\mathbf{r})$, $\delta\phi_a(\mathbf{r})$, $\psi_{\beta,a}^{(\pm)}(\mathbf{r})$ and $\widetilde{\psi}_{\beta,a}^{(\pm)}(\mathbf{r})$ solutions of the linear systems

$$\begin{aligned}&[H_{KS}+\gamma P_v-(\varepsilon_a\pm iu)]|\Delta^\beta\phi_a^{(\pm)}\rangle = -(1-P_v)\Delta^\beta V|\phi_a\rangle \\ &[H_{KS}+\gamma P_v-\varepsilon_a]|\delta\phi_a\rangle = -(1-P_v)[V_x-v_x]\phi_a\rangle \\ &[H_{KS}+\gamma P_v-(\varepsilon_a\pm iu)]|\psi_{\beta,a}^{(\pm)}\rangle = -(1-P_v)|t_{\beta,a}^{(\pm)}\rangle \\ &[H_{KS}+\gamma P_v-(\varepsilon_a\pm iu)]|\widetilde{\psi}_{\beta,a}^{(\pm)}\rangle = -(1-P_v)|\widetilde{t}_{\beta,a}^{(\pm)}\rangle\end{aligned} \tag{B.6}$$

where the constant terms $t^{(\pm)}_{\beta,a}(\mathbf{r})$ and $\widetilde{t}^{(\pm)}_{\beta,a}(\mathbf{r})$ in the linear sistem for $\psi^{(\pm)}_{\beta,a}(\mathbf{r})$ and $\widetilde{\psi}^{(\pm)}_{\beta,a}(\mathbf{r})$ are given by

$$\begin{aligned}
t^{(\pm)}_{\beta,a}(\mathbf{r}) = &-\sum_b^{occ}\int d\mathbf{r}'\phi^*_b(\mathbf{r}')\frac{e^2}{|\mathbf{r}-\mathbf{r}'|}\phi_a(\mathbf{r}')\Delta^\beta\phi^{(\pm)}_b(\mathbf{r}) \\
&-\sum_b^{occ}\Delta^\beta\phi^{(\pm)}_b(\mathbf{r})\langle\phi_b|V_x-v_x|\phi_a\rangle-\sum_b^{occ}\delta\phi_b(\mathbf{r})\langle\phi_b|\Delta^\beta V|\phi_a\rangle \\
&+[V_x-v_x]\,|\Delta^\beta\phi^{(\pm)}_a(\mathbf{r})\rangle+\Delta^\beta V(\mathbf{r})\delta\phi_a(\mathbf{r}); \\
\widetilde{t}^{(\pm)}_{\beta,a}(\mathbf{r}) = &-\sum_b^{occ}\int d\mathbf{r}'\left[\Delta^\beta\phi^{(\pm)}_b(\mathbf{r}')\right]^*\frac{e^2}{|\mathbf{r}-\mathbf{r}'|}\phi_a(\mathbf{r}')\phi_b(\mathbf{r}).
\end{aligned} \tag{B.7}$$

Finally the matrix elements of h_x follows from Eq. (B.5) and are simply given by

$$h^{\alpha\beta}_x = \langle\Delta^\alpha V|\chi_0 f_x\chi_0|\Delta^\beta V\rangle = \int d\mathbf{r}\Delta^\alpha V^*(\mathbf{r})\delta\Delta^\beta n_x(\mathbf{r}). \tag{B.8}$$

Although a bit involved this approach clearly shows that matrix elements of h_{Hx} and its action on a trial potential are simply given in terms of KS single particle wavefunctions $\phi_a(\mathbf{r})$ and its variations $\Delta\phi^{(\pm)}_a(\mathbf{r})$, $\delta\phi_a(\mathbf{r})$, $\psi^{(\pm)}_a(\mathbf{r})$ and $\widetilde{\psi}^{(\pm)}_a(\mathbf{r})$, which can be efficiently computed resorting to linear response technique of DFPT (Eq. (B.6)).

All the formula above are valid for a generic system. In the specific case of a periodic system we can replace $a \to (\mathbf{k}, v)$ and similarly $b \to (\mathbf{p}, v')$ and taking into account that the perturbation ΔV has a wave-vector $\mathbf{q}$ and that the wavefunctions at different $\mathbf{k}$-point are orthogonal, Eq. (B.5) becomes

$$\begin{aligned}
\delta\Delta n^{\mathbf{q}}_x(\mathbf{r}) = h^{\mathbf{q}}_x(iu)|\Delta V\rangle = &+\sum_{\mathbf{k},v}^{occ}\phi^*_{\mathbf{k},v}(\mathbf{r})[\psi^{(-)}_{\mathbf{k}+\mathbf{q},v}(\mathbf{r})+\psi^{(+)}_{\mathbf{k}+\mathbf{q},v}(\mathbf{r})] \\
&+\sum_{\mathbf{k},v}^{occ}[\widetilde{\psi}^{(-)}_{\mathbf{k}-\mathbf{q},v}(\mathbf{r})+\widetilde{\psi}^{(+)}_{\mathbf{k}-\mathbf{q},v}(\mathbf{r})]^*\phi_{\mathbf{k},v}(\mathbf{r}) \\
&+\sum_{\mathbf{k},v}^{occ}\delta\phi^*_{\mathbf{k},v}(\mathbf{r})[\Delta\phi^{(+)}_{\mathbf{k}+\mathbf{q}}(\mathbf{r})+\Delta\phi^{(-)}_{\mathbf{k}+\mathbf{q}}(\mathbf{r})] \\
&-\sum_{\mathbf{k},v,v'}^{occ}\langle\delta\phi_{\mathbf{k}+\mathbf{q},v}|\Delta\phi^{(+)}_{\mathbf{k}+\mathbf{q},v'}+\Delta\phi^{(-)}_{\mathbf{k}+\mathbf{q},v'}\rangle\phi^*_{\mathbf{k},v'}(\mathbf{r})\phi_{\mathbf{k}+\mathbf{q},v}(\mathbf{r}).
\end{aligned} \tag{B.9}$$

In the second line the variations $\widetilde{\psi}^{(\pm)}(\mathbf{r})$ have a wave-vector $\mathbf{k}-\mathbf{q}$ and are the solution of the linear problem

$$[H_{KS}(\mathbf{r})+\gamma P^{\mathbf{k}-\mathbf{q}}_v-(\varepsilon_{\mathbf{k},v}\pm iu)]|\widetilde{\psi}^{(\pm)}_{\mathbf{k}-\mathbf{q},v}\rangle = -(1-P^{\mathbf{k}-\mathbf{q}}_v)|\widetilde{t}^{(\pm)}_{\mathbf{k}-\mathbf{q},v}\rangle \tag{B.10}$$

which require, in principle, the knowledge of the projector and hence of the unperturbed wavefunctions at wave-vector $\mathbf{k}-\mathbf{q}$. However one can change the index in the sum in the

second line of Eq. (B.9) sending $\mathbf{k} \rightarrow \mathbf{k}+\mathbf{q}$, and then rename it as $\mathbf{k}$ under the assumption of an infinite dense grid of $\mathbf{k}$ and $\mathbf{q}$ points, leading to an equivalent expression for the second line

$$\sum_{\mathbf{k},v}^{occ}[\widetilde{\psi}^{(-)}_{\mathbf{k}-\mathbf{q},v}(\mathbf{r})+\widetilde{\psi}^{(+)}_{\mathbf{k}-\mathbf{q},v}(\mathbf{r})]^*\phi_{\mathbf{k},v}(\mathbf{r}) = \sum_{\mathbf{k},v}^{occ}[\widetilde{\psi}^{(-)}_{\mathbf{k},v}(\mathbf{r})+\widetilde{\psi}^{(+)}_{\mathbf{k},v}(\mathbf{r})]^*\phi_{\mathbf{k}+\mathbf{q},v}(\mathbf{r}) \tag{B.11}$$

where now the linear problems for $\widetilde{\psi}^{(\pm)}_{\mathbf{k},v}(\mathbf{r})$

$$[H_{KS}(\mathbf{r})+\gamma P_v^{\mathbf{k}}-(\varepsilon_{\mathbf{k}+\mathbf{q},v}\pm iu)]|\widetilde{\psi}^{(\pm)}_{\mathbf{k},v}\rangle = -(1-P_v^{\mathbf{k}})|\widetilde{t}^{(\pm)}_{\mathbf{k},v}\rangle, \tag{B.12}$$

do not contain anymore the unknown unperturbed wavefunctions $\phi_{\mathbf{k}-\mathbf{q},v}(\mathbf{r})$.

Compared to the RPA implementation based on the dielectric function diagonalization, where the basic operation is the calculation of the non-interacting response to a trial potential, i.e. the density variation $\Delta n(\mathbf{r}) = \chi_0|\Delta V\rangle = \sum_a \phi_a^*(\mathbf{r})[\Delta\phi_a^{(-)}(\mathbf{r})+\Delta\phi_a^{(+)}(\mathbf{r})]$, the additional operations required in our implemetation are the solutions of the linear sistems for $\delta\phi_a(\mathbf{r})$, $\psi_a^{(\pm)}(\mathbf{r})$ and $\widetilde{\psi}_a^{(\pm)}(\mathbf{r})$. While the former does not depend on trial perturbing potentials, the latters have to be solved for each ΔV and its computational cost is comparable to the one needed for computing $\Delta\phi_a^{(\pm)}(\mathbf{r})$. We therefore expect that the workload increase passing from RPA to RPAx correlation energy calculation should be restrained and accounted for by a multiplicative prefactor in front of the RPA computational cost estimated to be $4-5$.

Bibliography

[1] P. A. M. Dirac, "Quantum mechanics of many-electron systems," *Proceedings of the Royal Society of London. Series A, Containing Papers of a Mathematical and Physical Character*, vol. 123, pp. 714–733, Apr. 1929. 1

[2] W. Kohn, "Nobel lecture: Electronic structure of matterâwave functions and density functionals," *Reviews of Modern Physics*, vol. 71, pp. 1253–1266, Oct. 1999. 1, 2

[3] P. Hohenberg and W. Kohn, "Inhomogeneous electron gas," *Physical Review*, vol. 136, pp. B864–B871, Nov. 1964. 1, 8

[4] W. Kohn and L. J. Sham, "Self-consistent equations including exchange and correlation effects," *Physical Review*, vol. 140, pp. A1133–A1138, Nov. 1965. 1, 2, 9

[5] O. Gunnarsson and B. I. Lundqvist, "Exchange and correlation in atoms, molecules, and solids by the spin-density-functional formalism," *Physical Review B*, vol. 13, pp. 4274–4298, May 1976. 2, 3, 16

[6] A. D. Becke, "Density-functional exchange-energy approximation with correct asymptotic behavior," *Physical Review A*, vol. 38, pp. 3098–3100, Sept. 1988. 2, 15

[7] J. P. Perdew, K. Burke, and M. Ernzerhof, "Generalized gradient approximation made simple," *Physical Review Letters*, vol. 77, pp. 3865–3868, Oct. 1996. 2, 15

[8] J. P. Perdew and A. Zunger, "Self-interaction correction to density-functional approximations for many-electron systems," *Physical Review B*, vol. 23, pp. 5048–5079, May 1981. 2, 14, 53, 60

[9] J. Heyd, G. E. Scuseria, and M. Ernzerhof, "Hybrid functionals based on a screened coulomb potential," *The Journal of Chemical Physics*, vol. 118, pp. 8207–8215, May 2003. 2, 67

[10] V. I. Anisimov, J. Zaanen, and O. K. Andersen, "Band theory and mott insulators: Hubbard u instead of stoner i," *Physical Review B*, vol. 44, pp. 943–954, July 1991. 2

[11] D. C. Langreth and J. P. Perdew, "The exchange-correlation energy of a metallic surface," *Solid State Communications*, vol. 17, pp. 1425–1429, Dec. 1975. 3, 16

[12] D. C. Langreth and J. P. Perdew, "Exchange-correlation energy of a metallic surface: Wave-vector analysis," *Physical Review B*, vol. 15, pp. 2884–2901, Mar. 1977. 3, 16

[13] M. Dion, H. Rydberg, E. Schröder, D. C. Langreth, and B. I. Lundqvist, "Van der waals density functional for general geometries," *Phys. Rev. Lett.*, vol. 92, p. 246401, Jun 2004. 3, 64, 65, 66

[14] T. Thonhauser, V. R. Cooper, S. Li, A. Puzder, P. Hyldgaard, and D. C. Langreth, "Van der waals density functional: Self-consistent potential and the nature of the van der waals bond," *Physical Review B*, vol. 76, p. 125112, Sept. 2007. 3

[15] K. Lee, E. D. Murray, L. Kong, B. I. Lundqvist, and D. C. Langreth, "Higher-accuracy van der waals density functional," *Phys. Rev. B*, vol. 82, p. 081101, Aug 2010. 3, 64, 65, 66

[16] M. Fuchs and X. Gonze, "Accurate density functionals:ÂÂapproaches using the adiabatic-connection fluctuation-dissipation theorem," *Physical Review B*, vol. 65, p. 235109, June 2002. 3, 70, 71

[17] A. Marini, P. Garciá-González, and A. Rubio, "First-principles description of correlation effects in layered materials," *Phys. Rev. Lett.*, vol. 96, p. 136404, Apr 2006. 3

[18] J. Harl and G. Kresse, "Cohesive energy curves for noble gas solids calculated by adiabatic connection fluctuation-dissipation theory," *Physical Review B*, vol. 77, p. 045136, Jan. 2008. 3, 23

[19] H.-V. Nguyen and G. Galli, "A first-principles study of weakly bound molecules using exact exchange and the random phase approximation," *The Journal of Chemical Physics*, vol. 132, p. 044109, Jan. 2010. 3, 25, 71, 72

[20] F. Furche, "Molecular tests of the random phase approximation to the exchange-correlation energy functional," *Physical Review B*, vol. 64, p. 195120, Oct. 2001. 3, 25, 26, 67

[21] M. Fuchs, Y.-M. Niquet, X. Gonze, and K. Burke, "Describing static correlation in bond dissociation by kohnâsham density functional theory," *The Journal of Chemical Physics*, vol. 122, p. 094116, Mar. 2005. 3, 23, 67, 69

[22] A. Heßelmann and A. Görling, "Random phase approximation correlation energies with exact kohn-sham exchange," *Mol. Phys.*, vol. 108, pp. 359–372, Jan 2010. 4, 31, 32

[23] M. Hellgren and U. v. Barth, "Correlation energy functional and potential from time-dependent exact-exchange theory," *The Journal of Chemical Physics*, vol. 132, p. 044101, Jan. 2010. 4, 32

[24] P. Bleiziffer, A. Heßelmann, and A. Görling, "Resolution of identity approach for the kohn-sham correlation energy within the exact-exchange random-phase approximation," *The Journal of Chemical Physics*, vol. 136, no. 13, pp. –, 2012. 4, 31, 32

[25] M. Born and R. Oppenheimer, "Zur quantentheorie der molekeln," *Annalen der Physik*, vol. 389, pp. 457–484, Jan. 1927. 6

[26] D. R. Hartree, "The wave mechanics of an atom with a non-coulomb central field. part III. term values and intensities in series in optical spectra," *Mathematical Proceedings of the Cambridge Philosophical Society*, vol. 24, no. 03, pp. 426–437, 1928. 7

[27] V. Fock, "Näherungsmethode zur lösung des quantenmechanischen mehrkörperproblems," *Zeitschrift für Physik*, vol. 61, no. 1-2, pp. 126–148, 1930. 7

[28] C. Møller and M. S. Plesset, "Note on an approximation treatment for many-electron systems," *Phys. Rev.*, vol. 46, pp. 618–622, Oct 1934. 7

[29] A. Szabo and N. S. Ostlund, *Modern Quantum Chemistry: Introduction to Advanced Electronic Structure Theory*. Mineola, N.Y.: Dover Pubns, revised. edizione ed., July 1996. 7

[30] J. Čížek, "On the correlation problem in atomic and molecular systems. calculation of wavefunction components in ursellâtype expansion using quantum-field theoretical methods," *The Journal of Chemical Physics*, vol. 45, no. 11, pp. 4256–4266, 1966. 7

[31] L. H. Thomas, "The calculation of atomic fields," *Mathematical Proceedings of the Cambridge Philosophical Society*, vol. 23, no. 05, pp. 542–548, 1927. 8

[32] E. Fermi, "Un modello statistico per la determinazione di alcune proprietà dall'atomo," *Rend. Accad. Naz. Licei*, vol. 6, pp. 602–607, 1927. 8

[33] R. M. Martin, *Electronic Structure: Basic Theory and Practical Methods*. Cambridge, UK; New York: Cambridge University Press, 1 edizione ed., Oct. 2008. 11, 12

[34] N. W. Ashcroft, *Solid State Physics*. New York: Holt Rinehart & Winston, Nov. 1976. 12, 51

[35] D. R. Hamann, M. SchlÃ$\frac{1}{4}$ter, and C. Chiang, "Norm-conserving pseudopotentials," *Physical Review Letters*, vol. 43, pp. 1494–1497, Nov. 1979. 14, 65

[36] D. Vanderbilt, "Soft self-consistent pseudopotentials in a generalized eigenvalue formalism," *Physical Review B*, vol. 41, pp. 7892–7895, Apr. 1990. 14

[37] S. H. Vosko, L. Wilk, and M. Nusair, "Accurate spin-dependent electron liquid correlation energies for local spin density calculations: a critical analysis," *Canadian Journal of Physics*, vol. 58, pp. 1200–1211, Aug. 1980. 14, 53, 60, 61

[38] J. P. Perdew and Y. Wang, "Accurate and simple analytic representation of the electron-gas correlation energy," *Physical Review B*, vol. 45, pp. 13244–13249, June 1992. 14, 53, 60, 61

[39] D. M. Ceperley and B. J. Alder, "Ground state of the electron gas by a stochastic method," *Physical Review Letters*, vol. 45, pp. 566–569, Aug. 1980. 14, 53, 54, 55, 78

[40] C. Lee, W. Yang, and R. G. Parr, "Development of the colle-salvetti correlation-energy formula into a functional of the electron density," *Physical Review B*, vol. 37, pp. 785–789, Jan. 1988. 15

[41] H. B. Callen and T. A. Welton, "Irreversibility and generalized noise," *Physical Review*, vol. 83, pp. 34–40, July 1951. 19

[42] R. Kubo, "The fluctuation-dissipation theorem," *Reports on Progress in Physics*, vol. 29, p. 255, Jan. 1966. 19

[43] E. Runge and E. K. U. Gross, "Density-functional theory for time-dependent systems," *Physical Review Letters*, vol. 52, pp. 997–1000, Mar. 1984. 20

[44] M. Petersilka, U. J. Gossmann, and E. K. U. Gross, "Excitation energies from time-dependent density-functional theory," *Physical Review Letters*, vol. 76, pp. 1212–1215, Feb. 1996. 21, 22

[45] E. K. U. Gross and W. Kohn, "Local density-functional theory of frequency-dependent linear response," *Physical Review Letters*, vol. 55, pp. 2850–2852, Dec. 1985. 22

[46] R. F. Nalewajski, *Density Functional Theory II: Relativistic and Time Dependent Extensions*. Springer Verlag, Nov. 1996. 22

[47] D. Bohm and D. Pines, "A collective description of electron interactions. i. magnetic interactions," *Physical Review*, vol. 82, pp. 625–634, June 1951. 22

[48] D. Pines and D. Bohm, "A collective description of electron interactions: II. collective vs individual particle aspects of the interactions," *Physical Review*, vol. 85, pp. 338–353, Jan. 1952. 22

[49] D. Bohm and D. Pines, "A collective description of electron interactions: III. coulomb interactions in a degenerate electron gas," *Physical Review*, vol. 92, pp. 609–625, Nov. 1953. 22

[50] D. Pines, "A collective description of electron interactions: IV. electron interaction in metals," *Physical Review*, vol. 92, pp. 626–636, Nov. 1953. 22

[51] J. F. Dobson, "Quasi-local-density approximation for a van der waals energy functional," *arXiv:cond-mat/0311371*, Nov. 2003. arXiv: cond-mat/0311371. 23, 64

[52] A. Heßelmann and A. Görling, "Correct description of the bond dissociation limit without breaking spin symmetry by a random-phase-approximation correlation functional," *Physical Review Letters*, vol. 106, p. 093001, Feb. 2011. 23, 32, 68

[53] H. Jiang and E. Engel, "Random-phase-approximation-based correlation energy functionals: Benchmark results for atoms," *The Journal of Chemical Physics*, vol. 127, p. 184108, Nov. 2007. 23

[54] M. Hellgren and U. von Barth, "Correlation potential in density functional theory at the GWA level: Spherical atoms," *Physical Review B*, vol. 76, p. 075107, Aug. 2007. 23, 25, 34

[55] S. Kurth and J. P. Perdew, "Density-functional correction of random-phase-approximation correlation with results for jellium surface energies," *Physical Review B*, vol. 59, pp. 10461–10468, Apr. 1999. 23, 26, 68

[56] J. Toulouse, I. C. Gerber, G. Jansen, A. Savin, and J. G. Ángyán, "Adiabatic-connection fluctuation-dissipation density-functional theory based on range separation," *Physical Review Letters*, vol. 102, p. 096404, Mar. 2009. 23, 26

[57] X. Ren, A. Tkatchenko, P. Rinke, and M. Scheffler, "Beyond the random-phase approximation for the electron correlation energy: The importance of single excitations," *Physical Review Letters*, vol. 106, p. 153003, Apr. 2011. 23, 26

[58] H.-V. Nguyen and S. de Gironcoli, "Efficient calculation of exact exchange and RPA correlation energies in the adiabatic-connection fluctuation-dissipation theory," *Physical Review B*, vol. 79, p. 205114, May 2009. 23, 24, 25, 33, 37, 47, 48, 71

[59] H.-V. Nguyen, *Efficient calculation of RPA correlation energy in the Adiabatic Connection Fluctuation-Dissipation theory*. PhD Thesis, Scuola Internazionale Superiore di Studi Avanzati, Oct. 2008. 23, 24, 33, 37, 48

[60] D. Lu, Y. Li, D. Rocca, and G. Galli, "Ab-initio calculation of van der waals bonded molecular crystals," *Physical Review Letters*, vol. 102, p. 206411, May 2009. 23

[61] S. Baroni, S. de Gironcoli, A. Dal Corso, and P. Giannozzi, "Phonons and related crystal properties from density-functional perturbation theory," *Reviews of Modern Physics*, vol. 73, pp. 515–562, July 2001. 23, 34

[62] H. F. Wilson, F. Gygi, and G. Galli, "Efficient iterative method for calculations of dielectric matrices," *Physical Review B*, vol. 78, p. 113303, Sept. 2008. 24

[63] R. W. Godby, M. Schlüter, and L. J. Sham, "Accurate exchange-correlation potential for silicon and its discontinuity on addition of an electron," *Physical Review Letters*, vol. 56, pp. 2415–2418, June 1986. 25

[64] R. W. Godby, M. Schlüter, and L. J. Sham, "Self-energy operators and exchange-correlation potentials in semiconductors," *Physical Review B*, vol. 37, pp. 10159–10175, June 1988. 25

[65] P. Verma and R. J. Bartlett, "Increasing the applicability of density functional theory. II. correlation potentials from the random phase approximation and beyond," *The Journal of Chemical Physics*, vol. 136, p. 044105, Jan. 2012. 25

[66] M. Hellgren, D. R. Rohr, and E. K. U. Gross, "Correlation potentials for molecular bond dissociation within the self-consistent random phase approximation," *The Journal of Chemical Physics*, vol. 136, p. 034106, Jan. 2012. 25

[67] F. Caruso, D. R. Rohr, M. Hellgren, X. Ren, P. Rinke, A. Rubio, and M. Scheffler, "Bond breaking and bond formation: How electron correlation is captured in many-body perturbation theory and density-functional theory," *Physical Review Letters*, vol. 110, p. 146403, Apr. 2013. 25

[68] P. Bleiziffer, A. Heßelmann, and A. Görling, "Efficient self-consistent treatment of electron correlation within the random phase approximation," *The Journal of Chemical Physics*, vol. 139, p. 084113, Aug. 2013. 25

[69] N. L. Nguyen, N. Colonna, and S. de Gironcoli, "Ab initio self-consistent total-energy calculations within the EXX/RPA formalism," *Physical Review B*, vol. 90, p. 045138, July 2014. 25, 37, 65, 71, 72

[70] N. L. Nguyen, *Toward realistic DFT description of complex systems: ethylene epoxidation on Ag-Cu alloy and RPA correlation in van der Waals molecules*. PhD Thesis, Scuola Internazionale Superiore di Studi Avanzati, Mar. 2012. 25, 37, 72

[71] J. Paier, X. Ren, P. Rinke, G. E. Scuseria, A. Grüneis, G. Kresse, and M. Scheffler, "Assessment of correlation energies based on the random-phase approximation," *New Journal of Physics*, vol. 14, no. 4, p. 043002, 2012. 26

[72] E. Gross, J. Dobson, and M. Petersilka, *Topics in Current Chemistry*, vol. 181. Springer-Verlag, 1996. 27

[73] G. Giuliani and G. Vignale, *Quantum Theory of the Electron Liquid*. Cambridge University Press, 2005. 27, 32, 52, 53, 55, 82

[74] M. Lein, E. K. U. Gross, and J. P. Perdew, "Electron correlation energies from scaled exchange-correlation kernels: Importance of spatial versus temporal nonlocality," *Physical Review B*, vol. 61, pp. 13431–13437, May 2000. 27

[75] J. B. Krieger, Y. Li, and G. J. Iafrate, "Derivation and application of an accurate kohn-sham potential with integer discontinuity," *Physics Letters A*, vol. 146, pp. 256–260, May 1990. 27

[76] A. Görling, "Exact exchange kernel for time-dependent density-functional theory," *International Journal of Quantum Chemistry*, vol. 69, no. 3, pp. 265–277, 1998. 27, 34

[77] A. Görling, "Exact exchange-correlation kernel for dynamic response properties and excitation energies in density-functional theory," *Phys. Rev. A*, vol. 57, pp. 3433–3436, May 1998. 27, 32, 34

[78] Y.-H. Kim and A. Görling, "Exact kohn-sham exchange kernel for insulators and its long-wavelength behavior," *Phys. Rev. B*, vol. 66, p. 035114, Jul 2002. 27

[79] M. Hellgren and U. von Barth, "Linear density response function within the time-dependent exact-exchange approximation," *Physical Review B*, vol. 78, p. 115107, Sept. 2008. 27, 31, 32, 34

[80] M. Hellgren and U. v. Barth, "Exact-exchange kernel of time-dependent density functional theory: Frequency dependence and photoabsorption spectra of atoms," *The Journal of Chemical Physics*, vol. 131, p. 044110, July 2009. 27

[81] A. Görling and M. Levy, "Correlation-energy functional and its high-density limit obtained from a coupling-constant perturbation expansion," *Phys. Rev. B*, vol. 47, pp. 13105–13113, May 1993. 27, 30, 32

[82] A. Görling, "Time-dependent kohn-sham formalism," *Phys. Rev. A*, vol. 55, pp. 2630–2639, Apr 1997. 32

[83] M. Gell-Mann and K. A. Brueckner, "Correlation energy of an electron gas at high density," *Physical Review*, vol. 106, pp. 364–368, Apr. 1957. 32

[84] P. Giannozzi, S. Baroni, N. Bonini, M. Calandra, R. Car, C. Cavazzoni, D. Ceresoli, G. L. Chiarotti, M. Cococcioni, I. Dabo, A. D. Corso, S. d. Gironcoli, S. Fabris, G. Fratesi, R. Gebauer, U. Gerstmann, C. Gougoussis, A. Kokalj, M. Lazzeri, L. Martin-Samos, N. Marzari, F. Mauri, R. Mazzarello, S. Paolini, A. Pasquarello, L. Paulatto, C. Sbraccia, S. Scandolo, G. Sclauzero, A. P. Seitsonen, A. Smogunov, P. Umari, and R. M. Wentzcovitch, "QUANTUM ESPRESSO: a modular and open-source software project for quantum simulations of materials," *Journal of Physics: Condensed Matter*, vol. 21, p. 395502, Sept. 2009. 37, 47

[85] H. J. Monkhorst and J. D. Pack, "Special points for brillouin-zone integrations," *Physical Review B*, vol. 13, pp. 5188–5192, June 1976. 38

[86] A. Baldereschi, "Mean-value point in the brillouin zone," *Physical Review B*, vol. 7, pp. 5212–5215, June 1973. 38

[87] D. J. Chadi and M. L. Cohen, "Electronic structure of $Hg_{1-x}Cd_xTe$ alloys and charge-density calculations using representative k points," *Phys. Rev. B*, vol. 7, pp. 692–699, Jan 1973. 38

[88] F. Gygi and A. Baldereschi, "Self-consistent hartree-fock and screened-exchange calculations in solids: Application to silicon," *Physical Review B*, vol. 34, pp. 4405–4408, Sept. 1986. 48

[89] E. Wigner, "On the interaction of electrons in metals," *Physical Review*, vol. 46, pp. 1002–1011, Dec. 1934. 51, 52

[90] G. Ortiz and P. Ballone, "Correlation energy, structure factor, radial distribution function, and momentum distribution of the spin-polarized uniform electron gas," *Physical Review B*, vol. 50, pp. 1391–1405, July 1994. 53, 60, 61

[91] D. Geldart and R. Taylor, "Wave-number dependence of the static screening function of an interacting electron gas. i. lowest-order hartree-fock corrections," *Can. J. Phys.*, vol. 48, p. 155, 1970. 54

[92] P. R. Antoniewicz and L. Kleinman, "Kohn-sham exchange potential exact to first order in $\rho(\mathbf{K})/\rho_0$," *Phys. Rev. B*, vol. 31, pp. 6779–6781, May 1985. 54

[93] J. A. Chevary and S. H. Vosko, "Importance of pauli-principle restrictions for accurate numerical evaluation of the exchange-only screening function," *Physical Review B*, vol. 42, pp. 5320–5323, Sept. 1990. 54

[94] E. Engel and S. H. Vosko, "Wave-vector dependence of the exchange contribution to the electron-gas response functions: An analytic derivation," *Physical Review B*, vol. 42, pp. 4940–4953, Sept. 1990. 54

[95] E. Engel and S. H. Vosko, "Erratum: Wave-vector dependence of the exchange contribution to the electron-gas response functions: An analytic derivation," *Physical Review B*, vol. 44, pp. 1446–1446, July 1991. 54

[96] F. Brosens, L. F. Lemmens, and J. T. Devreese, "Frequency-dependent exchange correction to the dielectric function of the electron gas," *physica status solidi (b)*, vol. 74, pp. 45–55, Mar. 1976. 54

[97] F. Brosens, J. T. Devreese, and L. F. Lemmens, "Frequency-dependent exchange correction to the dielectric function of the electron gas (II)," *physica status solidi (b)*, vol. 80, pp. 99–107, Mar. 1977. 54

[98] C. F. Richardson and N. W. Ashcroft, "Dynamical local-field factors and effective interactions in the three-dimensional electron liquid," *Physical Review B*, vol. 50, pp. 8170–8181, Sept. 1994. 54

[99] A. W. Overhauser, "Spin density waves in an electron gas," *Physical Review*, vol. 128, pp. 1437–1452, Nov. 1962. 55

[100] J. E. Bates and F. Furche, "Communication: Random phase approximation renormalized many-body perturbation theory," *The Journal of Chemical Physics*, vol. 139, p. 171103, Nov. 2013. 56

[101] S. Moroni, D. M. Ceperley, and G. Senatore, "Static response and local field factor of the electron gas," *Physical Review Letters*, vol. 75, pp. 689–692, July 1995. 57, 58

[102] G. L. Oliver and J. P. Perdew, "Spin-density gradient expansion for the kinetic energy," *Physical Review A*, vol. 20, pp. 397–403, Aug. 1979. 59

[103] U. v. Barth and L. Hedin, "A local exchange-correlation potential for the spin polarized case. i," *Journal of Physics C: Solid State Physics*, vol. 5, p. 1629, July 1972. 60

[104] K. T. Tang and J. P. Toennies, "The van der waals potentials between all the rare gas atoms from he to rn," *The Journal of Chemical Physics*, vol. 118, pp. 4976–4983, Mar. 2003. 63, 66

[105] A. D. Becke and E. R. Johnson, "Exchange-hole dipole moment and the dispersion interaction revisited," *The Journal of Chemical Physics*, vol. 127, p. 154108, Oct. 2007. 63

[106] P. L. Silvestrelli, "Van der waals interactions in DFT made easy by wannier functions," *Physical Review Letters*, vol. 100, p. 053002, Feb. 2008. 63

[107] P. L. Silvestrelli, "van der waals interactions in density functional theory using wannier functions," *The Journal of Physical Chemistry A*, vol. 113, pp. 5224–5234, Apr. 2009. 63

[108] A. Tkatchenko and M. Scheffler, "Accurate molecular van der waals interactions from ground-state electron density and free-atom reference data," *Physical Review Letters*, vol. 102, p. 073005, Feb. 2009. 63

[109] S. Grimme, J. Antony, S. Ehrlich, and H. Krieg, "A consistent and accurate ab initio parametrization of density functional dispersion correction (DFT-d) for the 94 elements h-pu," *The Journal of Chemical Physics*, vol. 132, p. 154104, Apr. 2010. 63

[110] R. Sabatini, T. Gorni, and S. de Gironcoli, "Nonlocal van der waals density functional made simple and efficient," *Physical Review B*, vol. 87, p. 041108, Jan. 2013. 65, 66

[111] O. A. Vydrov and T. V. Voorhis, "Nonlocal van der waals density functional: The simpler the better," *The Journal of Chemical Physics*, vol. 133, p. 244103, Dec. 2010. 66

[112] J. Heyd, G. E. Scuseria, and M. Ernzerhof, "Erratum: âhybrid functionals based on a screened coulomb potentialâ [j. chem. phys.118, 8207 (2003)]," *The Journal of Chemical Physics*, vol. 124, p. 219906, June 2006. 67

[113] W. Kolos and L. Wolniewicz, "Potential-energy curves for the $x1\sigma g+$, $b3\sigma u+$, and $c1\pi u$ states of the hydrogen molecule," *The Journal of Chemical Physics*, vol. 43, no. 7, pp. 2429–2441, 1965. 68, 69

[114] R. J. Gdanitz, "Accurately solving the electronic schrodinger equation of atoms and molecules using explicitly correlated ($r_{12}-$)mr-ci: the ground state potential energy curve of n_2," *Chemical Physics Letters*, vol. 283, no. 5â6, pp. 253 – 261, 1998. 69, 70

[115] M. Marchi, S. Azadi, M. Casula, and S. Sorella, "Resonating valence bond wave function with molecular orbitals: Application to first-row molecules," *The Journal of Chemical Physics*, vol. 131, p. 154116, Oct. 2009. 70

[116] M. Casula, C. Filippi, and S. Sorella, "Diffusion monteÂ carlo method with lattice regularization," *Physical Review Letters*, vol. 95, p. 100201, Sept. 2005. 70

[117] V. F. Lotrich, R. J. Bartlett, and I. Grabowski, "Intermolecular potential energy surfaces of weakly bound dimers computed from ab initio density functional theory: The right answer for the right reason," *Chemical Physics Letters*, vol. 405, pp. 43–48, Mar. 2005. 70, 71

[118] I. Roeggen and L. Veseth, "Interatomic potential for the $x1\sigma + g$ state of be_2, revisited," *International Journal of Quantum Chemistry*, vol. 101, no. 2, pp. 201–210, 2005. 71

[119] J. M. Merritt, V. E. Bondybey, and M. C. Heaven, "Beryllium dimerâcaught in the act of bonding," *Science*, vol. 324, pp. 1548–1551, June 2009. 71, 74

[120] A. L. Fetter and J. D. Walecka, *Quantum Theory of Many-Particle Systems*. Mineola, N.Y.: Dover Pubns, June 2003. 82

ACKNOWLEDGMENTS

First of all, I would like to thank my supervisor Prof. Stefano de Gironcoli. I'm extremely grateful to Stefano for having constantly guided and supported me during my PhD at SISSA. I owe him for all the time he spent trying to patiently understand and give a sense to my twisted ideas.
A special thank goes to Dr. Ngoc Linh Nguyen who helped me to implement the code and to Dr. Maria Hellgren for the usefull discussions and suggestions.

These years spent in Trieste wouldn't be such a pleasant journey without all the new friends I met: Matteo, Guglielmo, Marcello, Monica, Angelo, Cristiano, Ivan and the whole A-TEAM; thank you all for the beautiful moments spent together.

Last but not least I'm heartfelt grateful to my family for her love, support and understanding. Thanks to my parents who made all that possible and for always being present; to my brothers Angelo and Rossella for criticizing me when needed and encouraging me always; to my grandparents for being an example to me. I would like to dedicate this work to them all. My last and greatest thanks goes to Cristina who shared with me all the beautiful, sad, difficult, happy and wonderful moments in these years. Thank you for always being by my side.

Grazie!
Nicola

31 October 2014